

IOWA STATE UNIVERSITY

Digital Repository

Retrospective Theses and Dissertations

Iowa State University Capstones, Theses and
Dissertations

2004

Traffic grooming in IP over WDM optical networks

Jing Fang
Iowa State University

Follow this and additional works at: <https://lib.dr.iastate.edu/rtd>



Part of the [Computer Sciences Commons](#), and the [Electrical and Electronics Commons](#)

Recommended Citation

Fang, Jing, "Traffic grooming in IP over WDM optical networks " (2004). *Retrospective Theses and Dissertations*. 1158.
<https://lib.dr.iastate.edu/rtd/1158>

This Dissertation is brought to you for free and open access by the Iowa State University Capstones, Theses and Dissertations at Iowa State University Digital Repository. It has been accepted for inclusion in Retrospective Theses and Dissertations by an authorized administrator of Iowa State University Digital Repository. For more information, please contact digirep@iastate.edu.

Traffic grooming in IP over WDM optical networks

by

Jing Fang

A dissertation submitted to the graduate faculty
in partial fulfillment of the requirements for the degree of
DOCTOR OF PHILOSOPHY

Major: Computer Engineering

Program of Study Committee:
Arun K. Soman, Major Professor
Manimaran Govindarasu
Ahmed E. Kamal
Mani Mina
Lu Ruan

Iowa State University

Ames, Iowa

2004

Copyright © Jing Fang, 2004. All rights reserved.

UMI Number: 3158331

INFORMATION TO USERS

The quality of this reproduction is dependent upon the quality of the copy submitted. Broken or indistinct print, colored or poor quality illustrations and photographs, print bleed-through, substandard margins, and improper alignment can adversely affect reproduction.

In the unlikely event that the author did not send a complete manuscript and there are missing pages, these will be noted. Also, if unauthorized copyright material had to be removed, a note will indicate the deletion.



UMI Microform 3158331

Copyright 2005 by ProQuest Information and Learning Company.
All rights reserved. This microform edition is protected against
unauthorized copying under Title 17, United States Code.

ProQuest Information and Learning Company
300 North Zeeb Road
P.O. Box 1346
Ann Arbor, MI 48106-1346

Graduate College
Iowa State University

This is to certify that the doctoral dissertation of
Jing Fang
has met the dissertation requirements of Iowa State University

Signature was redacted for privacy.

Major Professor

Signature was redacted for privacy.

For the Major Program

DEDICATION

To my grandparents and my parents.

TABLE OF CONTENTS

LIST OF TABLES	viii
LIST OF FIGURES	ix
ACKNOWLEDGEMENTS	xii
ABSTRACT	xiv
CHAPTER 1. Introduction	1
1.1 A Brief History of Optical Networks	1
1.1.1 SONET/SDH	2
1.1.2 WDM	3
1.2 IP over WDM	5
1.3 IP over WDM Networking Architecture	8
1.3.1 IP over Point-to-Point WDM	9
1.3.2 IP over Reconfigurable WDM	10
1.4 Motivation and Approach	13
1.4.1 Routing and Wavelength Usage Constraint	13
1.4.2 IP Traffic Grooming	15
1.4.3 Traffic Grooming in Light Trail Architecture	17
1.4.4 Survivable Grooming Network Design	22
CHAPTER 2. Network Models and Notations	24
2.1 Grooming WDM Network Models	25
2.1.1 WDM Grooming Networks	25
2.1.2 Grooming Nodes in WDM Networks	25

2.2	Restoration Models	26
2.3	Notations	27
CHAPTER 3.	Wavelength Usage Constraint	29
3.1	Introduction	29
3.1.1	Two Solutions: An Example	29
3.2	Network Model and Assumptions	31
3.3	Analysis	31
3.3.1	Free Wavelength Distribution	34
3.3.2	Estimation of Call Arrival Rates on a Link	36
3.4	Results and Discussion	37
3.5	Summary	42
CHAPTER 4.	IP Traffic Grooming in WDM Networks	43
4.1	Introduction	43
4.1.1	Related Work	44
4.1.2	IP Traffic Grooming Issues	45
4.2	IP Traffic Grooming Problem Formulation	46
4.3	Network Model	46
4.4	Solution for Optimal Strategy	48
4.4.1	Problem Statement	48
4.4.2	Notations	49
4.4.3	Problem Formulation	49
4.5	Heuristic Approach	51
4.5.1	Bounds	51
4.5.2	Traffic Aggregation Algorithm	52
4.5.3	Complexity Analysis	55
4.5.4	Example of Traffic Aggregation	55
4.6	Solutions and Numerical Results	56
4.6.1	Observations	57

4.7	Performance Study	60
4.7.1	Performance Metrics	60
4.7.2	Examples	62
4.8	Dynamic Routing in the Virtual Topology	67
4.8.1	Dynamic Traffic	67
4.8.2	Routing Strategies	67
4.8.3	Performance Analysis	69
4.9	Summary	73
CHAPTER 5. Traffic Grooming in Light Trail Architectures		76
5.1	Light Trail Architecture	76
5.1.1	Light Trail Example	77
5.1.2	Node Structure	77
5.1.3	Light Trail Characteristics	80
5.2	Light Trail Design	81
5.2.1	Step I: Traffic Matrix Preprocessing	82
5.2.2	Step II: ILP Formulation	82
5.2.3	Notations	83
5.2.4	Solution Consideration	85
5.3	Light Trail Design: Heuristic Approaches	86
5.3.1	The Best-Fit Approach	86
5.3.2	Algorithm Design	87
5.3.3	Discussions	88
5.4	Performance Study	88
5.4.1	Light Trail Hop-Length Limit: $Tl_{max} = 4$	91
5.4.2	Light Trail Hop-Length Limit: $Tl_{max} = 3$	91
5.4.3	Light Trail Hop-Length Limit: $Tl_{max} = 5$	93
5.4.4	Discussions	95
5.5	Summary	96

CHAPTER 6. Survivable Grooming Network Design	97
6.1 Introduction	97
6.1.1 Related Work	98
6.2 Formulation of the Optimization Problem	101
6.2.1 Network Model	101
6.2.2 Restoration Models	101
6.2.3 Assumptions	103
6.2.4 Notations	104
6.2.5 ILP Formulation I: Backup Multiplexing	105
6.2.6 ILP Formulation II: Dedicated Backup with MLPS	108
6.3 Numerical Results	109
6.3.1 Experimental Design	109
6.3.2 Experiment I	109
6.3.3 Experiment II	113
6.4 Partial Protection	116
6.4.1 Optimal Design for Partial Protection	116
6.4.2 ILP Formulation I: Resource Minimization	117
6.4.3 ILP Formulation II: Protection Maximization	118
6.4.4 Experimental Results	119
6.4.5 Shortest-Available-Least-Congested Routing	123
6.4.6 Simulation Results	124
6.5 Summary	128
CHAPTER 7. Summary and Future Work	130
BIBLIOGRAPHY	134

LIST OF TABLES

Table 4.1	Requests matrix for a 6-node network	57
Table 4.2	Resulting routes in virtual topologies	59
Table 5.1	Traffic matrix for a 10-node network.	90
Table 5.2	ILP: Resulting light trails $Tl_{max} = 4$	91
Table 5.3	Local Best-Fit: Resulting light trails $Tl_{max} = 4$	92
Table 5.4	Traffic matrix for a 10-node network: After traffic matrix preprocessing.	92
Table 5.5	ILP: Resulting light trails $Tl_{max} = 3$	93
Table 5.6	Local Best-Fit: Resulting light trails $Tl_{max} = 3$	94
Table 5.7	ILP: Resulting light trails $Tl_{max} = 5$	94
Table 5.8	Local Best-Fit: Resulting light trails $Tl_{max} = 5$	95
Table 6.1	Solution from ILP formulation I: Requires 21 wavelength-links.	110
Table 6.2	Solution from ILP formulation II: Requires 21 wavelength-links.	111
Table 6.3	Solution without traffic grooming: Requires 52 wavelength-links.	112
Table 6.4	Traffic matrix for the 10-node-14-link network.	113
Table 6.5	Solution from ILP formulation I: Requires 28 wavelength-links.	114
Table 6.6	Solution from ILP formulation II: Requires 33 wavelength-links.	115
Table 6.7	Solution with full protection: Requires 33 wavelength-links.	120
Table 6.8	Solution with partial protection ($P_{ratio} = 0.6$): Requires 28 wavelength-links.	121
Table 6.9	Traffic matrix for the 10-node-14-link network: 50 requests.	122
Table 6.10	Requests with improved protection: Given $P_{ratio} = 0.5$	122

LIST OF FIGURES

Figure 1.1	Increased network capacity - TDM.	4
Figure 1.2	Increased network capacity - WDM.	4
Figure 1.3	Possible layering architectures.	6
Figure 1.4	Router interconnections in the IP over point-to-point WDM architecture.	10
Figure 1.5	Router interconnections in the IP over reconfigurable WDM architecture.	10
Figure 1.6	Overlay IP over WDM network model.	11
Figure 1.7	Augmented IP over WDM network model.	12
Figure 1.8	Peer IP over WDM network model.	13
Figure 3.1	A two-link network. (a) 2 wavelengths per fiber with no wavelength conversion. (b) 2 wavelengths per fiber with wavelength conversion. (c) 3 wavelengths per fiber with at-most 2 usable at any given time and no wavelength conversion.	30
Figure 3.2	A z-link path model	32
Figure 3.3	Wavelength occupancy on a 2-hop path.	35
Figure 3.4	Blocking probability versus the link offered load for a bidirectional ring network with 25 nodes.	39
Figure 3.5	Blocking probability versus the link offered load for a bidirectional 5×5 Mesh-Torus network.	39
Figure 3.6	Comparison of random and first-fit wavelength assignment schemes for a bi-directional ring network with 25 nodes.	40
Figure 3.7	Comparison of random and first-fit wavelength assignment schemes for a bidirectional 5×5 mesh-torus network.	41

Figure 4.1	Network representation for integrated routing computation.	44
Figure 4.2	Illustrative example of IP traffic grooming.	47
Figure 4.3	Approximate approach: Traffic aggregation	54
Figure 4.4	An illustrative example of traffic aggregation algorithm.	56
Figure 4.5	Comparison of ILP solution and heuristic approach: An illustrative example. (a) Results obtained by solving ILP optimization problem with hop-length limit 3. (b) Results obtained from traffic aggregation approach.	58
Figure 4.6	Resource requirement in a 16-node bi-directional ring network.	63
Figure 4.7	Resource requirement in a 4×4 bi-directional mesh torus network.	63
Figure 4.8	Wavelength utilization in a 16-node bi-directional ring network.	64
Figure 4.9	Wavelength utilization in a 4×4 bi-directional mesh torus network.	64
Figure 4.10	The 20-node-31-link ARPANET topology.	65
Figure 4.11	Resource requirement in the 20-node-31-link bi-directional ARPANET.	65
Figure 4.12	Wavelength utilization in the 20-node-31-link bi-directional ARPANET.	66
Figure 4.13	Virtual topology solution with designed load on each link.	68
Figure 4.14	Blocking performance in virtual topology in Figure 4.13 with random traffic, $ Diff = 0$	69
Figure 4.15	Blocking performance in virtual topology in Figure 4.13 with random traffic with $ Diff = 2$	70
Figure 4.16	Blocking performance in virtual topology in Figure 4.13 with random traffic with $ Diff = 4$	70
Figure 4.17	Virtual topology solution with designed load on each link.	71
Figure 4.18	Blocking performance in virtual topology in Figure 4.17 with random traffic, $ Diff = 0$	72
Figure 4.19	Blocking performance in virtual topology in Figure 4.17 with random traffic with $ Diff = 2$	72

Figure 4.20	Blocking performance in virtual topology in Figure 4.17 with random traffic with $ Diff = 4$	73
Figure 5.1	Illustrative example of traffic streams in a light trail	77
Figure 5.2	An example node structure in light trail framework	78
Figure 5.3	An example light trail node structure with three input fibers with two wavelengths on each fiber	79
Figure 5.4	An example node configuration in light trail framework	79
Figure 5.5	Detailed node configuration of the light trail in Figure 5.4	80
Figure 5.6	Light trail design step 1: Traffic matrix preprocessing	83
Figure 5.7	Light trail design step 2: Best-Fit approach	89
Figure 5.8	A 10-node example network	90
Figure 6.1	An example of layered network model with $W = 3$, $K = 2$	102
Figure 6.2	Physical topologies used in experiments	110
Figure 6.3	Physical topologies used in experiments	119
Figure 6.4	Blocking performance for traffic capacity varies from OC-1 to OC-36	125
Figure 6.5	Number of call blocked due to primary blocking	126
Figure 6.6	Number of call blocked due to backup blocking	126
Figure 6.7	Blocking performance for traffic capacity varies from OC-24 to OC-36	127
Figure 6.8	Number of call blocked due to primary blocking	127
Figure 6.9	Number of call blocked due to backup blocking	128

ACKNOWLEDGEMENTS

First and foremost, I would like to express my utmost gratitude to Professor Arun Soman, for his guidance during my study at Iowa State University. I often feel I have been a lucky person since I joined his lab. He is a remarkable mentor in every aspect. He has always been and will always be my role model.

Special thanks to Professor Lu Ruan and Professor Mani Mina for their helpful advice in matters technical and beyond. I would like to thank Professor Ahmed Kamal for reading my dissertation meticulously and offering insightful comments to improve the quality of the dissertation. My thanks to Professor Manimaran Govindarasu for his valuable technical feedback and comments.

I would like to thank my friends Zhiqi Liu, Xuan Fu, Dan Gui, Suihong Liang, Weiling Deng and Daan He, for helping me during my difficult times and for inspiring me to pursue a PhD degree. Thanks to Yisheng Xue, for always being there when I need to talk, even though we have never met. My special thanks to my uncle Qi Li and aunt Yan Ma, for their generous help, and to Keri Li, my favorite cousin, for brightening my dull school days.

Thanks to my lab seniors, Sashisekaran Thiagarajan, Srinivasan Ramasubramanian, Murari Sridharan, Liang Zhao, Jianwei Zhou, Huesung Kim, Rama Sangireddy, and Tao Wu for all the help that made me survive and for the wonderful time we spent together; thanks to Abu Sebastian for teaching me how to drive and bravely sitting in my car to explore Iowa together; thanks to Murali Viswanathan for being a patient listener and a wonderful friend; thanks to Samyukta Sankaran, Nagapratima Kunapareddy, and Anirban Chakrabarti for the brainy coffee room discussions in Coover; thanks to my fellow lab-mates for their companionship and support that made my study and research a delightful experience: Wensheng He, Srivatsan

Balasubramanian, Yana Ong, Heng(Sam) Xu, Pallab Datta, Rohit Gupta, Rakesh Raghavan, Varun Sekhri, Mahadevan Gomathisankaran and David Lastine.

Four years are gone before I notice. The people here in Ames have changed me. I have been expecting this opportunity to express how grateful I am to all my friends. My special thanks to Helen He Mu for being a true friend to me during my ups and downs. Thanks to Lei Zhang for bringing so many laughters to my life. My thanks to Wenzheng Qiu and Lu Li for always being supportive and encouraging. Special thanks to Lu Li for establishing our photography club and setting a high standard for us. Thanks to Chao Cheng and Huafei Zheng, I have enjoyed reading every email from them through these years. Thanks to Bo Wang, Zhong Gu, Yang Yang and Jinchun Xia for their friendship. I have learned great a lot from all of my friends and I know I am not alone here because of them.

I would also like to give my most sincere thanks to Grand Master Young Chin Pak, for helping me to realize that the best way to get motivated is to challenge myself. When others are trying to make us feel like a fool, he makes us believe that we are the best. When others are trying to prove something is worthless, he is looking for the merits out it. He changed my attitude towards life, as a result, my life was changed. I enjoy every moment spent in the Do-jang, where I am not judged by my grades and degree, where I am always encouraged to do things that I never thought I would be able to do. Master Pak is a respectable martial artist, a true mentor. My thanks also go to all the teaching assistants in my Taekwondo class: David Niedergeses, Oesa Weaver, Amber Barnes and Brandy Witte.

In closing, my profound thanks go to my grandparents and my parents. Words cannot express my deepest gratitude to them. They have always put their faith in me and cherished my successes even more than I did myself. Without their sacrifices and support, I would never have completed this dissertation.

ABSTRACT

Telecommunication networks evolve as technology advances and society changes. Optical communications employing Wavelength Division Multiplexing (WDM) has become the dominant technology for use in backbone networks. As IP gains in popularity, the traffic pattern in carrier networks shift from being voice centric to being data centric. This has led to a change in the network infrastructure and many researchers believe that networks are evolving towards the slim two-layer model of IP over WDM. Although IP routers are becoming faster, eliminating the need for ATM and SONET/SDH, there still exists a significant bandwidth mismatch between the sub-wavelength level IP packets and wavelength capacity. The process of multiplexing, demultiplexing and switching lower rate traffic stream onto and off of higher capacity wavelengths is defined as *traffic grooming*. In this dissertation, we address several fundamental issues of the grooming network design and operation in the context of IP over WDM.

First, we provide an introduction to the evolution of optical network architectures from SONET/SDH to WDM. We describe the principles of routing and wavelength assignment in IP over WDM networks, and explain how wavelength continuity constraint and wavelength usage constraint affect network performance. We develop a mathematical model to analyze the blocking performance of the optical networks with wavelength usage constraint. We conclude that in the practical WDM networks with wavelength usage constraint, increasing the total number of available wavelengths in a fiber is an attractive alternative to employing wavelength conversion.

Next, to make the network viable and cost-effective for carrying IP centric traffic, it must be able to offer sub-wavelength level services and must have the capability to pack these services effectively onto a wavelength. This motivates the study of traffic grooming problems in the

IP over WDM framework. We investigate the traffic grooming performed in IP layer, where the sub-wavelength level IP packets are grouped together in electrical domain before they are sent to the WDM layer. This is referred to as IP traffic grooming. Similarly, the grooming performed in WDM layer is called WDM wavelength grooming. We study IP traffic grooming problem with the objective to minimize the number of transmitters and receivers needed in the WDM layer. The resulting topology is called the virtual topology. We also propose three routing strategies for allocating dynamic traffic requests in the designed virtual topologies. Their blocking performance is studied and compared through simulations.

The third issue addressed in this dissertation is IP traffic grooming in a recently proposed architecture called light trails. After a brief introduction to the light trail architecture, we define the light trail design problem and identify the minimum number of light trails to carry the given traffic demand. An ILP is formulated for solving the light trail design problem with given static traffic requirement. Two heuristic approaches are also developed for obtaining fast solutions in large networks. In our numerical examples, our heuristic approaches give very fast and good solutions in comparison to the results obtained from solving the ILP formulations.

We finally address the issue of fault management in grooming networks. Although fault tolerance in WDM network has been extensively studied in literature, the research on survivability issues in grooming networks is still a relatively new area. We study shared and dedicated protection against single link failure in WDM grooming networks and develop an ILP formulation for each of them respectively. We extend our research on the full protection design to partial protection where the backup capacity is smaller than the primary capacity. This problem is decomposed into two sub-problems, namely resource minimization and protection maximization. We present ILP formulations for each of the sub-problems, and further design a dynamic routing strategy named *shortest-available-least-congested* routing. We show that partial protection is a useful feature in grooming networks.

CHAPTER 1. Introduction

1.1 A Brief History of Optical Networks

An optical network is a data network built using fiber-optics technology, which sends data digitally, as *light*, through joined fiber strands. Optical fiber offers low-loss transmission over an enormous frequency range of about 25 THz, which is several orders of magnitude more than the bandwidth available in copper cables. Additionally, optical fiber offers lower bit error rates than any other transmission media and is less susceptible to various kinds of electromagnetic interferences and other undesirable effects. Consequently, optical networks offer an enormous increase in both transmission capacity and reliability over the traditional copper wire-based networks.

The first fiber-optic communication system was installed by AT&T and GTE in 1977. Since then, the tremendous cost savings and improved network service quality has led to many advances in the technologies required for optical networks. Fiber-optics today is used almost exclusively in the physical layers of wide-area networks around the globe, and the development of metropolitan optical networks is already underway.

Telecommunications networks evolves along with the technological advances and the social changes. The first digital networks were asynchronous networks, where each network element's internal clock source timed its transmitted signal. Due to the fact that each clock had a certain amount of variation, signals arriving and transmitting could have a large variation in timing, which often results in bit errors. Furthermore, as optical-fiber deployment advances, no standards existed to mandate how network elements should format the optical signal. The emergence of numerous proprietary methods makes it difficult to interconnect equipment from different vendors.

1.1.1 SONET/SDH

The need for optical standards leads to the creation of the synchronous optical network (SONET). SONET is a standard for optical communications transport formulated by the Exchange Carriers Standards Association (ECSA) for the American National Standards Institute (ANSI), which sets industry standards in the U.S. for telecommunications and other industries.

Following the development of the SONET standard by ANSI, the CCITT undertook to define a synchronization standard that would address interworking between the CCITT and ANSI transmission hierarchies. That effort finished off in 1989 with CCITT's publication of the synchronous digital hierarchy (SDH) standards. SDH is a world standard, and SONET can be considered as a subset of SDH.

A synchronous mode of transmission means that the optical signals transmitted through a fiber-optic system have been synchronized to an external clock. The resulting benefit is that data streams carrying voice, data, and images through the fiber system in a steady, regulated manner so that each stream of light can easily be identified and extracted from delivery or routing. In a synchronous system such as SONET, the average frequency of all clocks in the system is the same (synchronous) or nearly the same (plesiochronous). Every clock can be traced back to a highly stable reference supply. For instance, the STS-1 rate remains at a nominal 51.84 Mbps, allowing many synchronous STS-1 signals to be stacked together when multiplexed without any bit-stuffing. Thus, the STS-1s are easily accessed at a higher STS-N rate.

SONET and SDH are two closely related standards, they provide the foundation to transform the transport networks that we know today. SONET/SDH governs interface parameters, rates, formats, and multiplexing methods, and operations, administration, maintenance, and provisioning (OAM&P) for high-speed transmission of bits of information in flashing laser-light streams. It is SONET/SDH that enables network providers to use different vendor's optical equipment with the confidence of at least basic interoperability.

1.1.2 WDM

SONET has survived during a time of tremendous changes in network capacity needs. The main reason is its scalability. According to its open ended growth plan for higher bit rates, theoretically no upper limit exists for SONET bit rates. However, as bit rates increase, physical limitations in the laser sources and optical fiber begin to make the bit rate increasing on each signal impractical.

Additionally, connection to the networks through access rings also have increased requirements. Customers are carrying more and different types of data traffic and demand more services and options. To provide full end-to-end connectivity, a new paradigm needed to be developed to meet all the high capacity and varied needs. Optical networks provide the required bandwidth and flexibility to enable end-to-end wavelength services.

Facing the challenges of increased service needs, fiber exhaust, and layered bandwidth management, service providers need options to provide an economical solution. One way to alleviate the shortage of fiber is to lay more fibers. However, this solution is not always viable mainly due to the fact that the cost of laying new fibers is prohibitively high, especially in densely populated metropolitan areas. Besides, the rights-of-way issues are complicated and add the difficulties to lay new fiber.

A second choice is to increase the network capacity using time division multiplexing (TDM), where TDM increases the fiber capacity by slicing time into smaller intervals so that more data can be transmitted per second, as shown in Figure 1.1. It allows flexible traffic management on the fixed bandwidth but requires O-E-O and electrical multiplex/demultiplex function.

Traditionally, this has been method of choice (DS-1, DS-2, DS-3, etc.) in the industry. However, when service providers use this approach exclusively, they must make the leap to the higher bit rate in one jump, requiring the purchase of more capacity than they initially needed. Based on the SONET hierarchy, the next incremental step from 10 Gbps TDM is 40 Gbps - a quantum leap that many believe will not be possible for TDM technology in the near future. TDM has also been used with transport networks that are based on either SONET or SDH.

The third choice for service providers is to use wavelength division multiplexing (WDM),

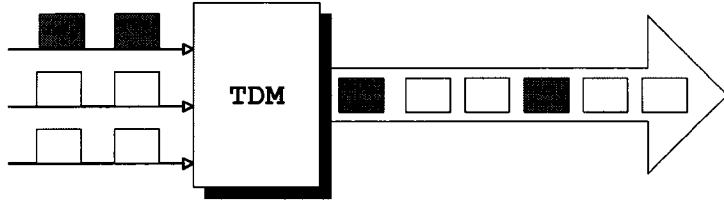


Figure 1.1 Increased network capacity - TDM.

which increases the capacity of embedded fiber by first assigning incoming optical signals to specific frequencies (wavelength, lambda) within a designated frequency band and then multiplexing the resulting signals out onto the fiber. This wavelength spacial reuse reduces the cost of the expensive electrical multiplex/demultiplex function. Since incoming signals are never terminated in the optical layer, the interface can be bit-rate and format independent. This bit rate and protocol transparency allows service providers to easily integrate the WDM technology with existing equipment in the network and access to the untapped capacity in the embedded fiber at the same time.

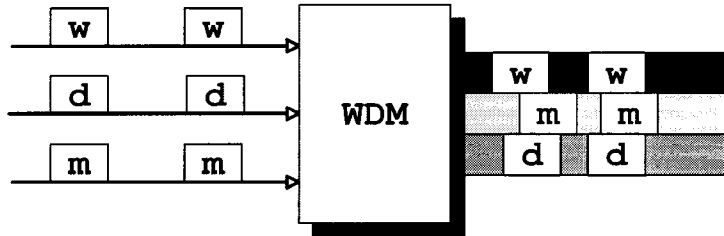


Figure 1.2 Increased network capacity - WDM.

WDM combines multiple optical signals so that they can be amplified as a group and transported over a single fiber to increase capacity, as shown in Figure 1.2. Each signal carried can be at a different rate (OC-3, -12, -24, etc.) and in a different format (SONET, ATM, data, etc.). When the inter gap between two wavelength channels is smaller than 100 GHz (~ 0.80 nm), such multiplexing is also referred to dense WDM (DWDM).

Consider a highway analogy where one fiber can be thought of as a multilane highway. Traditional TDM systems use a single lane of this highway and increase capacity by moving

closer on this single lane by using wider vehicles. WDM optical networking is analogous to accessing multiple lanes on the highway by using narrower vehicles (increasing the number of wavelengths on the embedded fiber base) to gain access to the fiber wavelength capacity. An additional benefit of optical networking is that the highway is blind to the type of traffic that travels on it. Consequently, the vehicles on the highway can carry ATM packets, SONET, as well as IP traffic.

1.2 IP over WDM

The popularity of the Internet and Internet protocol (IP)-based intranet is promising enormous growth in data traffic originating from IP endpoints. This growth is being fueled by various Web-based applications and by the indirect impact of increased computing power and storage capacity in the end systems. The advent of new services with increasing intelligence and bandwidth demands are further adding to the traffic growth. New access technologies such as Asymmetric Digital Subscriber Line (ADSL), High-bit-rate Digital Subscriber Line (HDSL), and fiber to the home (FTTH) would remove the access bottlenecks and enforce an even faster growth of demand on the backbone network. These changing trends have led to a fundamental shift in traffic patterns. The amount of data traffic on carrier networks now exceeds that of voice traffic. The cross-over happened for many carriers in 1998 [1]. This shift in traffic patterns in carrier networks has led to a change in the way that networks need to be organized.

In the past, the amount of data traffic on carrier networks was small compared with voice-centric traffic. Therefore, the carrier networks were designed mainly for voice traffic, and data networks were on the edges. For example, data clients would use leased constant bit rate lines to carry data traffic over voice networks. As the amount of data traffic has surpassed that of voice traffic, the data domain has become a remunerative market for the voice network providers. Furthermore, the voice revenue traffic has continued to decline due to market competition. These two effects leads to a trend where the core networks are designed primarily for data with voice networks on the edges. The voice can be carried in the core networks using “voice-

over-IP” or similar paradigms. Such architectures have resulted in the need for better quality of service (QoS), protection and availability guarantees in IP networks. To meet these growing demands, WDM has moved from the research laboratories and is emerging as a dominating trend for use in backbone networks.

WDM significantly increases the fiber capacity utilization by dividing the available bandwidth into non-overlapping channels, namely *wavelengths*, each operating at peak electronic speed. Connections between users are supported by establishing an all-optical channel, namely *lightpath*, between the two end nodes of each connection. On lightpaths signals can be at different rates and use different formats as the signals are never terminated inside the core network. This bit-rate and protocol transparency is a key feature of an optical backbone network. A wavelength converter is a device that allows the optical signal on a wavelength to be converted onto another wavelength. In the absence of wavelength converters, a lightpath should occupy the same wavelength on all the links it traverses. This property is known as the *wavelength-continuity constraint*.

Today’s Internet is dominated by applications and services based on IP protocol, almost all end-user communication applications in practice make use of TCP/IP. Most network designers believe that IP is going to be the common traffic convergence layer in communication networks. Consequently, IP over WDM has been envisioned as the winning combination of the network architecture [2, 3].

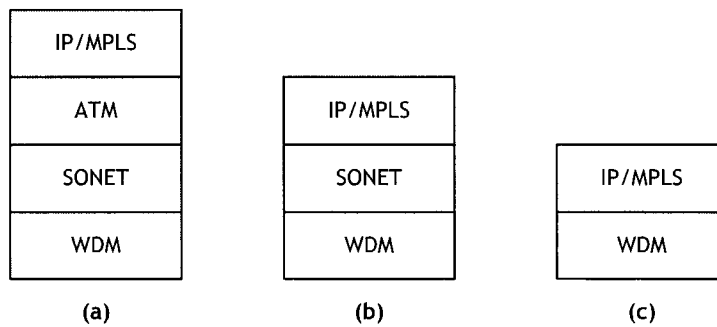


Figure 1.3 Possible layering architectures.

At present, WDM is mostly deployed point-to-point and the current four-layer architecture is shown in Figure 1.3 (a), in which IP routers are connected to ATM switches and then send ATM cells over SONET devices that were connected to a WDM transport system. ATM switches are required for multi-service integration (integrating voice and data). In addition, routers are limited generally in speed compared to ATM switches. SONET is required for aggregation - combining 155 Mb/s ATM streams to OC-48 SONET streams - and protection.

As IP routers are becoming significantly faster along with the introduction of quality of service (QoS) in IP, the need for ATM is diminishing. Beginning in 1996, packet over SONET or IP over PPP over SONET started becoming a popular approach. The four-layer model depicted in Figure 1.3 (a) was hence reduced to a three-layer architecture as shown in Figure 1.3 (b), where IP data traffic is transmitted over SONET approach doing without ATM layer.

In 1999, several router manufacturers announced fast OC-192 interfaces. Therefore the need for traffic aggregation using SONET is now under reconsideration. Routers with SONET interfaces that can fill an entire wavelengths have started becoming available. Moreover, the protection and restoration function that is provided by SONET add-drop multiplexers (ADMs) can be subdivided between IP and WDM equipment. In 2000, Ethernet framing also started gaining a foothold with the evolution of 10 Gigabit Ethernet. Some are predicting that eventually, SONET will not be required and Ethernet will be running end-to-end. Regardless of what the data link layer framing (SONET/PPP/Ethernet) is used, the reduced architecture is called “IP over WDM” where IP and WDM are the only two layers that are needed. This two-layer model is shown in Figure 1.3 (c), which aims at a direct integration of IP with WDM optical layers [2, 3].

MPLS (Multi-protocol label switching) may provide an integration structure between IP and WDM layer. A generalized multi-protocol label switching (GMPLS), also referred to as Multi-protocol lambda switching (MP λ S), which supports not only devices that perform packet switching, but also those that perform switching in the time, wavelength, and space domain has also been proposed [4]. In an MPLS network, incoming packets are assigned a “label” by a “label edge router (LER)”. Packets are forwarded along a “label-switched path (LSP)” where

each “label-switched router (LSR)” makes forwarding decisions based solely on the contents of the label. At each hop, the LSR strips off the existing label and applies a new label which tells the next hop how to forward the packet.

MPLS evolved from numerous prior technologies including Cisco’s “Tag Switching”, IBM’s “ARIS”, and Toshiba’s “Cell-Switched Router”. The initial goal of label based switching was to bring the speed of Layer 2 (such as ATM, Frame Relay or Ethernet) switching to Layer 3 (such as IP) by replacing the complex IP address based route lookup with the fast Label based switching methods. This initial justification for techniques as MPLS is no longer perceived as the main benefit, as Layer 3 switches are now able to perform route lookups at sufficient speeds to support most interface types. However, MPLS brings many other benefits to IP-based networks such as,

- Traffic Engineering
- VPNs(Virtual Private Networks)
- Elimination of Multiple Layers.

Typically most carrier networks employ an overlay model where SONET/SDH is deployed at Layer 1, ATM is used at Layer 2 and IP is used at Layer 3. Using MPLS, carriers can migrate many of the functions of the SONET/SDH and ATM control plane to Layer 3, thereby simplifying network management and network complexity. Eventually, carrier networks may be able to migrate away from SONET/SDH and ATM all-together.

1.3 IP over WDM Networking Architecture

The development of IP over WDM technology and networking architecture can be broadly classified into three generations [5]:

- *First Generation:* In the first-generation, WDM (or DWDM) systems are used mainly for point-to-point high-bandwidth pipes between adjacent IP routers. IP packets are encapsulated in SONET frames using Packet-over-SONET schemes. Precisely speaking,

this is still a three-layer architecture as shown in Figure 1.3 (b). Many IP routers and WDM equipment vendors have products commercially available today that can support IP over point-to-point DWDM. Point-to-point DWDM systems have seen widespread deployment in long distance carriers.

- *Second Generation:* In the second-generation IP over WDM systems, WDM channels are routed in WDM networks using crossconnects enabling more efficient WDM bandwidth utilization and IP router interface utilization. Due to the reconfigurability afforded in this generation of products, there is a drive to move protection switching and restoration directly to WDM layer, thereby, eliminating SONET layer for the first time. Many WDM vendors have announced WDM crossconnect products that will enable this second-generation IP over WDM networking.
- *Third Generation:* In the third generation, IP packets are directly transported and switched by WDM packet switches that leads to much finer granularity in traffic multiplexing on the respective wavelength channels. WDM packet switching [6, 7, 8] has been successfully demonstrated in laboratory trials, including the DARPA funded optical Label Switching Project [9]. However, this technique is still yet maturing and it remains to be seen whether such optical packet switching technologies can mature and be made commercially available in the near future.

1.3.1 IP over Point-to-Point WDM

In an IP over point-to-point WDM architecture, IP routers are directly interconnected via WDM fiber links. As illustrated in Figure 1.4, the neighboring routers for a given router interface is fixed. In the IP over point-to-point WDM architecture, the network topology is fixed and the network configuration is static with typically centralized network management and limited interaction between IP and WDM layers.

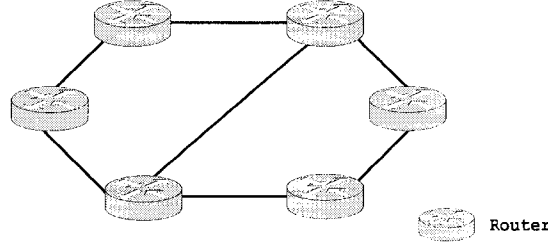


Figure 1.4 Router interconnections in the IP over point-to-point WDM architecture.

1.3.2 IP over Reconfigurable WDM

In an IP over reconfigurable WDM architecture, IP routers are connected to the ports of WDM crossconnects as shown in Figure 1.5. A WDM crossconnect can then connect any of its input port to any of its output port. In other words, the WDM crossconnects are themselves interconnected in a mesh configuration with WDM fiber links. Therefore, by appropriately configuring the WDM crossconnects, a given router interface can be connected to any other router interface. As a result, the neighboring router for a given router interface is configurable under this architecture.

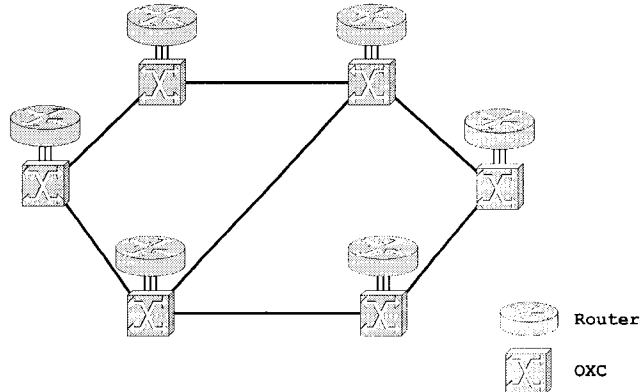


Figure 1.5 Router interconnections in the IP over reconfigurable WDM architecture.

The IP and WDM layers can be combined in several different models [10].

- *Overlay model* where the two layers relate to each other in a client-server relationship, with IP being the client to the WDM layer. The IP network layer links are realized by the corresponding WDM layer connections. Under the overlay model, IP domain is more or less independent of the WDM layer. The IP/MPLS routing protocols are independent of the routing and signaling protocols of the WDM layer. The overlay model may be statically provisioned using a Network Management System or may be dynamically provisioned. Static provisioning solution may not be scalable though.

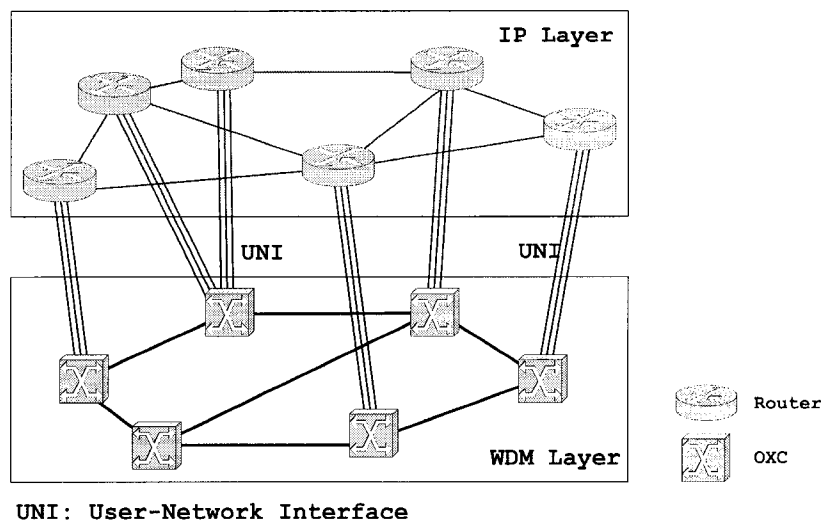


Figure 1.6 Overlay IP over WDM network model.

- *Augmented model* where IP and WDM have a single addressing plane, but separate routing instances. For example, IP addresses could be assigned to optical network elements and carried by optical routing protocols to allow routing (reachability) information to be shared with the IP domain to support some degree of automated discovery. In augmented model, control information is passed on from one instance to another. Static configuration or border gateway protocol (BGP) can be used to bridge the two routing instances.
- *Peer model* where devices from the IP and WDM networks relate to each other in a peer-to-peer relationship, and there is only one instance of a routing protocol running in

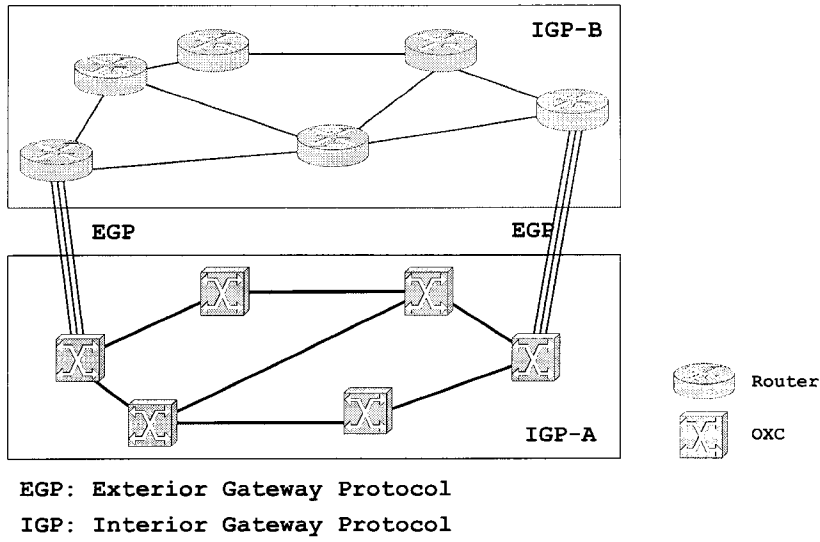


Figure 1.7 Augmented IP over WDM network model.

the optical domain as well as in the IP domain. In this model, MPLS and its lambda variant MP λ S can be used to provide a uniform control plane. The assumption in this model is that all the WDM crossconnects and the IP routers have a common addressing scheme.

The overlay model, which is aligned with the carrier practice of organizing their operational units into transport and switching units, is of particular interests to carriers and is likely to be adopted in near-term immediate deployment. Proponents of the other models may argue that due to the overall simplified management and control structures, their models are likely to be adopted in the long-term for highly dynamic IP over WDM networks.

Notice that regardless of the model being adopted, logically a reconfigurable IP over WDM network always sees a *virtual topology* (or *logical topology*), which is dynamically reconfigurable. In the overlay model, the dynamic virtual topology is the one formed by IP links. In the augmented and peer model, the dynamic virtual topology is the lightpath tunnel topology. In all cases, fine-grained IP traffic is routed over the respective virtual topology.

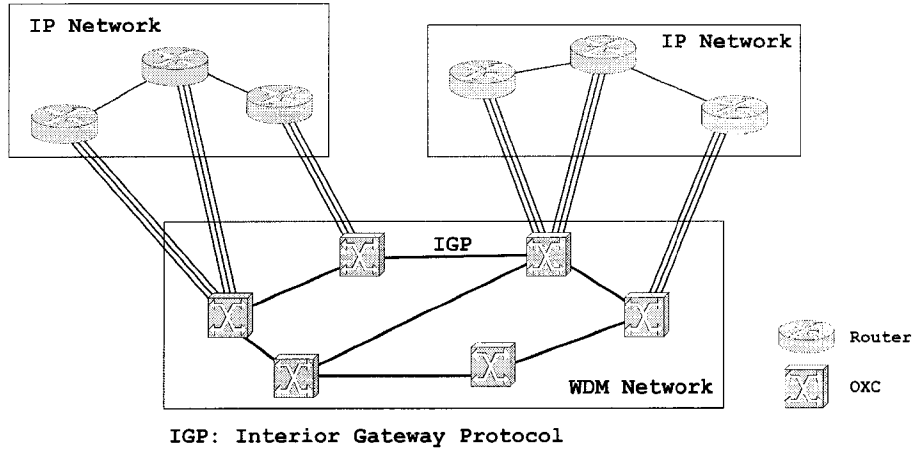


Figure 1.8 Peer IP over WDM network model.

1.4 Motivation and Approach

The fundamental properties of the WDM system are exploited to form an all optical layer. Bit rate and protocol transparency enables transport of native enterprise data traffic like Gigabit Ethernet, ATM, SONET, IP etc. on different channels. It also brings in more flexibility so that the system can be connected directly to any signal format without extra equipment. The optical transport architecture will employ both transport networking and enhanced service layers, working together in a complementary and inter-operative manner.

We address several prominent issues of optical layer in the context of IP over WDM.

1.4.1 Routing and Wavelength Usage Constraint

In the two-layer IP over WDM architecture, proponents of all-optical networks (AONs) have predicted that IP over WDM can become a reality only when all the end-to-end services are offered optically. In wavelength routed WDM networks, connections between users are supported by an all-optical channel, namely lightpath. However, the wavelength continuity constraint leads to higher call blocking probability in a network without wavelength conversion than it does in a network that employ full-wavelength conversion at all nodes. Although wavelength conversion improves network blocking performance, the high cost of wavelength

converters have made it impractical to employ full-wavelength converters at all nodes. The benefit of using wavelength converters in wavelength routed WDM networks and wavelength converter placement problems have been extensively studied in literature.

Another practical problem is that not all the wavelengths can be used at any given instant in time due to power constraints. This restriction is referred to as the *wavelength usage constraint* [11]. Such a scenario could arise due to the restriction on the power carried in the fiber or the power limit on the optical components on the path such as amplifiers, re-generators, etc. The reason behind is that fiber nonlinearity effects, such as stimulated Brillouin scattering (SBS), simulated Raman scattering (SRS), four wave mixing (FWM), self-phase modulation (SPM), cross-phase modulation (XPM), and intermodulation (mixing), arise as the optical power levels increases in an optical fiber. In fact, these fiber nonlinearities present a new realm of barriers that need special attention when designing state-of-the-art fiber optic systems.

Wavelength routing remains to be a fundamental problem in IP over WDM networks. It is highly desired that the traffic is efficiently packed and uses minimum number of wavelengths to avoid employing expensive equipment like wavelength converters, transmitters and receivers. However, as the data traffic keeps increasing and the WDM network resource is still limited, wavelength routing will appear to be a predominant problem. In order to satisfy both wavelength continuity constraint and wavelength usage constraint and still achieve good network blocking performance, two alternatives can be employed: (1) Employing wavelength converters with the number of wavelengths carried in the fiber being the same as the maximum number of usable wavelengths; or (2) Employing more wavelengths in a fiber but restricting the number of usable wavelengths to a certain maximum without employing wavelength converters. This leads to the following research problems.

How to achieve good network blocking performance without employing wavelength converters? When the number of usable wavelengths is fixed, would adding more wavelengths be a better choice than employing wavelength converters in the networks? How would the wavelength be assigned? What is the performance of network with wavelength usage constraint?

In Chapter 3, we develop an analytical model for evaluating the blocking performance

of WDM optical networks with wavelength usage constraint employing random wavelength assignment scheme. The analytical model is shown to be accurate by comparing the results with that of simulations for two different network topologies that have high and low link load correlation. We evaluate the performance of first-fit wavelength assignment strategy and compare its performance with that of random wavelength assignment strategy. It is observed that with an increase of few extra wavelengths in the fiber, the blocking performance is similar to that when full-wavelength conversion is employed. The simulation results also show that the number of extra wavelength required to achieve a certain blocking performance is lesser when first-fit wavelength assignment strategy is employed. We conclude that employing extra wavelengths in practical networks is an attractive alternative compared to full-wavelength conversion even in the presence of power budget constraints.

1.4.2 IP Traffic Grooming

One critical issues that the two-layer IP over WDM networks are facing is the big gap between available bandwidth on a wavelength capacity and the existing low-rate traffic connections. The bandwidth on a wavelength is close to the peak electronic transmission speed and has been steadily increased from OC-48 (2.5 Gbps) to OC-192 (10Gbps), and is expected to increase up to OC-768 (40 Gbps). This wavelength capacity is becoming too large for certain data traffic requirements and the networks are required to provide dynamic service to the users at much lower capacity than that available on a wavelength channel. These sub-rate traffic connections can vary from STS-1 (51.84 Mbps) to the full wavelength capacity. Moreover, in networks of practical sizes, the number of source-destination traffic connections is still an order of magnitude higher than the number of available wavelengths.

Several further traffic multiplexing techniques on a wavelength are thus proposed. One approach to provisioning fractional wavelength capacity is to multiplex traffic on the wavelength. The act of multiplexing, demultiplexing and switching lower rate traffic streams onto higher capacity wavelengths is defined as *traffic grooming* [12, 13, 14]. The resulting networks are referred to as WDM grooming networks.

In the two-layer IP over WDM networks, SONET ADMs are eliminated and the function of multiplexing traffic onto wavelengths will be passed onto the IP/MPLS routers as well as optical crossconnects. Consequently, traffic grooming can be performed in both layers, namely, IP traffic grooming and WDM wavelength grooming. IP traffic grooming, that is, the traffic aggregation performed at IP routers, would help to alleviate the complexity of performing sub-wavelength level grooming in WDM layer. In this dissertation, we address several fundamental issues related to the design and operation of traffic grooming in IP over WDM networks. Specifically, we answer the following important questions:

- What is the role and classification of traffic grooming in IP over WDM optical networks? How should IP traffic be processed before it is sent to optical layer? How to groom the IP traffic such that the number of transmitters and receivers required in optical layer is minimized?
- In WDM grooming networks, due to the high bandwidth involved, any link failure that results into fiber being unusable will have catastrophic results. How should we provide protection and restoration for WDM grooming networks? How can we efficiently groom multiple working and protection paths in the network?

In Chapter 4 we study the IP traffic grooming problem in IP over WDM framework. We use the concept of virtual topology to solve the IP traffic grooming problem with objective to minimize the network cost in terms of number of transmitters and receivers. To minimize transmitters and receivers inevitably introduces overhead IP traffic in the networks and impacts networks performance such as wavelength utilization, throughput and average delay. This is a tradeoff we have to make.

This transmitter/receiver minimization problem is formulated as an ILP (Integer Linear Programming) optimization problem. A lower bound of this minimization problem is derived from the traffic matrix. The complexity of the ILP formulation can be reduced by adding hop-length limit constraints. It may still yield a good solution with carefully selected maximum hop-length. This model provides a general formulation and various constraints, such as maximum

node degree, can be easily integrated into it.

The ILP formulation produces the optimal solution for static traffic demands, however, applying this technique to dynamic traffic in large networks is not very practical due to its large computation time. To solve the IP traffic grooming problem with static estimated traffic in big networks, we develop the *traffic aggregation algorithm* as a heuristic approach. Both ILP and heuristic approaches give a virtual topology design for a given estimated traffic. In the virtual topology, each link corresponds to a lightpath in the optical layer. We further develop three different routing and wavelength assignment strategies based on the designed virtual topology, where the actual traffic seen by the IP layer varies from the estimated traffic. The performance of the proposed routing and wavelength assignment schemes is evaluated and compared in terms of blocking probability.

1.4.3 Traffic Grooming in Light Trail Architecture

In order to transport IP traffic effectively over optical networks, several different switching techniques in optical layer have been proposed in literature.

1.4.3.1 Optical Packet Switching

Optical packet switching (OPS) [6, 7, 8] is one alternative technology to circuit switching in backbone networks. The major advantages of OPS is the flexible and efficient bandwidth usage, which enables the support of diverse services. Pure OPS technology in which packet header recognition and control are performed in all-optical domain is still many years away from becoming reality. OPS with electronic header processing and control is more realistic for medium-term network scenarios. A practical OPS experiment has been performed under the European ACT KEOPS (KEys to Optical Packet Switching) project[15]. In KEOPS, the header is sent with data (payload), but at a lower bit rate, and the header processing is still in electrical domain. This potentially requires an optical buffering at the input port to allow the header processing circuits to finish its job.

However, there are still several critical technological challenges need to be overcome before

a practical OPS network becomes a reality.

Firstly, the lack of an efficient way to store information in optical domain is the major difficulty in the implementation of OPS nodes. At present, the buffering technology is not mature and has to overcome a number of technological constraints, such as large and varying size of optical buffers.

Secondly, in highly dynamic traffic environment as OPS, wavelength converters are required and play an important role in contention resolution. Wavelength converters can be integrated to the design of optical buffer and switch architecture in OPS networks. An all-optical wavelength converter is desirable for OPS. However, the fabrication techniques for such wavelength converters are still not practical.

The third issue is the high speed header processing in OPS. Currently, the processing of the header is performed in electrical domain. All-optical header processing has received considerable attention [16, 17], but the technology is still in its early stage.

A key enabling technology in OPS is the optical switch fabrics. To deal with packet-by-packet requests, an OPS node requires the switch fabric that is capable of rapid reconfiguration. For instance, when the data rate is at 40 Gbps and beyond, the switching times have to be on the order of a few nanoseconds.

Finally, the other critical requirements include the reliability and scalability of the technology to high port counts, low loss and crosstalk, efficient energy usage and so on. Unfortunately, none of today's available fabric technologies is eligible to build such a reliable and cost-effective high-performance optical packet switches.

1.4.3.2 Optical Burst Switching

The concept of burst switching has been proposed for conventional telephone networks in early 1980's [18]. Fast circuit switching has been originally developed to support statistical multiplexing of voice circuits, but it was also suitable for data communication at moderate rates. Starting from the middle 1980's, fast packet and cell switching took the place of the circuit switching. At that time, fast circuit switching was implemented using time-division

multiplexing in electrical domain to provide distinct channels (time slots). This is essentially similar to the ATM technology. The concept of burst switching has been extended for ATM networks. The International Telecommunication Union - Telecommunication Standardization Sector (ITU-T) standard for burst switching in ATM networks is known as *ATM block transfer* (ABT) [19]. Burst switching for optical networks, namely, optical burst switching, was proposed in late 1990's [20, 21].

Optical burst switching (OBS) maybe a viable alternative switching technology to transport IP traffic directly over WDM networks. In wavelength switched network, once a lightpath is established, it remains in place for a relatively long time, perhaps months or even years. In OBS, the goal is to set up a wavelength channel for each single burst to be transmitted. At the ingress node of an OBS network, various types of data are assembled as data *burst*, which, for example, can carry one or more IP packets. In OBS, a burst is dynamically assigned to a wavelength channel upon its arrival and is later disassembled at the egress node. To establish a connection for an incoming burst, the ingress nodes sends an associated control packet (request or set-up) over a dedicated wavelength channel or a non-optical channel before the burst is transmitted. The data burst is switched all-optically using the OBS fabric.

Two primary techniques to transmit data are *tell-and-wait*(TAW) and *tell-and-go*(TAG). In *tell-and-wait* scheme [22], a burst is buffered while the control packet is being sent to set up switches and reserve bandwidth for establishing a connection. In *tell-and-go* scheme [22, 23] a burst is sent immediately after its control packet without receiving a confirmation. If a switch along the path cannot carry the burst due to congestion, the burst is dropped. In this scheme, it may still be necessary to buffer the burst in the optical burst switch until its control packet has been processed [19]. Other schemes, known as *just-enough-time* (JET) [21] and *just-in-time* (JIT) [24], have also been proposed in literature. An OBS architecture is described in [25]. An amount of research papers on OBS technology and its applications have been published by researcher around the world. Among them, a vast majority are based on JET. In the JET scheme, there is a delay between transmission of the control packet and transmission of the optical burst. This delay can be set to be long enough, for example, larger than the total

processing time of the control packet along the path. Therefore, when a burst arrives at an intermediate node, the control packet has been processed and a channel on the output port has been reserved. Thus, there is no need to buffer the burst at the intermediate nodes. This is a very important feature of the JET scheme, since optical buffers are still difficult to implement. Improvements and variations of JET have also been studied extensively in literature.

Given burst switching's limited success in the 1980's, one may question why burst switching should be a promising approach to the high speed data communications now. As aforementioned, burst switching is essentially very similar to ATM, however, the flexibility of ATM outperformed burst switching in electrical domain. Some researchers believe that since optical fibers have provided virtually unlimited bandwidth resource, it makes sense to carry control information in a dedicated parallel channel so as to keep the data path simple. Besides, it is best to avoid queueing as much as possible, because both electrical and optical buffers are expensive at gigabit data rates. For this reason, many believe that OBS achieves good statistical multiplexing performance by transmitting many independent data channels in parallel.

1.4.3.3 Challenges to OBS

Just like OPS, OBS has to overcome several critical technological challenges before it really becomes practical. One important issue is the synchronization at terminal nodes [25]. Consider an OBS network using passive optical components with no re-timing of the data. A terminal that receives this burst must synchronize the received data at the bit level and the burst level. To use re-timing elements throughout the OBS network could be an alternate solution, however this puts too many complicated requirements on transmission components. And eventually, this complexity makes the implementation of OBS even more difficult.

In OBS, guard bands are used in each burst to accommodate possible timing jitters along the path from source to destination in OBS. Due to the relatively low speed of optical switching elements, a significant guard time has to be provided between control and data segments, which results in another significant overhead for OBS. Therefore, taking into account the large ratio between switching delay and IP burst duration, the network might be severely underutilized.

It is also worth mentioning that JET does not completely remove optical buffers from OBS networks. Notice that optical buffers are still required at the ingress nodes to generate the initial delay between a data burst and its control packet. The need of high speed optical buffers remains as a notably intractable problem for OBS. Additionally, since the number of control channels are limited in optical networks, the control channels can become bottleneck for the performance of the OBS networks. Currently, commercial OBS networks do not exist. It is yet not clear whether OBS will become an alternative technique for the core optical network or it is just an intermediate step towards all-optical packet switching.

1.4.3.4 Light Trail Architecture

The *Light trail* [26] has been proposed as a novel architecture designed for carrying finer granularity IP traffic. A light trail is a unidirectional *optical trail* between the start node and the end node. It is similar to a lightpath with one important difference that the intermediate nodes can also access this unidirectional trail. A lightpath is an end-to-end system in which no further wavelength multiplexing between the multiple intermediate nodes along the lightpath is allowed. While in light trails, the wavelength is shared in time and the medium access is arbitrated by control protocol among the nodes that try to transmit data simultaneously, that is, upstream nodes have higher priorities than lower stream nodes.

Light trail architecture brings up various issues in designing optical networks for transporting IP centric traffic: *How to identify a set of light trails at the design phase for the given traffic? What are the new constraints introduced by light trail architecture? How hard is this problem? How good can we achieve in terms of wavelength utilization and how?*

In Chapter 5 we propose an exact ILP formulation for obtaining optimal light trail design with minimum cost (in terms of number of light trails as well as the number of wavelengths). A simplified formulation is also given as well as possible LP-relaxations. Two algorithms, namely *local best-fit increasing packing* and *local best-fit decreasing packing* are developed for solving the light trail design problem. Even though the heuristic algorithms do not guarantee global optimality, their capability of obtaining fast solutions with local optimality is still preferred

especially when the problem is unmanagcable to ILP approaches.

1.4.4 Survivable Grooming Network Design

Protection and restoration have always been an important issue in the design and operation of WDM optical networks. Due to the huge amount of traffic carried in the WDM network, any single failure can be catastrophic. However, the research on emerging survivability issues in WDM grooming network is still a relatively new territory.

In Chapter 6 we address two important issues in WDM network design, survivability and traffic grooming. The aim is to enable subwavelength level traffic grooming in survivable WDM network design. In order to provide 100% protection under single link failure, two link-disjoint alternate paths for each connection are pre-computed. The path selection and wavelength assignment schemes are formulated as ILP optimization problems. Two exact formulations are given for employing backup multiplexing and dedicated backup with Minimum-Link-Primary-Sharing(MLPS) respectively. Illustrative examples are given to show the improvement of wavelength utilization of the two schemes and the difference path selections.

Backup multiplexing has been extensively studied in mesh-restoration WDM networks. It saves the amount of the reserved restoration capacity by allowing different backup paths to share the same wavelength on their common links if their corresponding primary paths are link disjoint. Backup multiplexing is still applicable in WDM grooming network, however, it becomes much more expensive in computation than it is in networks without traffic grooming. As the wavelength utilization improved by the network grooming capability, it becomes affordable to use dedicated backup reservation to provide 100 % restoration for the single link failure. Furthermore, by minimizing the total link-primary-sharing (MLPS), the number of affected working paths due to single link failure is reduced, thereby the recovering signalling is simplified. It would be ideal to employ both backup multiplexing and MLPS schemes, however this would be too costly in computation and hence infeasible for practical usage.

Our design approach for survivable grooming network that provides 100 % protection again single link failures can be easily extended to grooming networks providing partial protection.

In partial protection network, due to the constraints on available network resource, the reserved backup capacity is less than or equal to the capacity of its primary path. The ratio of the minimum backup capacity to its primary capacity is called the *protection ratio*, denoted by P_{ratio} . In general, for any request, $P_{ratio} = 0$ implies no protection, $P_{ratio} = 1$ indicates full protection, and when $0 < P_{ratio} < 1$, a request is partially protected. We decompose the partial protection problem into two subproblems, namely *resource minimization* and *protection maximization*. The first step is to use the minimum resource to meet the partial protection requirement. In the second step, the residual network resource is optimally distributed to provide better protection to some if not all of the requests. We develop ILP formulations for solving the partial protection design with given static traffic. We also designed the *shortest-available-least-congested* routing algorithm for solving this problem with dynamic unknown traffic. Results obtained from solving ILP formulations and performing simulations are presented. The study shows that to provide partial protection is an effective compromise for grooming networks with restrained resource and hence a useful feature of WDM grooming networks.

CHAPTER 2. Network Models and Notations

Wavelength Division Multiplexing (WDM) has emerged as the promising technology to meet the ever-increasing demand for bandwidth. WDM divides the available fiber bandwidth into WDM channels, called *wavelengths*, each operating at peak electronic rate. Connections between users are supported by establishing an all-optical channel between the end nodes. The all-optical connections are referred to as *lightpaths* [27]. Signals on lightpaths can be at different rates and may use different formats as the signals are never terminated inside the core network. This bit-rate and protocol transparency is a key feature that is very desirable in the backbone network.

A wavelength converter is a device that allows the optical signal on a wavelength to be converted into another wavelength. In the absence of wavelength converters, a lightpath should occupy the same wavelength on all the links it traverses. This property is known as the *wavelength-continuity constraint*. Hence a connection request encounters higher blocking probability in a network without wavelength conversion than it does in a network that employs full-wavelength conversion at all nodes.

The role of wavelength converters in wavelength-routed networks has been studied extensively in the literature [28, 29, 30, 31, 32, 33]. The role of sparse-wavelength conversion, where only a few nodes in the network have full-wavelength conversion capability, has been analyzed in [33]. The effect of limited-wavelength conversion, where a given input wavelength can be converted into a set of (but not all) output wavelengths, has been studied in [34] and [35]. Multi-fiber multi-wavelength wavelength-routed networks have been shown to offer blocking performance similar to that of networks that employ limited- or sparse-wavelength conversion [36, 37, 38]. A generalized framework for analyzing optical networks that employ both

wavelength and time division multiplexing has been recently proposed in [14] from which most of the models discussed above can be derived. Although wavelength converters improve network blocking performance, the high cost of wavelength converters have made it impractical to employ full-wavelength converters at all nodes.

2.1 Grooming WDM Network Models

The act of multiplexing, demultiplexing, and switching lower rate traffic streams onto higher capacity wavelengths is defined as traffic grooming. The resulting WDM optical networks are referred to as WDM grooming networks.

2.1.1 WDM Grooming Networks

WDM grooming networks can be classified into two categories [38]: dedicated-wavelength grooming (DWG) networks and shared-wavelength grooming (SWG) networks. In DWG networks source destination pairs (s-d pairs) are connected by *lightpaths* and connections between the s-d pair are multiplexed onto the lightpath. A new lightpath to the destination is established when the requested bandwidth is not available on any of the existing lightpaths to the destination. On the other hand, in SWG networks, if a request cannot be accommodated on an existing lightpath to its destination, it is multiplexed onto an existing lightpath to an intermediate node. This connection is then switched at the intermediate node towards the final destination either directly or through other intermediate nodes. If we define each lightpath as one *hop*, then, a request between an s-d pair takes a single hop to reach its destination in DWG networks, while it may take multiple hops in SWG networks. The performance of WDM grooming networks depends on the efficient aggregation of requests into full or almost-full wavelength requirements.

2.1.2 Grooming Nodes in WDM Networks

The grooming nodes in WDM networks can be classified into various categories depending on the level of grooming capability it provides. If a node can multiplex and demultiplex low-

rate traffic only on *dropped* wavelengths at an add-drop multiplexer (ADM), it is referred to as a *ADM-constrained grooming node*. If a node can switch connections across different lightpaths, but cannot switch between different wavelengths, it is termed as a *wavelength continuity constrained grooming node*. If a node can switch connections in any permutation from one wavelength to another, it is then termed as a *full grooming node* [39].

2.2 Restoration Models

Network survivability can be achieved by using link-, path- or segment based protection mechanism [40, 41]. Link-based method reroute disrupted traffic around the failed link, while path-based rerouting replaces the whole path between the source and destination of a demand. Segment-based method reroutes the affected path-segments when failure occurs. We employ path-based protection for each request in this dissertation.

Capacity sharing among the primary and restoration paths can be dedicated or shared. The dedicated technique uses 1 : 1 protection, where each primary path has a corresponding restoration path. In the shared case, several primary paths can have the same backup paths share the same wavelength w on link l as long as the primaries are node and/or link disjoint. This scheme is called the backup multiplexing technique [42]. It is still 1 : 1 protection as long as only one link fails. However, the path is assigned upon the actual failure. This improves wavelength utilization, while providing guaranteed protection under the single fault assumption. This is due to the fact that no single failure will cause two primary paths to contend for the same backup capacity. We have the following constraints in our restoration models.

- Number of connections (lightpaths) on each link is bounded
- Levels of protection
 - **Full protection:** (i) Every demand is assigned a primary and a backup path (ii) The primary and backup paths are allocated the same capacity

- **Partial protection:** (i) Every demand is assigned a primary path and a backup path
 (ii) The reserved capacity for backup path is smaller than or equal to that of the corresponding primary path
- **No protection:** Every demand is assigned only primary path
- **Best-effort protection:** (i) Every demand is assigned a primary path. A backup path is assigned if resources are available (ii) Accept as many demands as possible with or without backup
- No backups are admitted without a primary path.
- Primary and backup paths for a given demand should be node disjoint.

We use full protection model by default if it is not mentioned.

2.3 Notations

The physical topology of a WDM network is represented as a weighted directed graph $G_p = (V, E)$ with V be the set of network nodes and E the set of physical links (edges). $|V| = N$ and $|E| = L$. Nodes correspond to network nodes and links correspond to the fibers between nodes.

Since we will be using ILP based optimization approach to solve many problems, the following notations will be used in problem formulations.

- W : Maximum number of wavelengths in each direction in a bidirectional fiber (technology dependent data)
- C : Maximum capacity of each wavelength. (We assuming each wavelength has the same capacity.)
- $m, n, s, t = 1, 2, \dots, N$: Number assigned to each node in the network.
- $l = 1, 2, \dots, L$: Number assigned to each link in the network.
- $w = 1, 2, \dots, W$: Number assigned to each wavelength.

- $i, j = 1, 2, \dots, N \times (N - 1)$: Number assigned to each demand (s-d pair).
- $K = 2$: Number of alternate routes between every s-d pair.
- $p, r = 1, 2, \dots, KW$: Number assigned to a path for each s-d pair. A path has an associated wavelength (lightpath). Each route between every s-d pair has W wavelength continuous paths. The first $1 \leq p, r \leq W$ paths belong to route 1 and $W + 1 \leq p, r \leq 2W$ paths belong to route 2.
- $\bar{p}, \bar{r} = 1, 2, \dots, KW$: If $1 \leq p, r \leq W$ (route 1), then $W + 1 \leq \bar{p}, \bar{r} \leq 2W$ (route 2) and vice versa.
- $D_{N \times N} = \{d_i\}$: Traffic matrix. d_i indicates the required capacity of low-speed traffic requests in units of OC-1.
- $H_{N \times N} = \{h_{st}\}$: Distance matrix. h_{st} indicates the physical distance from node s to t .

CHAPTER 3. Wavelength Usage Constraint

3.1 Introduction

Wavelength routing remains to be an important problem in IP over WDM framework due to the fact that the data traffic keeps increasing, more and more lightpaths need to be setup in order to satisfy the traffic requirement. Hence, the network resource needs to be utilized efficiently so as to minimize the call blocking probability.

In WDM optical networks, the available fiber bandwidth can be divided into a large number of wavelengths while maintaining the operating speed of each wavelength to be around the peak electronic speeds. However, due to power constraints not all the wavelengths may be used at any given instant in time. This restriction is referred to as the *wavelength usage constraint*. Such a scenario could arise due to the restriction on the power carried in the fiber or the power limit on the optical components on the path such as amplifiers, re-generators, etc. Two alternatives can be employed to solve this wavelength usage constraint problem: (1) Employing wavelength converters with the number of wavelengths carried in the fiber being the same as the maximum number of usable wavelengths; or (2) Employing more wavelengths in a fiber but restricting the number of usable wavelengths to a certain maximum without employing wavelength converters.

3.1.1 Two Solutions: An Example

We illustrate the wavelength usage constraint and motivate the two solutions to the wavelength usage constraint problem through a simple example. Consider a two-link path of a network as shown in Figure 3.1(a). The nodes are assumed to be connected by a single-fiber link. Each fiber is assumed to carry signals in at-most two wavelengths at any given time due

to power considerations. Assume that two calls have been established in the path; the first call originating from Node 1 and destined for Node 2 is established on wavelength W_1 and second call originating from Node 2 and destined for Node 3 is established on wavelength W_2 .

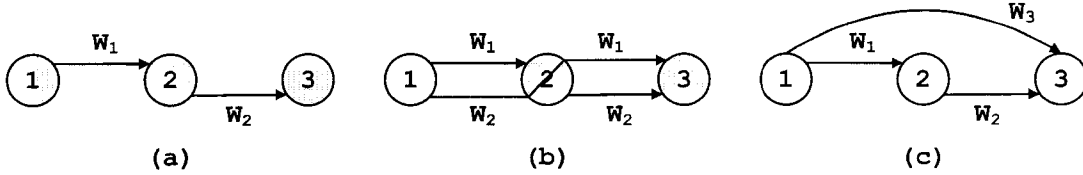


Figure 3.1 A two-link network. (a) 2 wavelengths per fiber with no wavelength conversion. (b) 2 wavelengths per fiber with wavelength conversion. (c) 3 wavelengths per fiber with at-most 2 usable at any given time and no wavelength conversion.

Consider a third call that originates from Node 1 destined for Node 3. If the fibers were to carry only two wavelengths and wavelength conversion is not employed, then the third call would be blocked. The third call would be accepted if wavelength conversion is employed at Node 2. A connection can be established from Node 1 to Node 3 by assigning wavelength W_1 on the first link and wavelength W_2 on the second, making use of the wavelength conversion capability at Node 2 as shown in Figure 3.1(b). An alternative to employing wavelength conversion is to increase the number of wavelengths available in a fiber. For example, if the fibers were to carry 3 wavelengths of which only two can be used at any given time, then the third call could be accommodated on wavelength W_3 without employing wavelength conversion as shown in Figure 3.1(c).

In this chapter, we form an analytical model for evaluating the blocking performance of wavelength-routed optical network with wavelength usage constraint. The analytical model is used to evaluate the above two alternatives. The remainder of the chapter is organized as follows: Section 3.2 provides the network model and assumptions that are used in developing the analytical model. The analytical model for computing the blocking performance of networks with wavelength usage constraint is developed in Section 3.3. Section 3.4 compares the analytical and simulation results and discusses the performance of the two alternatives on ring

and mesh-torus networks. Section 3.5 concludes the chapter.

3.2 Network Model and Assumptions

Let us consider an N nodes wavelength-routed optical network, where the nodes are connected by single fiber links. Each fiber is assumed to carry a total of W wavelengths of which at-most U wavelengths can be used at any given time ($W \geq U$).

The analytical model developed in this chapter is based on the following assumptions:

- Call requests arrive at each node according to a Poisson process with rate λ_n . Each call is equally likely to be destined to any of the remaining nodes.
- The holding time of calls are exponentially distributed with mean $1/\mu$. The load offered by a node is $\rho = \lambda_n/\mu$ Erlangs.
- The bandwidth requirement of calls are assumed to be of one wavelength capacity.
- No broadcast or multicast traffic is considered.
- The routing of calls follows fixed-path routing strategy. e.g., shortest-path routing. Although dynamic routing algorithms provide slightly better performance, it is much harder to study them analytically.
- The wavelength assigned for a connection is assumed to be chosen at random from the set of available wavelengths.
- The load on a link of a path is assumed to be correlated only to the load in the previous link of the path, referred to as the *Markovian Correlation*.
- Blocked calls are discarded and are not re-attempted.

3.3 Analysis

In this section, we develop an analytical model that has modest computation requirements. We use the previously proposed Trunk Switched Network models of [14] as a base model, and

extend it by restricting the number of usable wavelengths in a fiber.

The network blocking probability is computed as the average blocking probability experienced over different path lengths. Consider a z -link path model as shown in Figure 3.2.

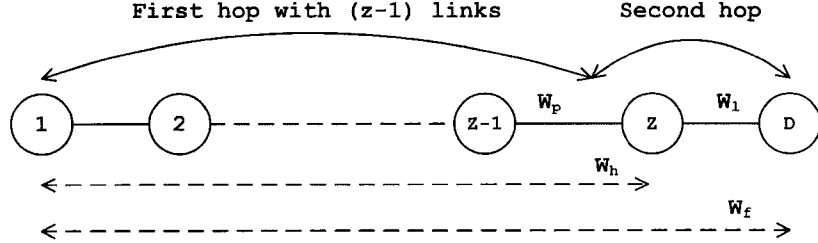


Figure 3.2 A z -link path model

Let $P_z(W_f)$ denote the probability of W_f wavelength continuous paths available on the z -link path. The network blocking probability, denoted by P_b , is given by:

$$P_b = \sum_{z=1}^{N-1} P_z(W_f = 0)p_z \quad (3.1)$$

where p_z is the probability of selecting a z -link path. The probability of choosing a path of a certain hop length can be computed based on the network topology and routing algorithm employed. $P_z(W_f = 0)$ denotes the blocking probability over the z -link path.

Let W_l denote the number of wavelengths free on the last link of the path. Let $P_z(W_f, W_l)$ denote the probability of W_f wavelengths being available on a z -link path with W_l wavelengths free on the last link. $P_z(W_f)$ is then written as:

$$P_z(W_f) = \sum_{W_l=W_f}^W P_z(W_f, W_l) \quad (3.2)$$

The z -link path is analyzed as a two-hop path by viewing the first $z - 1$ links as the first hop and the last two links as the second hop, as shown in Figure 3.2. It is to be noted that the destination node is not considered as the last node of the path. Let W_h and W_p denote the number of wavelengths available on the first hop and the number of free wavelengths on the last link of the first hop (link $z - 1$). $P_z(W_f, W_l)$ is recursively computed as:

$$P_z(W_f, W_l) = \sum_{W_h=W_f}^W \sum_{W_p=0}^W P_{z-1}(W_h, W_p) P(W_f, W_l | W_h, W_p) \quad (3.3)$$

The starting point of this recursion, for $z = 1$, is defined as:

$$P_1(W_f, W_l) = \begin{cases} P(W - U) & \text{if } W_f = 0 \\ P(W_l) & \text{if } W_f = W_l \text{ and } W_l > W - U \\ 0 & \text{otherwise} \end{cases} \quad (3.4)$$

where $P(W_l)$ denotes the probability of W_l free wavelengths on a link. $P(W_l)$ is computed using a two-link path model and is described in Section 3.3.1.

It is to be noted that when W_f ($W_f > 1$) wavelengths are said to be available on a z -link path, it is assumed that there is a choice of W_f wavelengths on which a call can be established. However, this does not guarantee that W_f calls can be accommodated on the z -link path as the wavelength usage constraint could be violated at some or all links on the path.

$P(W_f, W_l | W_h, W_p)$ is computed by conditioning on the number wavelengths free on the last link as:

$$P(W_f, W_l | W_h, W_p) = \begin{cases} P(W_f | W_h, W_p, W_l)P(W_l | W_h, W_p) & \text{if } W_h \geq W_f \\ 0 & \text{otherwise} \end{cases} \quad (3.5)$$

where $P(W_l | W_h, W_p)$ is the probability of W_l wavelengths being free on the last link given W_h wavelengths are available on the first hop and W_p wavelengths free on the last link of the first hop. With the assumption of Markovian correlation of link loads, W_l is independent of W_h . Hence, $P(W_l | W_h, W_p)$ is reduced to $P(W_l | W_p)$. The computation of $P(W_l | W_p)$ is based on a two-link model and is discussed in Section 3.3.1. Equation 3.5 is rewritten as:

$$P(W_f, W_l | W_h, W_p) = \begin{cases} P(W_f | W_h, W_p, W_l)P(W_l | W_p) & \text{if } W_h \geq W_f \\ 0 & \text{otherwise} \end{cases} \quad (3.6)$$

$P(W_f | W_h, W_p, W_l)$ denotes the probability of having W_f wavelengths available on a two-link path given that W_h wavelengths are free on the first hop with W_p wavelengths free on the last link of the first hop and W_l wavelengths free on the last link. This probability value is computed by considering two cases: (1) No wavelength conversion and (2) Full-wavelength conversion.

In case 1, there is no wavelength conversion in the network. Thus the *wavelength continuity constraint* is imposed on the connections. Let U_c denote the number of wavelengths that are used by connections that occupy both the links. $P(W_f|W_h, W_p, W_l)$ is then obtained as:

$$P(W_f|W_h, W_p, W_l) = \begin{cases} 1 & \text{if } W_f = 0 \text{ and } (W_p \leq W - U \text{ or } W_l \leq W - U) \\ \sum_{U_c=0}^{\min(W-W_p, W-W_l)} \frac{\binom{W_h}{W_f} \binom{W-W_h-U_c}{W_l-W_f}}{\binom{W-U_c}{W_l}} P(U_c|W_p, W_l) & \text{if } W_f > 0, W_p > W - U, W_l > W - U, \\ & \text{and } W_f \leq \min(W_h, W_l) \\ 0 & \text{otherwise} \end{cases} \quad (3.7)$$

In case 2, the number of wavelengths available on the path is the minimum number of free wavelengths of each link on the path, provided the total number of used wavelengths in the links are below the maximum value. Thus, a call is blocked only if either or both of the links have U wavelengths occupied. In this case $P(W_f|W_h, W_p, W_l)$ is computed as:

$$P(W_f|W_h, W_p, W_l) = \begin{cases} 1 & \text{if } W_f = 0, \text{ and } (W_p \leq W - U \text{ or } W_l \leq W - U) \\ 1 & \text{if } W_f > 0, W_p > W - U, W_l > W - U, \\ & \text{and } W_f = \min(W_h, W_l) \\ 0 & \text{otherwise} \end{cases} \quad (3.8)$$

The values of $P(U_c|W_p, W_l)$, $P(W_l|W_p)$, and $P(W_l)$ are obtained using a two-link path model as described in the following subsection.

3.3.1 Free Wavelength Distribution

Consider a two-link path model as shown in Figure 3.3. Let u_p , u_l , and u_c denote the number of wavelengths busy on the first link, the number of wavelengths busy on the second link, and the number of wavelengths occupied by calls that continue from the first link to the

second, respectively. Note that $u_c \leq \min(u_p, u_l)$ and $\max(u_p, u_l) \leq U$. Recall that at-most U wavelengths out of the total W wavelengths carried by a fiber can be used at any given time.

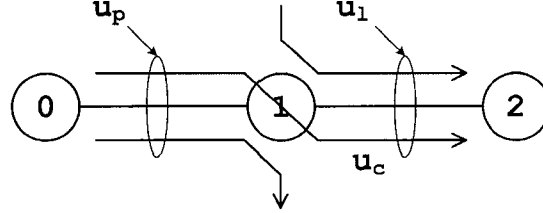


Figure 3.3 Wavelength occupancy on a 2-hop path.

Let λ_p denote the arrival rate for calls to the first link, λ_l denote the arrival rate for calls to the second link, and λ_c [$\lambda_c \leq \min(\lambda_p, \lambda_l)$] denote the arrival rate of calls to the first link that continue to the second link. If the link loads are assumed to be uniformly distributed, it follows that $\lambda_p = \lambda_l = \lambda$. The Erlang loads corresponding to the calls that occupy the first link, second link, and that which continue from the first to the second can be written as, $\rho_p = \frac{\lambda_p}{\mu}$, $\rho_l = \frac{\lambda_l}{\mu}$, and $\rho_c = \frac{\lambda_c}{\mu}$, respectively.

The wavelength distribution on a two-link path can be characterized as a 3-dimensional Markov chain. The state-space is denoted by the 3-tuple (u_p, u_l, u_c) . The steady-state probability for the states can be computed as [43]:

$$\Pi(u_p, u_l, u_c) = \frac{(\rho_p - \rho_c)^{u_p - u_c} (\rho_c)^{u_c} (\rho_l - \rho_c)^{u_l - u_c}}{\sum_{j=0}^U \sum_{i=j}^U \sum_{k=j}^U \frac{(\rho_p - \rho_c)^{i-j}}{(i-j)!} \frac{(\rho_c)^j}{(j)!} \frac{(\rho_l - \rho_c)^{k-j}}{(k-j)!}} \quad (3.9)$$

where $0 \leq u_p \leq U$, $0 \leq u_l \leq U$, $0 \leq u_c \leq \min(u_p, u_l)$.

The following probabilities that are required to complete the analytical model are derived from the above steady-state probability.

$$P(W_l|W_p) = \begin{cases} \frac{\sum_{x_c=0}^{\min(W-W_l, W-W_p)} \Pi(W-W_p, W-W_l, x_c)}{\sum_{x_l=0}^U \sum_{x_c=0}^{\min(W-W_p, x_l)} \Pi(W-W_p, x_l, x_c)} & \text{for } W-U \leq W_l, W_p \leq W \\ 0 & \text{otherwise} \end{cases} \quad (3.10)$$

$$P(U_c|W_p, W_l) = \begin{cases} \frac{\Pi(W-W_p, W-W_l, U_c)}{\sum_{x_c=0}^{\min(W-W_p, W-W_l)} \Pi(W-W_p, W-W_l, x_c)} & \text{if } U_c \leq \min(W - W_p, W - W_l) \\ & \text{and } W - U \leq W_l, W_p \leq W \\ 0 & \text{otherwise} \end{cases} \quad (3.11)$$

$$P(W_l) = \begin{cases} \sum_{x_p=0}^U \sum_{x_c=0}^{\min(x_p, W-W_l)} \Pi(x_p, W - W_l, x_c) & \text{for } W - U \leq W_l \leq W \\ 0 & \text{otherwise} \end{cases} \quad (3.12)$$

3.3.2 Estimation of Call Arrival Rates on a Link

In the analytical model developed in Section 3.3, the network traffic is assumed to be known in term of *link load*. Typically the traffic in the network is specified in terms of set of offered loads between the source and destination node pairs. The call arrival rate has to be estimated from the arrival rates of calls to nodes [33].

Consider a network with N nodes and L links, the average path length of a connection in the network is given by:

$$Z_{av} = \sum_{z=1}^{N-1} z p_z \quad (3.13)$$

where p_z is the path-length distribution. Let λ_n denote the call arrival rate at a node. Let λ denote the average link arrival rate and is computed as:

$$\lambda = \frac{N\lambda_n Z_{av}}{L} \quad (3.14)$$

The fraction of traffic that is not destined for a node is obtained as the ratio of the number of links a path that are not the last hop to the total number of links in the path. For a path with z links, there are $(z - 1)$ intermediate links. Hence, the fraction of traffic on a link that would continue on any neighboring links at a node is written as:

$$\delta_c = \frac{\sum_{z=1}^{N-1} (z-1)p_z}{\sum_{z=1}^{N-1} zp_z} \quad (3.15)$$

$$= 1 - \frac{1}{Z_{av}} \quad (3.16)$$

It is to be noted that the above expression gives the fraction of the traffic that is not destined for a node. Such traffic could continue on any of the output links at the node. The link load correlation is defined as the probability that a call on a link would continue to a successive link on a chosen path and is given by:

$$\gamma_c = \left(1 - \frac{1}{Z_{av}}\right) \frac{1}{E} \quad (3.17)$$

where E denotes the number of links at a node that do not connect the node to any of the previous nodes in the path, referred to as *exit links*. Hence, the arrival rate of traffic on a link that would continue to a successive link on a path is given by $\lambda_c = \gamma_c \lambda$.

3.4 Results and Discussion

In this section, we assess the accuracy of the analytical model by comparing it with the simulation results. Two kinds of network topologies are considered for performance evaluation:

1. a 25-node bidirectional ring network
2. a 5×5 bidirectional mesh-torus network

The networks are assumed to employ shortest-path routing. If more than one shortest path is available, one of them is chosen at random. The path length distribution, p_z , and the number of exit nodes, E , for the two networks are given below:

1. Bidirectional Ring network with N nodes (if N is odd):

$$p_z = \frac{2}{N-1} \quad 1 \leq z \leq \frac{N-1}{2} \quad (3.18)$$

$$E = 1 \quad (3.19)$$

2. $M \times M$ bidirectional mesh-torus network (if M is odd):

$$p_z = \begin{cases} \frac{4z}{M^2-1} & 1 \leq z \leq \frac{M-1}{2} \\ \frac{4(M-z)}{M^2-1} & \frac{M-1}{2} < z \leq M-1 \end{cases} \quad (3.20)$$

$$E = 3 \quad (3.21)$$

The link load correlation factors for the 25-node bi-directional ring network and 5×5 bi-directional mesh-torus network are 0.846 and 0.2, respectively. The selection of these two networks for evaluating the accuracy of the proposed analytical model is due to the high and the low values for link correlation factors. Evaluating the analytical model at these extreme values of link correlation factors validates the model for a wide range of networks.

For each network, the number of usable wavelengths on each link is fixed as 16 ($U = 16$). The blocking performance is compared by varying the total number of wavelengths in each fiber. Three different values for the total number of wavelengths in a link are considered: $W = 16$; $W = 18$, and $W = 20$. It is assumed that the networks do not employ wavelength conversion for the above parameters. The blocking performance of networks with the above parameters are compared with that of a network employing 16 wavelengths per fiber and full-wavelength conversion at each node.

Figures 3.4 and 3.5 show the blocking performance versus the link load of the two network topologies considered. It is observed that the simulation and the analysis results match closely, thereby validating the analytical model developed in this paper. It is worth mentioning that the analysis and simulation results match better in the mesh-torus in comparison to the results in the ring topology. This is due to the fact that the link load correlation ratio of the mesh-torus is lower than it is of the ring topology with the same number of nodes.

It is also observed that there is a significant improvement in the blocking performance when the total number of wavelengths in a link is just a few more (4 in the examples shown

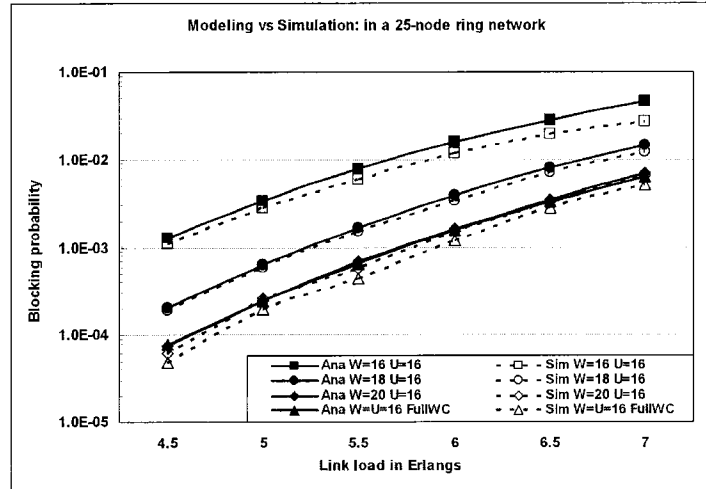


Figure 3.4 Blocking probability versus the link offered load for a bidirectional ring network with 25 nodes.

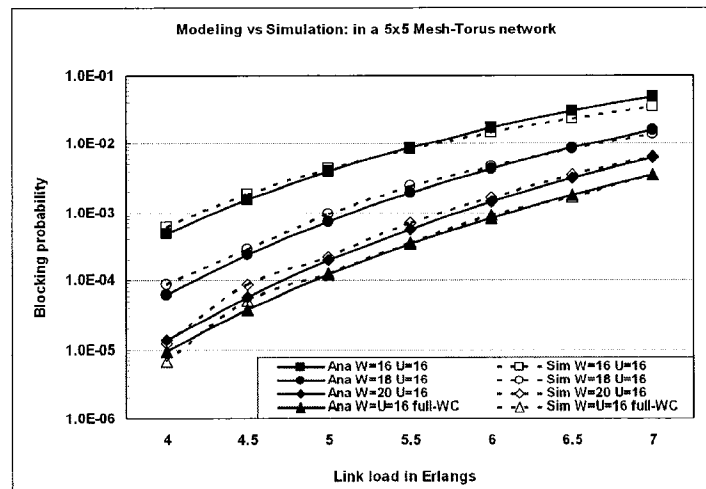


Figure 3.5 Blocking probability versus the link offered load for a bidirectional 5×5 Mesh-Torus network.

above) than the maximum that can be used at any instant of time. Specifically, for the above parameters, it is observed that a network employing 20 wavelengths per fiber with at-most 16 being usable at any given time has a blocking performance close that of a network employing 16 wavelengths per fiber with full-wavelength conversion capability at all nodes.

Figures 3.4 and 3.5 also shows that the blocking performance of networks with higher correlation ratio will benefit more compared to those with lower correlation with the extra wavelengths. From the graphs, it can be seen that the addition of four extra wavelengths results in almost the same blocking performance as the case with full-wavelength conversion in ring networks as compared to mesh-torus. This effect can be significant with the increase in the network size. This effect is also due to the fact that wavelength converters do not result in a drastic reduction in the blocking performance for networks with higher correlation ratio [14, 33]. As most of the existing real-life networks have sparse connectivity, therefore having a high link load correlation, the approach of providing extra wavelengths is attractive compared to employing full-wavelength conversion.

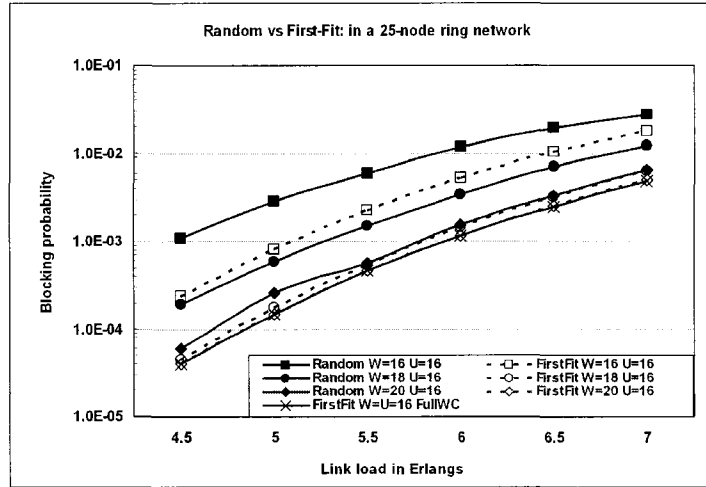


Figure 3.6 Comparison of random and first-fit wavelength assignment schemes for a bi-directional ring network with 25 nodes.

We assume random wavelength assignment for developing the analytical framework. However, the number of extra wavelengths required to achieve a certain performance would be

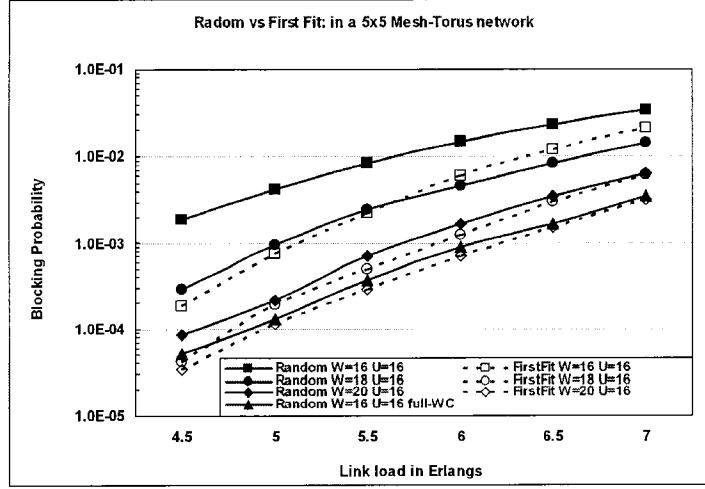


Figure 3.7 Comparison of random and first-fit wavelength assignment schemes for a bidirectional 5×5 mesh-torus network.

reduced if better wavelength assignment schemes are employed. To illustrate this claim, we consider first-fit assignment algorithm and evaluate its performance with the wavelength usage constraint on ring and mesh-torus networks. In this scheme, all wavelengths are numbered. When searching for available wavelengths, a lower numbered available wavelength is chosen to establish the connection. Figs. 3.6 and 3.7 show the performance comparison of random and first-fit wavelength assignment algorithms on ring and mesh-torus networks, respectively.

We observe that first-fit wavelength assignment algorithm performs better in term of blocking probability compared to random wavelength assignment. This is because first-fit wavelength assignment packs all the connections towards the lower end of the wavelength space. Such an arrangement results in more wavelength-continuous channels available from source to destination as compared to random wavelength assignment. Hence, the number of wavelengths required to obtain a certain blocking performance is smaller under first-fit wavelength assignment strategy. This further establishes the viability of employing more wavelengths with wavelength continuity constraint rather than having lesser number of wavelengths with full-wavelength conversion capability.

3.5 Summary

Wavelength routing remains to be an important issue in IP over WDM networks. As data traffic keeps increasing and the network resource becomes insufficient. In addition, the wavelength continuity constraint in the optical layer leads to higher call blocking probability in a network without wavelength conversion than it does in a network that employ full-wavelength conversion at all nodes. At present, the high price of wavelength converters make it impractical to be employed at every node. The problem we solve in this chapter provides a viable solution which avoids involving wavelength converters.

We consider the power budget scenario in optical networks when the total number of usable wavelengths in a fiber is limited to a certain maximum number due to power considerations. The total number of available wavelengths in the fiber can be more then the maximum usable number, referred to as the *wavelength usage constraint*. We developed an analytical model for evaluating the blocking performance of WDM optical networks with wavelength usage constraint employing random wavelength assignment scheme. The analytical model is shown to be accurate by comparing the results with that of the simulation for two different network topologies that have high and low link load correlation. We evaluate the performance of first-fit wavelength assignment strategy and compare its performance with that of random wavelength assignment strategy.

It is observed through our simulations that with an increase of 4 more wavelengths in the fiber while remain the number of usable wavelengths as 16, the blocking performance is similar to that when full-wavelength conversion is employed. Our results also show that the number of extra wavelength required to achieve a certain blocking performance is lesser when first-fit wavelength assignment strategy is employed. Thus employing extra wavelengths in practical networks is an attractive alternative compared to full-wavelength conversion even in the presence of power budget constraints.

CHAPTER 4. IP Traffic Grooming in WDM Networks

4.1 Introduction

The rapid growth of IP traffic demand has led to a paradigm shift in the telecommunications industry from voice-optimized to IP-centric networks. It is widely believed that, in the near future, data communications will be based on optical transportation networks (OTNs).

A challenging problem for carrying IP traffic over WDM optical networks is the huge opto-electronic bandwidth mismatch. The bandwidth on a wavelength is 10 Gbps today and is likely to increase, while the sub-rate traffic connections can vary from STS-1 (51.84 Mbps) to the full wavelength capacity. The bandwidth of a full wavelength is becoming too large for a single request. Therefore, the wavelength capacity might be underutilized for IP centric traffic unless it is filled up by efficiently aggregated traffic.

One approach to provisioning fractional wavelength capacity, as discussed earlier, is to divide a wavelength into multiple sub-channels using time-, frequency-, or code division multiplexing, and then multiplex traffic on the wavelength, i.e., *traffic grooming*. However, optical processing and buffer technologies are still not mature enough to achieve online routing decisions at high-speed. With the development of MPLS (MultiProtocol Label Switching) and GMPLS (Generalized MultiProtocol Label Switching) standards, it is possible to aggregate a set of IP packets for transport over a single lightpath. Therefore, traffic grooming in IP over WDM optical networks is performed at two layers, namely *IP traffic grooming* and *WDM traffic grooming*. IP traffic grooming is the aggregation of smaller granularity IP layer traffic streams. It is performed at MPLS/GMPLS enabled IP routers by using transmitters and receivers. This aggregated traffic streams are then sent to the optical layer where WDM traffic grooming (or wavelength level traffic grooming) is performed by utilizing optical add-drop multiplexors

(OADM). The two-layered grooming reduces the workload at both IP and optical layers.

4.1.1 Related Work

Most of the work in the literature on traffic grooming has been concentrated on providing efficient network designs in SONET/WDM rings for improving the overall network cost [12, 13, 44, 45, 46]. This is appropriate because today's backbone transport infrastructures are organized in rings. As networks are evolving to become more IP-centric, grooming for IP traffic in general networks is becoming an important area.

In the IP environment, the network topology is a general mesh and the traffic is typically neither static nor known in advance. Static and dynamic traffic grooming problems have been studied by various researchers. A novel algorithm for integrated dynamic routing of bandwidth guaranteed paths in MPLS networks is developed in [47]. In this work a node is viewed as W sub-nodes, where W denotes the number of wavelengths. A super-node is created for the node which has wavelength conversion capability. Three different types of nodes, namely routers, OXCs (with or without wavelength conversion capability) are considered. Different logical links are created accordingly so as to create a new network representation. Figure 4.1 gives an example of the network representation for integrated routing computation.

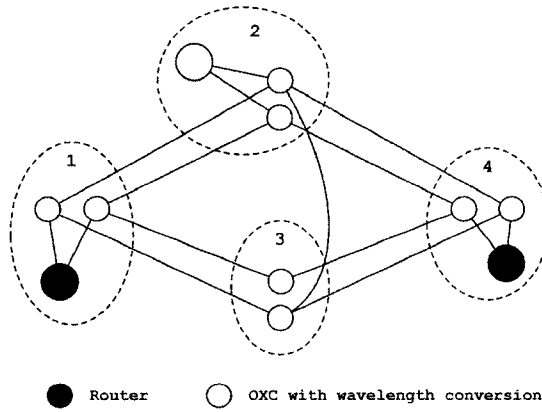


Figure 4.1 Network representation for integrated routing computation.

In this example, each link is assumed to have two wavelengths, λ_1 and λ_2 . Nodes 1 and

4 are routers, Node 2 is an OXC with wavelength conversion and Node 3 is an OXC without wavelength conversion. Consider a request for 0.1 unit from Node 1 to Node 4 in Figure 4.1. If this demand is routed from Node 1 to Node 3 to Node 4 using λ_1 , Node 3 cannot use λ_1 to route traffic along the path 2-3-4. This is due to the fact that Node 3 is OXC and cannot switch between different wavelengths.

Routing in such a network, therefore, is decided by taking into account the combined topology and resource usage information at the IP and optical layers, with constraints on the maximum delay or number of hops. However, the network representation of Figure 4.1 becomes very complex quickly with the increase in the number of wavelength. Therefore, it is hard to apply this algorithm in practical DWDM optical networks.

The study in [48] also proposed another auxiliary graph according to the given networking configuration. In this model a node is viewed as $W + 2$ layers with two nodes at each layer, one acting as the input and the other being the output. Apart from W layers with one for each wavelength, two layers named access layer and lightpath layer are added. This more general graph model is applicable in heterogeneous WDM mesh networks. An integrated traffic grooming algorithm and a integrated grooming procedure that jointly solve traffic grooming subproblems are developed. Several grooming policies are compared and evaluated through simulations. However, this approach may also face the scalability problem as the number of wavelength increases.

4.1.2 IP Traffic Grooming Issues

The main cost in IP traffic grooming is due to cost on the transmitters and receivers at the end nodes rather than number of wavelengths [49], which was the main cost for grooming ring network design. The studies in [12], [50] and [51] are the first to consider transmitter and receiver cost rather than number of wavelengths in grooming ring network design.

It has been shown that to minimize the number of transmitters and receivers required is equivalent to minimizing the number of lightpaths that are needed, since each lightpath needs one transmitter and one receiver. The problem of minimizing the number of transmitters and

receivers for a general topology is studied in [52]. The authors concentrate on the topology subproblem. They assume the virtual topologies are always implementable on the given physical topology and the traffic streams and lightpaths are full-duplex.

An ILP formulation is developed to solve the transmitter/receiver minimizing problem. A heuristic algorithm is presented based on the successively deleting lightpaths from an initial topology.

In this chapter, the design problem in a more general IP traffic grooming network is formulated as an ILP optimization problem. A lower- and upper-bound of the tranmisstter/receiver problem is developed and a heuristic algorithm based on traffic matrix transformation is also developed. The organization of this chapter is as follows: Section 4.3 defines the network models. An exact ILP (Integer Linear Programming) formulation is presented in Section 4.4. Due to the complexity of the problem itself, a fast heuristic algorithm is proposed in Section 4.5. Results of both approaches are compared and evaluated in Section 4.6 and 4.7. Dynamic routing in the resulting virtual topology is studied in Section 4.8. Section 4.9 presents our conclusions and discusses possible future work.

4.2 IP Traffic Grooming Problem Formulation

4.3 Network Model

There are two topologies associated with the WDM optical networks:

- *Physical topology*, a graph $G_p(V, E)$ with V being the set of nodes and E being the set of physical links;
- *Virtual topology (logical topology)*, a graph $G_l(V, L)$ with nodes corresponding to the nodes in the physical network and edges corresponding to the lightpaths.

Each lightpath may extend over several physical links (spans). Lightpaths can be viewed as chains of physical channels through which packets are moved from a router to another router toward their destinations. The link flow and link capacity for link (m, n) (from node m to node n) are denoted by x_{mn} and u_{mn} , respectively.

As mentioned earlier, the main cost in IP traffic grooming is due to the transmitters and receivers. The number of transmitters and receivers is equivalent to the number of lightpaths in the network. Figure 4.2 depicts an illustrative example that shows how IP traffic grooming helps to reduce the number of transmitters and receivers in a 3-node network.

Assume that each link has capacity of 100 units. The matrix in Figure 4.2 (a) is the original traffic matrix. It includes the location and capacity of three requests. Figure 4.2(a) depicts one solution in the absence of IP traffic grooming, it simply establishes a lightpath (connection) for each s-d pair. It requires one transmitter and one receiver at each node.

Figure 4.2(b) depicts another solution based on the fact that the capacity requested by s-d pair (1, 3) is relatively smaller. Thus, instead of reserving a separate lightpath for it, the spare capacity along lightpath 1 → 2 and 2 → 3 can be reused to accommodate the traffic of s-d pair (1, 3). That is, the traffic from Node 1 to Node 2 and 3 both take the route from Node 1 to Node 2, Node 2 receives and analyzes the traffic, drops the traffic that is destined for it and forwards the remaining traffic (from Node 1 to Node 3) along with its own traffic (from Node 2 to Node 3) to Node 3. This add-and-drop procedure is performed by transmitters and receivers at Node 2. In this scenario, the traffic carried by the optical layer is represented by the matrix in Figure 4.2 (b).

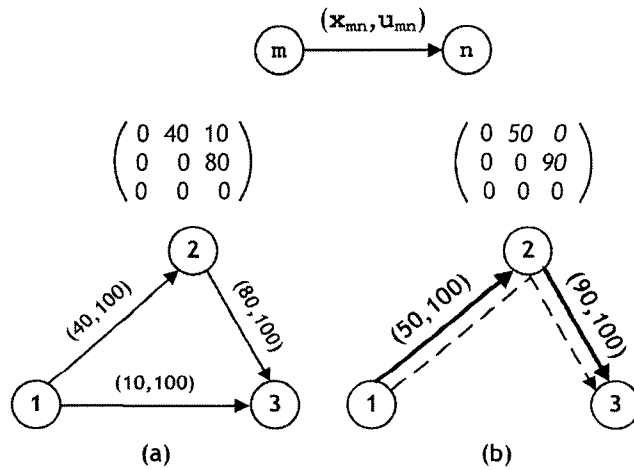


Figure 4.2 Illustrative example of IP traffic grooming.

The scheme shown in Figure 4.2 (b) results into one less transmitter and receiver in comparison to the scheme shown in Figure 4.2 (a). However, the lower size traffic request (1,3) takes a longer route in IP layer to avoid reserving an entire wavelength for it. This is the tradeoff we need to make in order to alleviate the wavelength underutilization in optical layer. A formal problem statement of the IP traffic grooming problem is given in the next section.

4.4 Solution for Optimal Strategy

4.4.1 Problem Statement

Unlike the other chapters, let us denote the traffic matrix as $D_{N \times N} = \{d_{st}\}$, where d_{st} denotes the traffic capacity required from source node s to destination node t , represents the capacity requirement of the systems.

The IP traffic grooming problem we study in this chapter can be described as follows.

Given a traffic matrix for a network, how to aggregate the traffic requests for transporting, such that the total number of transmitters (and receivers) required in the network is minimized.

In the virtual topology, each arc corresponds to a lightpath between the node pair. Hence the problem of minimizing the number of lightpaths is equivalent to minimizing the number of arcs required in the virtual topology.

Notice that if each request is assigned a dedicated lightpath, the virtual topology would be a full-connected network if there is a request for each node pair. The desired grooming network is the one with minimum number of transmitters and receivers, which is a solution with a minimum set of arcs in its virtual topology that is sufficient to carry the given traffic.

To simplify the problem, it is assumed that each request has capacity smaller than or equal to the full-wavelength capacity. Note that for a capacity requirement of more than a full wavelength, there has to be some full wavelength paths assigned to this request and its remaining capacity need would be fulfilled using the traffic grooming algorithm. The terms “link” and “arc” are used interchangeably here.

This problem is similar to a capacitated multicommodity flow design problem [53] with limited link capacities. Therefore, this problem can be formulated as an ILP optimization

problem. It is assumed that a request from the same s-d pair will always take the same route. Also, it is assumed that each link has the same capacity that is given by $W \times C$, where W denotes the number of wavelengths carried by a link, and C denotes the full-wavelength capacity.

4.4.2 Notations

4.4.2.1 Parameters

- L_{st}^k : (data) for each s-d node pair, list all possible routes from source node s to destination node t , excluding routes that pass through a node more than once, number them using k as an index. That is, $r_{1,6}^3$ indicates the 3rd route from Node 1 to Node 6.
- $A_{st}^{l,k}$: (binary data), takes value of 1 if arc l is on the k th path from node s to t ; zero otherwise.

4.4.2.2 Variables

- γ_{st}^k : binary variable, route usage indicator, takes value of 1 if route r_{st}^k is taken; zero otherwise.
- u_l : integer variable, logical link usage indicator, keeps an account of the number of lightpaths on arc l in the virtual topology.

4.4.3 Problem Formulation

1. Objective:

The objective is to minimize the number of arcs in the virtual topology. This reflects the minimum number of lightpaths in optical layer. Recall that variable u_l counts the number of lightpaths on arc i in the virtual topology. Here L is defined as the set of arc in the virtual topology. If the capacity carried by arc i exceeds the full wavelength capacity, multiple lightpaths between the same node pair are required. Thus the number of transmitters (and receivers) increase.

$$\min \sum_{l \in L} u_l \quad (4.1)$$

2. *Fiber link capacity constraint:* Let TC^l be the total capacity carried by link l , which is given by Equations (4.2). Constraint (4.3) guarantees that the aggregated capacity on any arc does not exceed the total fiber capacity, which is bounded by $W \times C$.

$$TC^l = \sum_{(s,t), s \neq t} \sum_k \gamma_{st}^k A_{st}^{l,k} d_{st} \quad (4.2)$$

$$TC^l \leq W \times C \quad (4.3)$$

3. *Traffic routes constraint:*

Equations (4.4) and (4.5) ensure that if there is a request from node s to t , one and only one route is assigned to the request. In another word, $d_{st} \geq 0$, set $\sum_k \gamma_{st}^k = 1$. Otherwise, there is no traffic request from node s to node t , none of the routes from node s to node t will be taken, hence, $\sum_k \gamma_{st}^k = 0$.

$$\sum_k \gamma_{st}^k \leq d_{st} \quad (4.4)$$

$$NC \sum_k \gamma_{st}^k \geq d_{st} \quad (4.5)$$

4. *Arc usage constraint:* Recall that arc usage indicator u_l counts the number of lightpaths required on arc l (logical link l) in order to carry the aggregated traffic TC^l . $u_l = \lceil TC^l / C \rceil$. This is obtained by using Equations (4.6) and (4.7). For example, if $C = 48$ and $TC^i = 62$, $\lceil 62/48 \rceil = 2$ lightpaths are required on logical link i from its start node to its end node.

$$C \times u_l \geq TC^l \quad (4.6)$$

$$C \times u_l \leq TC^l + C \quad (4.7)$$

Notice that from Equations (4.3) and (4.6), the total number of lightpaths on a logical link l is bounded by the number of wavelengths on the optical fiber. It can also be noticed that Equation 4.7 is not required for solving this problem, it is left in the formulation to help understand the definition of u_l .

Further constraints, such as the limited number of transmitters on each node, can be easily added to this formulation. This will help to capture the cost on each node in the network.

The limitation of this exact ILP formulation is that it enumerates all the possible routers for each s-d pair and search for an optimal set of arcs in virtual topology. In a fully connected network of N nodes, there are up to $\sum_{h=0}^{N-2} P_{N-2}^h$ possible routes for each s-d pair, where P_m^n is the permutation operation. This search requires large computation time as the network size increases. The formulation can be further simplified by adding a *hop-length constraint* such that the number of possible routes is reduced to a reasonable number, consequently, the computation time is saved. However, this network design problem is still a special case of multicommodity flow problem, which becomes unmanageable even for moderate sized networks. Therefore, we have to resort to heuristics to obtain “good” solutions in a reasonable amount of time that capture all the constraints of the ILP solution.

4.5 Heuristic Approach

4.5.1 Bounds

For a network $G(V, E)$, in the absence of IP traffic grooming, the number of transmitters and receivers required at node s , denoted by Tx_s^{max} and Rx_s^{max} respectively, can be derived from matrix $D_{N \times N}$.

$$Tx_s^{max} = \sum_{t:(s,t) \in E} \lceil \frac{d_{st}}{C} \rceil \quad (4.8)$$

$$Rx_s^{max} = \sum_{t:(t,s) \in E} \lceil \frac{d_{ts}}{C} \rceil \quad (4.9)$$

where C denotes the full wavelength capacity that can be utilized. This is because request d_{st} requires at most $\lceil d_{st}/C \rceil$ transmitters at node s to transmit traffic d_{st} , likewise, it requires at most $\lceil d_{st}/C \rceil$ receivers at node t to receive traffic d_{st} .

From the perspective of network flows, the total amount of outgoing traffic flows seen by node s is $\sum_{t \neq s} d_{st}$, the total amount of incoming flows to node s is $\sum_{t \neq s} d_{ts}$. Hence, the minimum number of transmitters and receivers needed in the network to carry the traffic in $D_{N \times N}$ can be derived using the following two equations.

$$Tx_s^{min} = \lceil \frac{\sum_{t:(s,t) \in E} d_{st}}{C} \rceil \quad (4.10)$$

$$Rx_s^{min} = \lceil \frac{\sum_{t:(t,s) \in E} d_{ts}}{C} \rceil. \quad (4.11)$$

In general, Tx_s^{min} and Rx_s^{min} are loose lower bounds. The reason is that in order to reduce the number of transmitters (and receivers) some s-d pairs may have to take multiple hops and hence increase the link load in the virtual topology. This overhead load is not captured in Equations (4.10) and (4.11), and it is dependent on the traffic pattern.

4.5.2 Traffic Aggregation Algorithm

To develop a *traffic aggregation* heuristic approach, the basic idea is to merge the smaller traffic request onto bigger bundles to reduce the number of transmitters and receivers. Although the total number of lightpaths required in the network is reduced, the finer granularity requests may take multiple-hop and longer routes. This may introduce delay for lower-rate requests. However, we believe that this is affordable in the future slim IP-over-WDM control plane, and this is a tradeoff we would have to make in order to reduce the overall network cost.

An element in traffic matrix can be *reallocated* by merging it with other traffic streams. Thus there will be no need to establish a direct path for that s-d pair. An element in traffic matrix can be *aggregated* if it is smaller than full capacity, i.e., has spare capacity on a wavelength

channel and allows other traffic streams to be merged on it. Each element in the traffic matrix can be viewed as in one of the three states,

- State 0: If it can be reallocated or be aggregated;
- State 1: If it cannot be reallocated, but can be aggregated;
- State 2: If it cannot be eliminated or aggregated. For example, if $d_{st} = 0$, there is no traffic to be reallocated, and there is no need to allocate traffic.

The goal of the traffic aggregation algorithm is to choose a traffic stream d_{st} that can be merged with some other traffic streams d_{sn} and d_{nt} , so that d_{st} can be carried using a multiple hop path and not burden the system to establish a new path for it. After selecting d_{st} , the basic traffic aggregation operation on traffic matrix D consists of the following three steps:

1. $d_{sn} \leftarrow d_{st} + d_{sn};$
2. $d_{nt} \leftarrow d_{st} + d_{nt};$
3. $d_{st} \leftarrow 0.$

After this operation, the traffic request between s-d pair (s, t) is aggregated on s-d pairs (s, n) and (n, t) . Let $TR(T_{s,t,n})$ be the number of transmitters (equals to the number of receivers) needed after merging d_{st} with d_{sn} and d_{nt} . $TR(T^0)$ is called the upper bound, where T^0 is the original traffic matrix.

The key here is to select d_{st} and node n to reduce the value of $TR(T_{s,t,n})$. In experimenting with the ILP formulation, we observed that the ILP solution uses multi-hop routes for smaller requests, while the bigger requests tend to use direct single hop path. We use this observation to develop an heuristic solution. Figure 4.3 gives the *traffic aggregation* algorithm. The resulting new traffic matrix gives the structure of a virtual topology and the required capacity on each physical link. The idea behind this is to integrate smaller traffic request, say d_{st} , to those bigger traffic requests, d_{sn} and d_{nt} , to saturate the existing wavelength paths before establishing a

INPUT: Graph $G(V, E)$ and a traffic matrix $D_{N \times N}$.

OUTPUT: Rearranged traffic matrix $D_{N \times N}$.

ALGORITHM:

1. Initialize s-d pair status:
If $d_{st} \geq 0$ then $d_{st}.state = 0$,
else $d_{st}.state = 2$.
2. $target = \min(d_{st} : d_{st}.state = 0)$.
3. If target = NULL, terminate.
4. else
 - (a) Set K =new stack. Pick node v that satisfies:
 - i. $d_{sv}.state \leq 1, d_{vt}.state \leq 1$;
 - ii. $d_{st} + d_{sv} \leq C, d_{st} + d_{vt} \leq C$;
 - iii. $TR(T_{s,t,v}) < TR(T)$. $K.push \{v\}$.
 - (b) Define $index(v) = \max(d_{sv}, d_{vt}), v \in K$.
 - (c) If $K = \emptyset$, then $d_{st}.state \leftarrow 1$, go to 2.
 - (d) else $n = \arg \max_{v \in K} \{index(v) : v \in K\}$.
 - (e) Update traffic matrix $D_{N \times N}$:
 - i. $d_{sn} \leftarrow d_{st} + d_{sn}$;
 - ii. $d_{nt} \leftarrow d_{st} + d_{nt}$;
 - iii. $d_{st} \leftarrow 0, d_{st}.state \leftarrow 2$.
5. Go to 2.

Figure 4.3 Approximate approach: Traffic aggregation

new one. This would force some smaller granularity traffic to take longer routes with multiple hops, while saving some lightpaths.

The algorithm starts by finding the s-d pair with minimum request capacity that is in state 0 (Step 2 in Figure 4.3), say d_{st} . Next it searches for a set of all eligible intermediate nodes, namely K (Step 4a in Figure 4.3). Define the index value of an item v in set K as $\text{index}(v) = \max(d_{sv}, d_{vt})$. The intermediate node n is selected from K to saturate some wavelengths. Hence, if K is not empty, n is chosen as the node with the maximum index value. Then the algorithm updates the current traffic matrix after an intermediate node is decided (Step 4e in Figure 4.3). If K is empty, no eligible intermediate node is found for this s-d pair, $d_{st}.\text{state}$ is changed from 0 to 1, which means request d_{st} cannot be reallocated, but could be aggregated. The algorithm keeps searching for the next s-d candidate for aggregation until there is no eligible s-d pairs in state 0 can be found.

4.5.3 Complexity Analysis

One s-d pair is changed from State 0 to either State 1 or State 2 in each step. Thus the algorithm terminates after at most N^2 passes. The run time for searching *target* in each loop is up to N^2 , it takes another N loops to find the set K . Thus, the overall computation complexity of this algorithm is $O(N^5)$. In practice one will never see this complexity and the algorithm terminates much faster. One way is to use effective data structures to make the search more efficient and faster.

4.5.4 Example of Traffic Aggregation

Figure 4.4 illustrates an example of how the traffic aggregation algorithm performs. Assume that each wavelength has capacity of OC-48 (2.5Gbps), and the minimum allocatable unit is OC-1. Thus, $C = 48$. Consider traffic matrix that is composed of random combination of OC-1, OC-3, and OC-12. An original traffic matrix includes all possible s-d pairs, shown as the top left matrix in Figure 4.4.

The algorithm starts by finding the minimum eligible s-d pair that can be reallocated, which

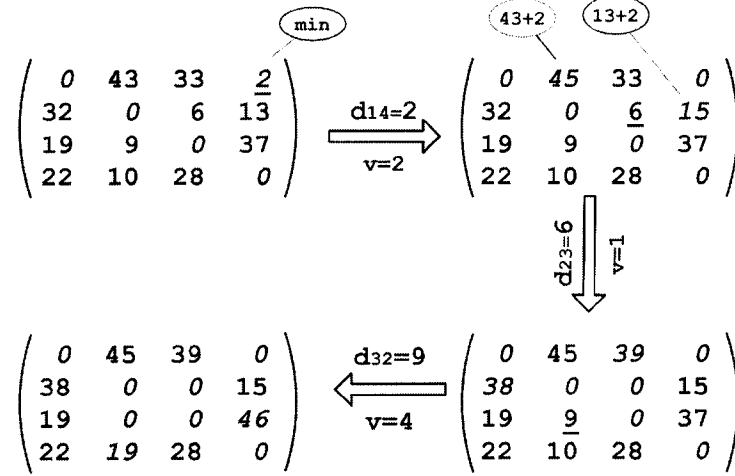


Figure 4.4 An illustrative example of traffic aggregation algorithm.

is $(1, 4)$ with $d_{1,4} = 2$ in this example. Next it finds the possible intermediate nodes to put into set K . It can be observed that $K = \{2, 3\}$ with $\text{index}(2) = 43$ and $\text{index}(3) = 37$. Amongst the candidates nodes in K , the one with highest index value is chosen, that is $n = 2$. Next, we update the current traffic matrix by removing $d_{1,4}$ from the original position and aggregating it with $d_{1,2}$ and $d_{2,4}$. This results into the matrix on the top right in Figure 4.4. Next it selects $d_{2,3} = 6$ and completes its processing by choosing $n = 1$. The algorithm continues until no more relocatable s-d pair exists as shown in Figure 4.4. The bottom left matrix shows the final results. Application of Equations (4.8) and (4.9) indicate that 12 transmitters (and receivers) are required for the original traffic matrix. After traffic aggregation, this number is reduced by 3. More detailed performance study is provided in Section 4.7.

4.6 Solutions and Numerical Results

The ILP formulation of Section 4.4 is solved by using CPLEX Linear Optimizer 7.0. We use the ILP formulation and the traffic aggregation approach to solve IP traffic grooming problem for a 6-node network, with $W = 6$, $C = 48$. Table 4.1 gives a traffic matrix with randomly generated 50 requests. The integer numbers indicates the request capacity in unit of OC-1 (51.84 Mbps). The objective is to design a network with as few logical links as possible.

Notice that there are totally $P_4^0 + P_4^1 + P_4^2 + P_4^3 + P_4^4 = 65$ routes for each s-d pair in a 6-node network, and this number increases dramatically as the network size increases. It would be a great burden and might be unnecessary as well to obtain optimality by searching among all the possible routes. In this 6-node network example, we performed experiments with maximum hop-length as 3, 4 and 5. It is observed that limiting the hop-length to 3 still yields close to optimal solution while the number of all candidate paths for each s-d pair is effectively reduced from 65 to $P_4^0 + P_4^1 + P_4^2 = 17$. This significantly reduces the computation complexity of solving the ILP optimization problem.

Table 4.1 Requests matrix for a 6-node network

	1	2	3	4	5	6
1	0	3	3+1+1	12+12	3+1+1	12+12
2	12+12+12+3	0	3	1+3	0	1+1+12
3	3	1	0	12+12	3+1+1	0
4	3	12	3+12+3+3	0	1	3+1+1+12
5	3	3+12	12	0	0	3+1
6	1+3	12	0	3+12	0	0

The results obtained from solving ILP with hop length = 3 and traffic aggregation approach are shown in Figure 4.5 (a) and Figure 4.5(b), respectively.

According to Equations (4.10) and (4.11), at least 9 transmitters (receivers) are required. Figure 4.5 (a) shows an optimal solution of 11 lightpaths by solving the ILP formulation with a maximum hop-length limit of 3. Figure 4.5 (b) shows solution with 12 transmitters (receivers) using traffic aggregation approach. Table 4.2 shows the virtual topology routing assignments obtained by solving the ILP formulation and the traffic aggregation heuristic algorithm.

4.6.1 Observations

Figure 4.5 also shows the similarity between the virtual topology design obtained from solving ILP formulation and heuristic approach. More specifically, the ILP formulation tends to keep bigger requests on shorter paths in virtual topology and tries to integrate smaller traffic streams onto bigger bundles. The ILP approach provides an optimal solution by performing

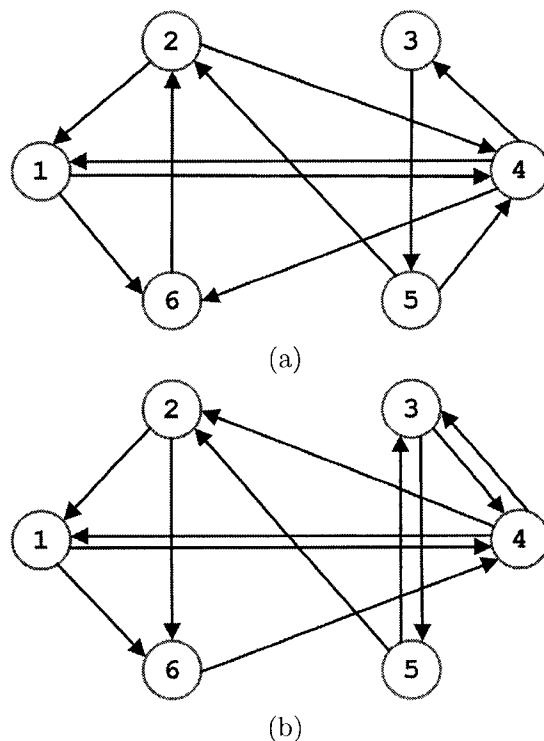


Figure 4.5 Comparison of ILP solution and heuristic approach: An illustrative example. (a) Results obtained by solving ILP optimization problem with hop-length limit 3. (b) Results obtained from traffic aggregation approach.

Table 4.2 Resulting routes in virtual topologies

Node pair	Requested Capacity	ILP Formulation	Traffic Aggregation
		Route on VT	Route on VT
1-2	3	1-6-2	1-4-2
1-3	5	1-4-3	1-4-3
1-4	24	1-4	1-4
1-5	5	1-4-3-5	1-4-3-5
1-6	24	1-6	1-6
2-1	39	2-1	2-1
2-3	3	2-4-3	2-1-4-3
2-4	4	2-4	2-6-4
2-6	14	2-4-6	2-6
3-1	3	3-5-2-1	3-4-1
3-2	1	3-5-2	3-4-2
3-4	24	3-5-4	3-4
3-5	5	3-5	3-5
4-1	3	4-1	4-1
4-2	12	4-6-2	4-2
4-3	21	4-3	4-3
4-5	1	4-3-5	4-3-5
4-6	17	4-6	4-2-6
5-1	3	5-4-1	5-2-1
5-2	15	5-2	5-2
5-3	12	5-2-4-3	5-3
5-6	4	5-4-6	5-2-6
6-1	4	6-2-1	6-4-1
6-2	12	6-2	6-4-2
6-4	15	6-2-4	6-4

exhaust search among all possible routes. The traffic aggregation heuristic algorithm also gives a pretty good solution in this example by just performing local search, which takes much less computation time. However, as an approximate approach, the traffic aggregation heuristic cannot guarantee any optimality.

The integration of the traffic helps to reduce the number of transmitters and receivers. On the other hand, it also introduces overhead traffic to the network and impact the resource utilization. Besides, it adds potential delays to the requests which have been reallocated to take multiple hops in the virtual topology. It can be observed from Table 4.2 that the average hop-length in the ILP solution is $80/50 = 1.6$. The average hop-length in the traffic aggregation heuristic is $77/50 = 1.54$, while without grooming, given enough resource, the minimum average hop-length is 1. The more we save on transmitters and receivers, the longer the average hop-length is, accordingly the longer average delay. This is the trade-off we cannot avoid.

The ILP approach becomes unmanageable quickly as the size of the network increases. The reason is that the number of all possible arcs in the corresponding fully connected network increases dramatically as the number of nodes increases. We study the performance of the IP traffic aggregation heuristic approach in terms of wavelength utilization in the following Section.

4.7 Performance Study

4.7.1 Performance Metrics

The performance study for the above algorithm is carried out using the following performance metrics.

Effective load. We study the performance in terms of *wavelength utilization*. With given traffic matrix $D_{N \times N}$, where d_{st} is the amount of requested wavelength capacity. Given a network's physical topology $G_p(V, E)$ with N nodes, we apply Dijkstra's shortest path algorithm to find the shortest path between all s-d pairs. This forms a distance matrix $H_{N \times N} = \{h_{st}\}$,

where h_{st} denotes the physical distance from node s to node t . More specifically, h_{st} here represents the shortest hop-length from node s to node t . If the number of wavelengths is sufficient, each request would use the corresponding shortest physical path. Thus we define the effective network load l_{eff} as,

$$l_{eff} = \sum_{(s,t)} d_{st} \times h_{st}. \quad (4.12)$$

This gives the minimum network resources in terms of the actual capacity used by that is needed for the given traffic requests.

Offered load. In the wavelength routed optical network without grooming capability, each request will be assigned a full wavelength capacity C , even though the actual requested capacity might be only a fraction of C . We define the minimum offered load of a WDM network in the absence of grooming as l_{WDM} . It is given by Equation (4.13) and represents the physical wavelength link product used without the grooming capacity.

$$l_{WDM} = \sum_{(s,t)} \lceil \frac{d_{st}}{C} \rceil \times C \times h_{st}. \quad (4.13)$$

Similarly, let l_{IP} be the offered load by setting up lightpaths based on the new traffic matrix $\bar{D}_{N \times N} = \{\bar{d}_{st}\}$, which is obtained by using the traffic aggregation approach. With sufficient wavelength resource, each s-d pair in \bar{D} would take its corresponding shortest path. Recall the distance matrix $H_{N \times N} = \{h_{st}\}$, l_{IP} can be obtained by using Equation (4.14). More specifically, this provides the lower bound on the actual reserved capacity for the lightpaths after aggregation.

$$l_{IP} = \sum_{(s,t)} \lceil \frac{\bar{d}_{st}}{C} \rceil \times h_{st} \times C. \quad (4.14)$$

Wavelength utilization. The wavelength utilization is defined as the ratio between the effective network load and the actual offered load. Hence, the wavelength utilization in

WDM network without grooming capability and in IP traffic grooming networks are given by Equations (4.15) and (4.16), respectively.

$$\eta_{WDM} = \frac{l_{eff}}{l_{WDM}} \quad (4.15)$$

$$\eta_{IP} = \frac{l_{eff}}{l_{IP}} \quad (4.16)$$

4.7.2 Examples

Figures 4.6 and 4.7 show a set of experiment results obtained from a 16-node bidirectional ring topology and a 4×4 mesh torus network, respectively. The traffic generation for ring, mesh and ARPENET are the same. The traffic is uniformly distributed among all source-destination pairs. For each s-d pair, we randomly generate a number between 0 and max allowable traffic. Thus the mean is $(max - 1)/2$. By increasing the value of max, we can increase the value of the mean traffic in the network. The wavelength utilization is shown in Figures 4.8 and 4.9 for the two topologies, respectively. The bars in the Figures 4.6 and 4.7 represent the number of equivalent OC-1 capacity units that are required in different network topologies with different traffic matrices. We consider only sub-rate traffic in the experiments. The traffic matrix is randomly generated and the effective load is increased by increasing the mean value of the sub-rate traffic capacity. Ten experiments are performed for each traffic pattern and the average values are presented as the final results.

Simulations on the 20-node-31-link ARPANET topology (shown in Figure 4.10) are conducted and the corresponding results are shown in Figures 4.11 and 4.12.

In the absence of traffic grooming, the capacity required in a WDM network (the middle bar) does not change much as the sub-rate traffic requests varies. This is because each connection is assigned an entire wavelength irrespective of whether it actually requires a full wavelength or a fractional wavelength capacity. Significant improvement on the reserved capacity can be observed when there are more finer granularity requests in the traffic matrix.

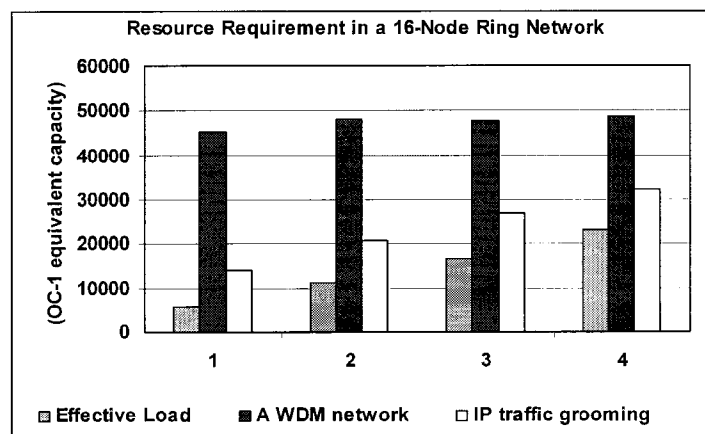


Figure 4.6 Resource requirement in a 16-node bi-directional ring network.

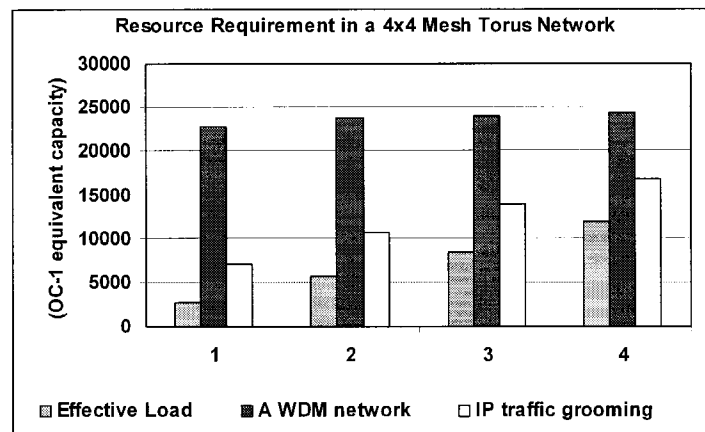


Figure 4.7 Resource requirement in a 4×4 bi-directional mesh torus network.

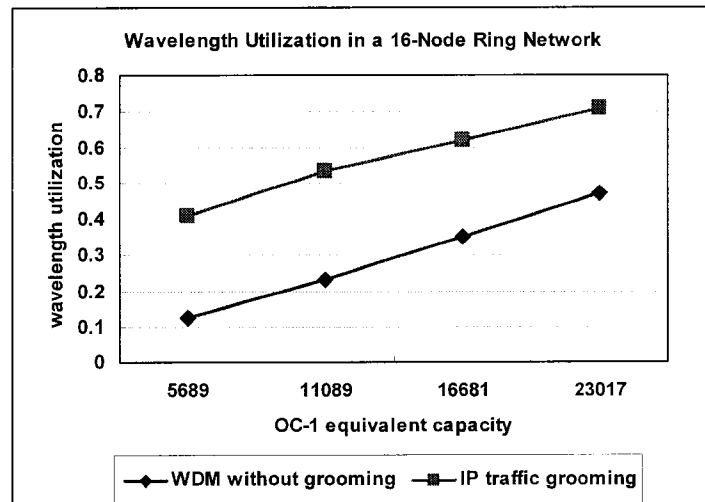


Figure 4.8 Wavelength utilization in a 16-node bi-directional ring network.

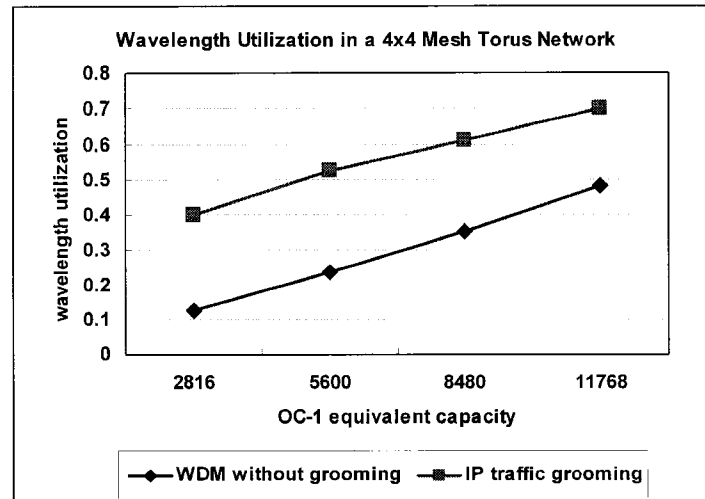


Figure 4.9 Wavelength utilization in a 4×4 bi-directional mesh torus network.

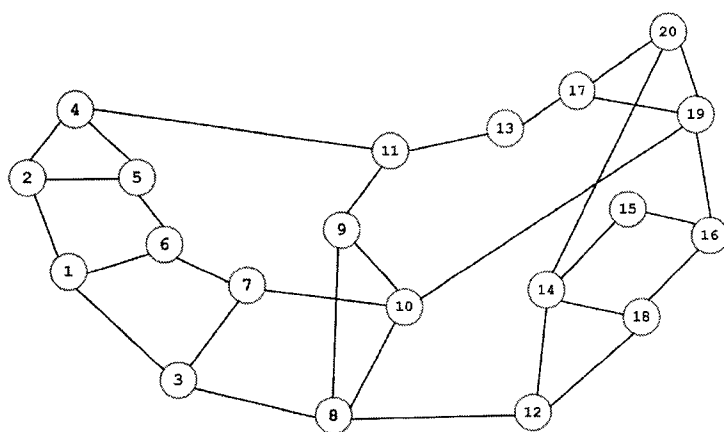


Figure 4.10 The 20-node-31-link ARPANET topology.

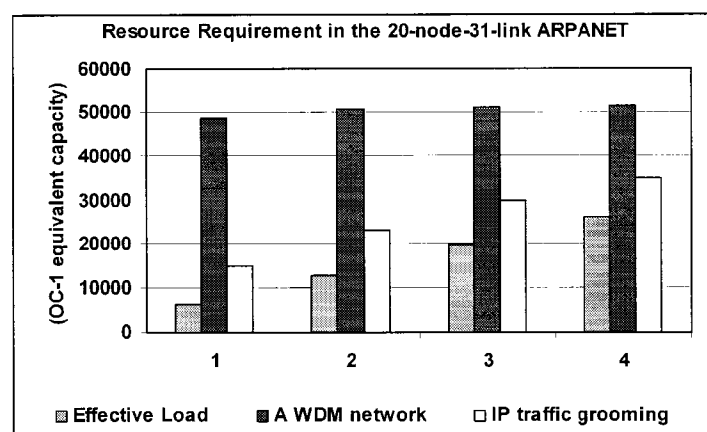


Figure 4.11 Resource requirement in the 20-node-31-link bi-directional ARPANET.

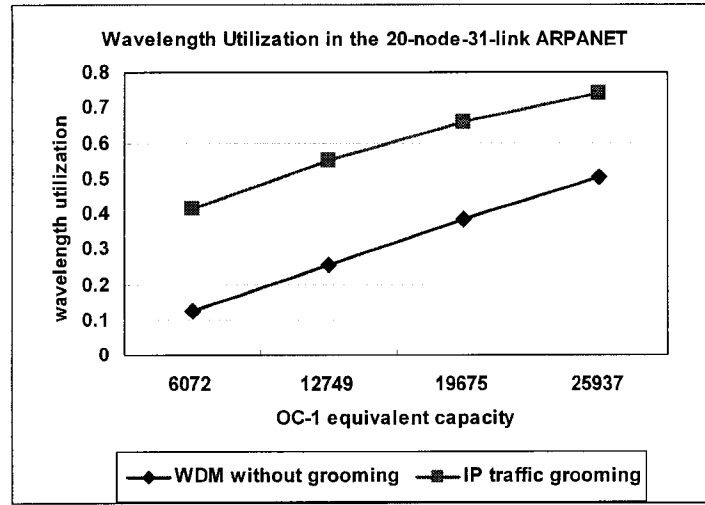


Figure 4.12 Wavelength utilization in the 20-node-31-link bi-directional ARPANET.

This is also because the wavelengths are severely under utilized in WDM networks without traffic grooming when most traffic requests are sub-rate traffic.

In comparison to the WDM networks without traffic grooming, the capacity reserved in IP traffic grooming networks goes up as the effective load increases. This reflects a wavelength sharing among sub-rate traffic streams, which also results in an improvement on wavelength utilizations.

Generally, given the same traffic matrix, more wavelength-links are required in a ring topology comparing with a mesh-like topology. This can also be observed from Figures 4.6 and 4.7 where the same traffic matrices are tested, the effective load in the 16-node ring is almost twice as that of in the 4×4 mesh torus network. This is partly due to the longer average path length in ring topology than in a mesh network with the same number of nodes. Besides, in a ring topology, each s-d pair has only two alternate paths, when establishing the same number of lightpaths. Thus more wavelengths are required in order to satisfy the wavelength continuity constraint. In these experiments, the performance of our algorithm in ring topology is almost as good as it is in the mesh torus topology.

4.8 Dynamic Routing in the Virtual Topology

The above design is based on the given static traffic matrix, or the estimated traffic matrix. The actual traffic varies from the given data. In this section we study the routing and wavelength assignment of dynamic traffic in the designed virtual topology.

4.8.1 Dynamic Traffic

The virtual topology is designed based on the given static traffic matrix, which is also referred to as the estimated traffic matrix. The requested capacity dynamic traffic varies from the corresponding estimated value. We define this difference as $|Diff|$, if the given requested capacity between node s and t is d_{st} , the capacity for each random request from s to t is uniformly distributed between $\max(d_{st} - |Diff|, 0)$ and $\min(d_{st} + |Diff|, C)$. The value of $|Diff|$ indicates the variation of the random traffic from the estimated traffic, and it is one of the parameters in our simulations. The blocking performance are compared as this range varies. Since the virtual topology is designed closely bascd on the given estimated traffic matrix, it is expected that as the value of $|Diff|$ goes up, the network will see an increasing blocking probability.

It is also assumed here that random requests arrive at each node according to a Poisson process with rate λ . Each request is equally likely to be destined to any of the remaining nodes. The holding time of the requests are exponentially distributed with mean $1/\mu$. Hence, the Erlang load offered by a node is $\rho = \lambda/\mu$.

4.8.2 Routing Strategies

To begin with, it is worth mentioning that both the ILP approach and the heuristic algorithms provide not only the virtual topology design, but also the routing for each request. From this we can calculate the designed load on each link in the virtual topology, which is, more specifically, the total capacity used on each corresponding lightpath in the physical topology. For instance, Figure 4.13 is the same virtual topology that we obtained in Section 4.6 with the estimated traffic matrix given in Table 4.1, with the designed load on each link marked.

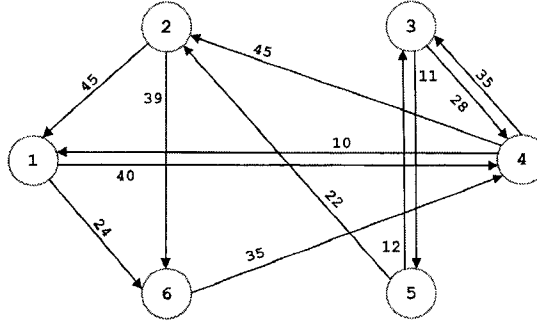


Figure 4.13 Virtual topology solution with designed load on each link.

Before starting the design of routing strategies, let us define the route that obtained from either ILP solution or heuristic algorithms as the *preferred route*, let us also refer to those design approaches as the *static design*. Once we have the virtual topology, we can apply shortest path algorithm repeatedly to find multiple routes for each node pair.

Notice that the preferred route for a node pair, which is obtained from the static design, does not necessarily to be the shortest route in the virtual topology.

Three different routing strategies are developed as follows. The wavelength assignment follows the rule of *first-fit*.

- *Fixed Path Routing (FPR)*: Only the *preferred route* is considered in the virtual topology, if there is no enough wavelength available along this route, the request is blocked, otherwise, the request is accepted.
- *Least Congested Routing (LCR)*: The least congested route is defined as the route which has the maximum amount of free capacity. If there is a tie, a shorter route is taken.
- *Preferred Path First (PPF)*: In this scheme, the preferred route is the first choice for each node pair. K shortest paths for the given virtual topology are pre-computed for each node pair, where K indicates the number of alternate paths. K takes the value of four in our simulations. If the preferred route is not available, the first available shortest path is chosen.

4.8.3 Performance Analysis

The performance of different routing strategies are studied in terms of blocking probability.

Figures 4.14, 4.15, 4.16 show the performance comparison of the proposed three routing strategies with different values of $|Diff|$ for the virtual topology in Figure 4.13. It can be observed that as expected earlier, when the value of $|Diff|$ increases, the network sees higher blocking probability. As stated earlier, this is due to the fact that the virtual topology is designed closely based on the given traffic matrix, as the actual traffic pattern goes away from the estimation, the blocking performance in the resulting virtual topology goes down. After certain point, virtual topology will need to be updated based on a better traffic estimation.

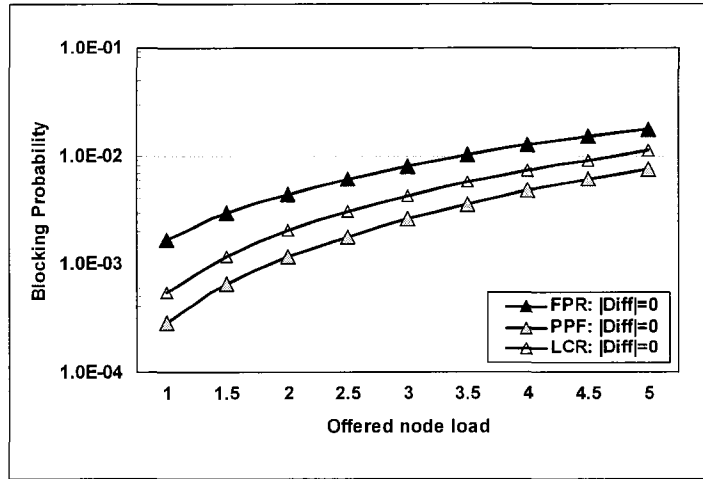


Figure 4.14 Blocking performance in virtual topology in Figure 4.13 with random traffic, $|Diff| = 0$.

The fixed path routing (FPR) approach considers only the preferred route obtained from the static design, it is actually independent to the resulting virtual topology. Also as a fixed path approach, it inevitably has the worst blocking performance among all the three routing schemes.

In contrast to FPR, the least congested routing (LCR) considers only the virtual topology. When the number of alternate paths is large enough, the preferred path will be included in the set of alternate paths. The preferred path first (PPF) approach takes both the static design

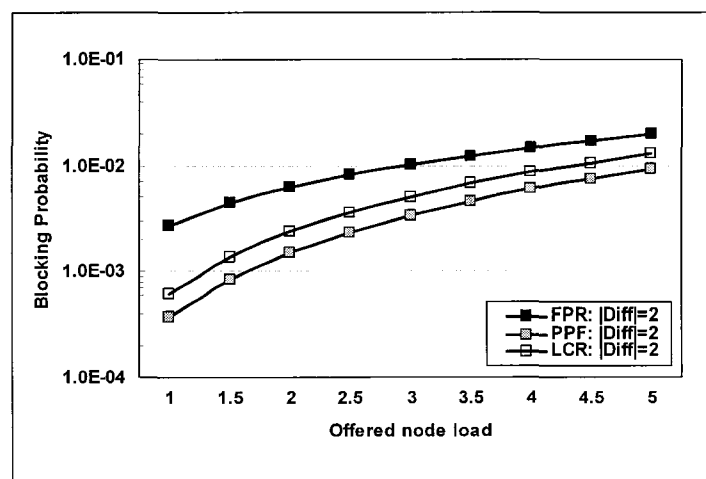


Figure 4.15 Blocking performance in virtual topology in Figure 4.13 with random traffic with $|Diff| = 2$.

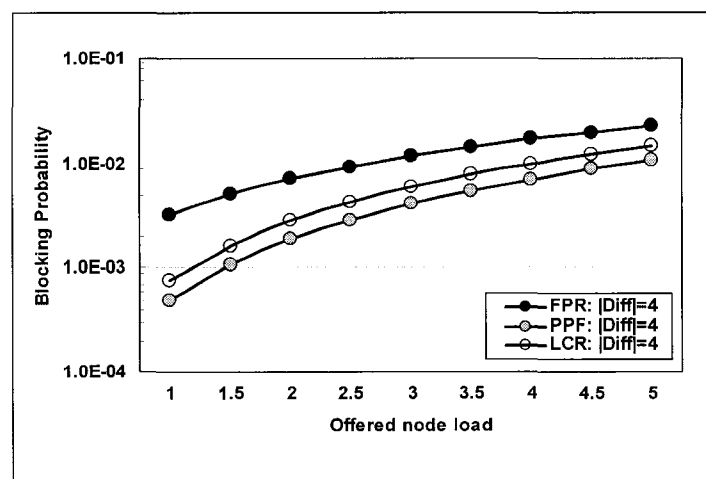


Figure 4.16 Blocking performance in virtual topology in Figure 4.13 with random traffic with $|Diff| = 4$.

and the virtual topology into account. Both LCR and PPF should perform better than FPR. And in this example, PPF performs even better than LCR.

Figure 4.17 gives another virtual topology design based on a different estimated traffic. Figures 4.18, 4.19, and 4.20 show another set of performance comparison among FPR, LCR and PPF. In this example, FPR still gives the worst blocking performance, while LCR always performs better than FPR and PPF.

The reason LCR performs better for the virtual topology given by Figure 4.17 while PPF is the best choice for the virtual topology given by Figure 4.13 is that the average designed load in Figure 4.13 is higher than that is in Figure 4.17. This also means that it is more critical for the requests to take the preferred routes. In other words, there is no much space for selecting alternate paths when the design link load is high. Therefore, PPF outperformed LCR in this scenario.

While in Figure 4.17, the designed link load is relatively lower, which leaves more possibility for the network to select an alternate path if the preferred path is unavailable. LCR becomes a better choice in comparison to PPF in this case.

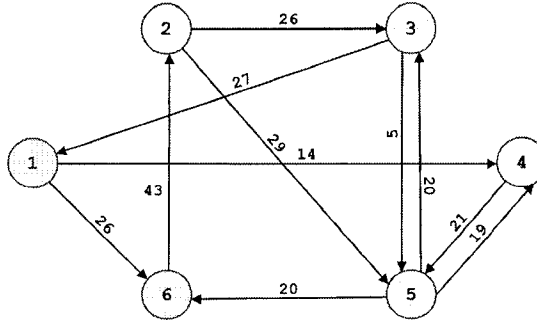


Figure 4.17 Virtual topology solution with designed load on each link.

We still can not conclude exactly in which situation PPF performs better than LCR. However, it is also can be observed that the performance of LCR and PPF is reasonable close. If the static design is an optimal solution, which means that all the estimated traffic requests are efficiently packed on each lightpath, the virtual topology should see a relatively high designed link load. In this case, it is proper to say that PPF is better choice is the static

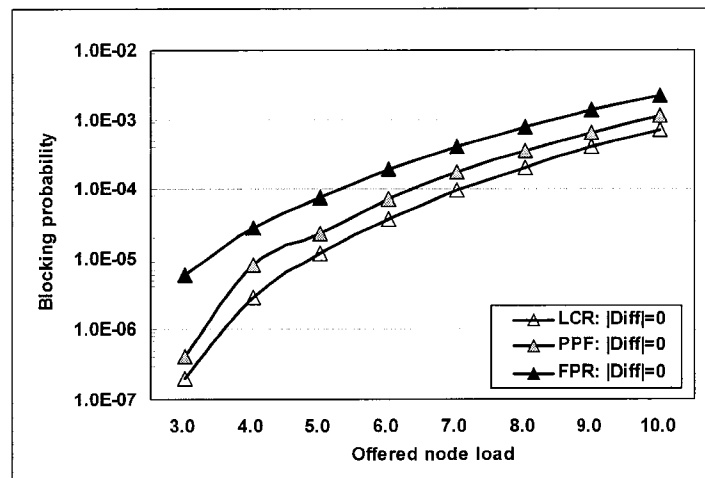


Figure 4.18 Blocking performance in virtual topology in Figure 4.17 with random traffic, $|Diff| = 0$.

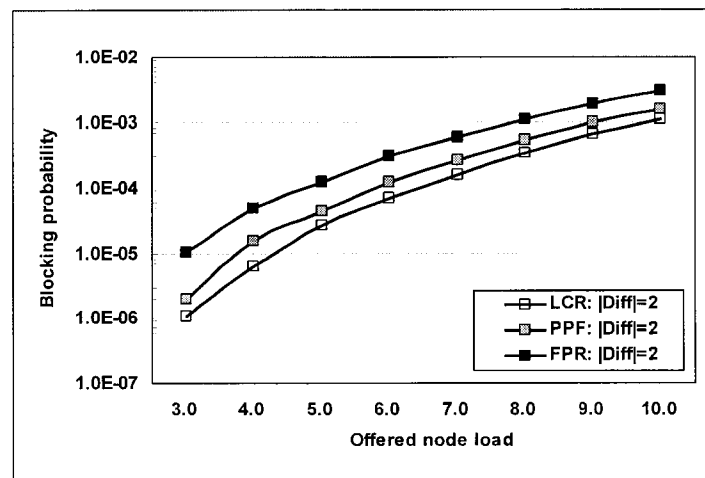


Figure 4.19 Blocking performance in virtual topology in Figure 4.17 with random traffic with $|Diff| = 2$.

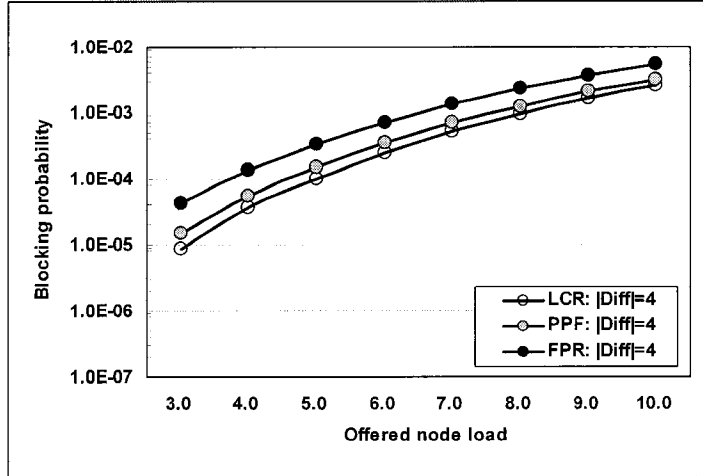


Figure 4.20 Blocking performance in virtual topology in Figure 4.17 with random traffic with $|Diff| = 4$.

design is an optimal one.

4.9 Summary

Traffic grooming is an essential issue in the evolution of future IP over WDM network architectures. IP traffic is characterized by its burstiness, high variability and sub-wavelength capacity requirements. Traffic grooming in optical networks has gained significant importance in the recent years due to the prevailing different and variable requirements of end users on single wavelength.

In this chapter, we studied the IP traffic grooming problem in IP over WDM framework. IP traffic grooming, that is, the traffic aggregation performed at IP routers, would help to alleviate the complexity of performing sub-wavelength level grooming in WDM layer. We used the concept of virtual topology to solve the IP traffic grooming problem with objective to minimize the network cost in terms of number of transmitters and receivers. To minimize transmitters and receivers inevitably introduces overhead IP traffic in the networks and impacts networks performance such as wavelength utilization, throughput and average delay. This is a tradeoff we have to make.

This transmitter/receiver minimization problem is formulated as an ILP optimization problem. The lower bound of this minimization problem is derived from the traffic matrix. The complexity of the ILP formulation can be reduced by adding hop-length limit constraints. It may still yield a good solution with carefully selected maximum hop-length. This model provides a general formulation and various constraints, such as maximum node degree, can be easily integrated into it.

The ILP formulation produces the optimal solution for static traffic demands, however, applying this technique to dynamic traffic in large networks is not practical due to its prohibitively large computation time. We also designed a simple fast heuristic approach, called the traffic aggregation algorithm. It is evaluated in Section 4.6 and 4.7. The IP traffic aggregation algorithm does not yield an optimal solution in terms of number of transmitters/receivers. However, it helps to effectively reduce the number of transmitters/receivers, and reduces the overhead IP traffic by reallocating smaller traffic streams first. The performance of IP traffic aggregation approach is studied in terms of wavelength utilization. We have shown that in comparison with WDM networks without traffic grooming, the IP traffic aggregation algorithm significantly improves the wavelength utilization in both ring and mesh torus topologies. Moreover, the polynomial computation complexity of the traffic aggregation algorithm makes it suitable for fast online IP traffic grooming.

It is worth mentioning that the IP traffic matrices, which contain the knowledge of the volume of traffic that flows between all possible sources and destinations, are not available to carriers today. Despite the lack of the information, it is still possible to capture the characteristics of IP traffic. Traffic matrix estimation has attracted more and more attention due to the benefits that would be derived by having access to accurate information of the size and the locality of the traffic flow [54, 55].

This traffic aggregation approach proposed in this chapter can be extended and applied in virtual private network design and upgradable network design. The wavelength utilization can be further improved by performing wavelength level traffic grooming in optical layer.

We also study the routing and wavelength assignment for dynamic traffic in the obtained

virtual topology. The dynamic traffic requests varies from the estimated traffic pattern. Three different routing strategies, namely, Fixed Path Routing (FPR), Least Congested Routing (LCR), and Preferred Path First (PPF) are proposed. The blocking performance of these three routing schemes is compared through simulation. The results show that as the dynamic traffic varies away from the estimated traffic, the blocking performance of all the three schemes goes down. FPR always gives the worst blocking performance. When the designed link load is high, PPF outperforms LCR.

CHAPTER 5. Traffic Grooming in Light Trail Architectures

To accommodate sub-rate IP bursts on OTNs is one of the key and still challenging problems in realizing the future optical Internet. Light trail [26] offers a strong candidate for supporting IP traffic over optical networks. We study this architecture in more detail and show how it can be effectively used. This chapter is devoted to the optimal design of light trails in WDM networks. The rest of the chapter is organized as follows. Section 5.1 is a brief introduction to light trail concept, light trail node structure, and a summary of light trail properties. A formal statement of light trail design problem is given in Section 5.2, followed by a two-step approach for solving this problem. The results obtained from our experiments are presented in Section 5.4. Section 5.5 presents our conclusions.

5.1 Light Trail Architecture

Current technologies that transport IP centric traffic in optical networks are often too expensive, due to their reliance on expensive optical and opto-electronic approach. Consumers generate diverse granularity traffic and service providers need technologies that are affordable and seamlessly upgradable. Recently, a concept called *light trail* was proposed to enable IP centric communications at the optical layer [26]. A light trail is a unidirectional *optical trail* between the start node and the end node. It is similar to a lightpath with one important difference that the intermediate nodes can also access this unidirectional trail. In light trails, the wavelength is shared in time and the medium access is arbitrated by control protocol among the nodes that try to transmit data simultaneously, that is, upstream nodes have higher priorities than lower stream nodes.

5.1.1 Light Trail Example

We depict a 4-node light trail in Figure 5.1. The light trail starts from Node 1, passes through Node 2, Node 3 and ends at Node 4. Each of the nodes 1, 2 and 3 are allowed to send data to any of their respective downstream nodes without the need for optical switch reconfiguration. Every node receives the data from the upstream nodes, but only the corresponding destination node(s) will accept the data packets while other nodes will ignore them. An out-of-band control signal carrying information pertaining to the set up, tear down and dimensioning of light trails is dropped and processed at each node in the light trail. Since a light trail is unidirectional, a light trail with N_T nodes offers up to $\frac{N_T(N_T-1)}{2}$ optical connections along the trail. The six paths for the 4-node light trail are shown in Figure 5.1.

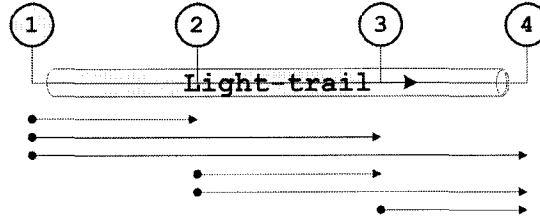


Figure 5.1 Illustrative example of traffic streams in a light trail.

The exclusion of fast switching at packet/burst level, combined with the flexible provisioning for diverse traffic granularity make the light trails superior to conventional circuit and burst switched architecture.

5.1.2 Node Structure

Figure 5.2 provides a typical node structure in light trail framework [26]. In Figure 5.2, the multiple wavelengths from the input link are de-multiplexed and then sent to corresponding light trail switches. A portion of the signal power goes to the local receiver, the remaining signal power passes through an optical shutter which is typically an AOTF (Acousto-Optic Tunable Filter). Thus a node receives signal from all wavelengths. If a particular wavelength is not being used by an upstream node (incoming fiber has no signal), the local host can insert

its own signal, otherwise it does not use the trail. The local signal is coupled with the incoming signal as shown in Figure 5.2.

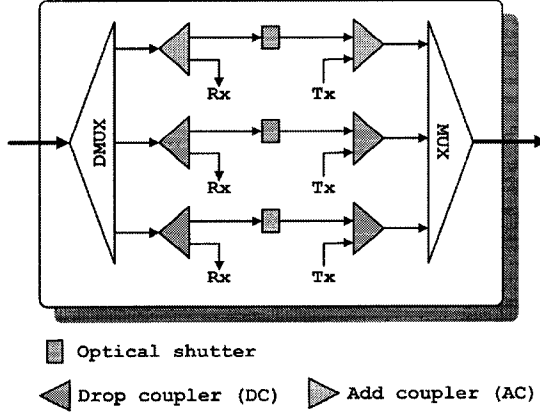


Figure 5.2 An example node structure in light trail framework.

Figure 5.3 provides a detailed light trail node structure with three input and three output fibers and two wavelengths on each fiber. The input signal is first demultiplexed, a portion of it is dropped and the remaining goes to the corresponding 3×3 wavelength switch, as depicted in Figure 5.3. The output of the wavelength switches goes through the optical shutter and along with the local added signals, are sent to the output ports of the light trail node. Notice that the optical shutter can locate either before the wavelength switch or after it at the output side.

Figure 5.4 gives a connection of 4-node light trail and the corresponding ON/OFF switch configurations. The direction of communication is from Node 1 to Node 4. The light trail on that wavelength is separately shown in Figure 5.5. The optical shutter is set to *OFF* state at the start and end nodes of the light trail such that the signal is blocked from traveling further. For an intermediate node along the light trail, the optical shutter is set to *ON* state to allow the signal to pass through the node.

A unidirectional light trail is thereby obtained from the start node to the end node as shown in Figure 5.5. No switch reconfiguration is required after the initial light trail setup.

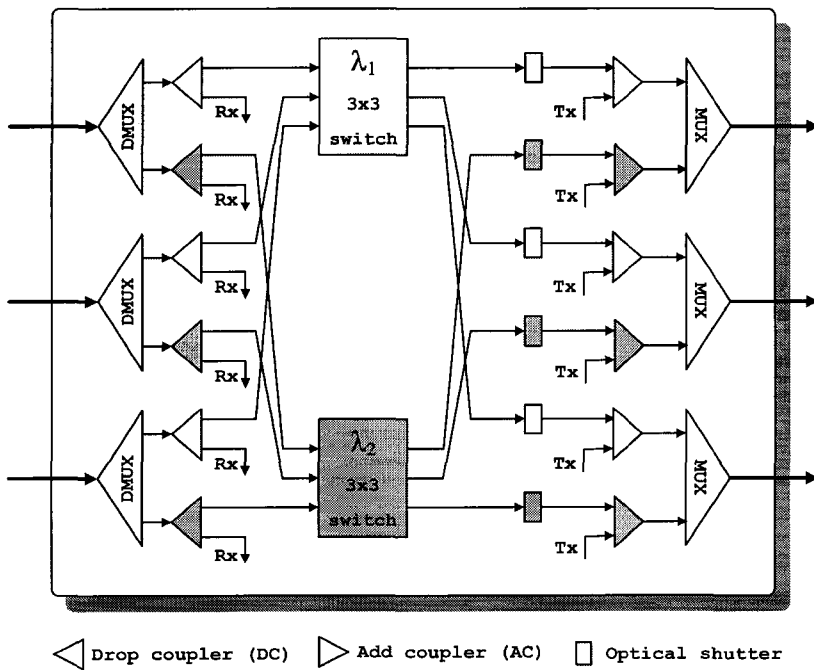


Figure 5.3 An example light trail node structure with three input fibers with two wavelengths on each fiber.

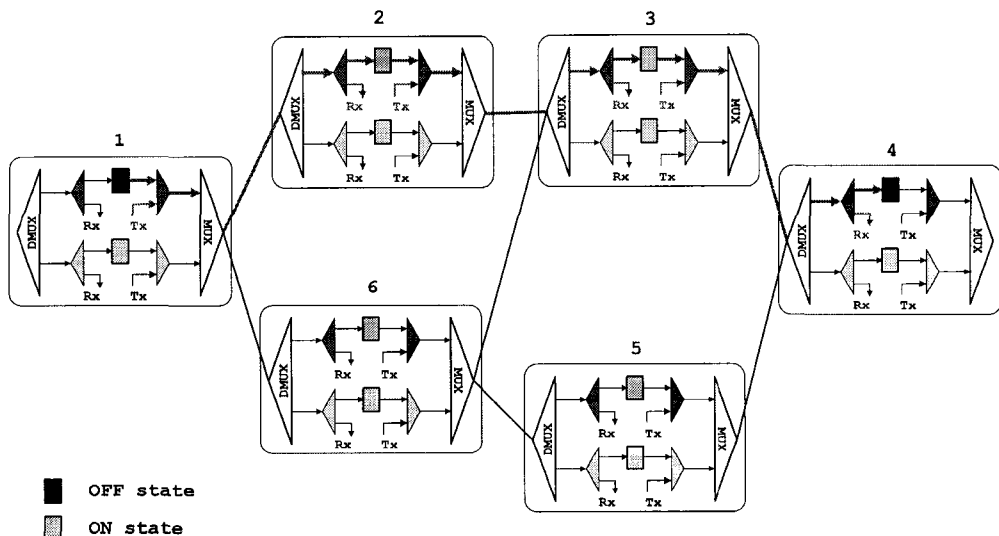


Figure 5.4 An example node configuration in light trail framework.

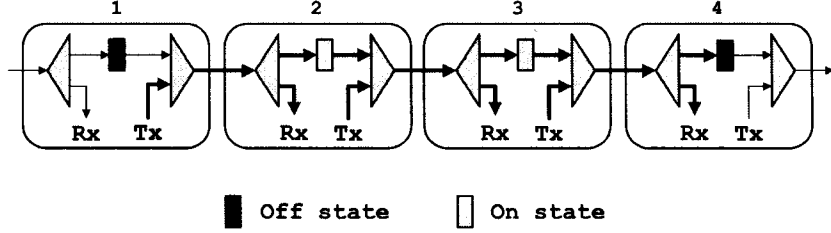


Figure 5.5 Detailed node configuration of the light trail in Figure 5.4.

Due to the power loss within the light trail, which mainly comes from the power splitting at each node, the length of a light trail is limited and is estimated in terms of hop-length. The expected length of a light trail is 4 to 6 hops, and a reasonable hop-length of a light trail is 5 [26].

5.1.3 Light Trail Characteristics

In contrast to OBS, we do not need to configure any switches when using light trails to carry IP bursts. This leads to an excellent provisioning time [26]. Moreover, the major advantage of using light trails for burst traffic, as compare to OBS, is the improved wavelength utilization. Utilization is defined as the ratio of capacity used over time for actual data transmission to the total reserved capacity. The study in [26] shows that the utilization in OBS is severely degraded comparing to that in light trails as the network load increases. More specifically, the utilization of light trails is an order of magnitude better than that in OBS under similar conditions.

Multicasting in optical layer is another salient feature of light trail architecture. Nodes in a light trail are able to send the same quanta of information to a set of downstream nodes without the need for a special processing or control arbitration.

In general, the light trail offers a technologically exclusive solution that enables a number of salient features and is practical. It exhibits a set of properties that distinguishes and differentiates light trails from other platforms. The following three characteristic properties of light trails make possible this differentiation:

- The light trail provides a way to groom traffic from many nodes to share a wavelength path to transmit their subwavelength capacity traffic.
- The light trail is built using mature components that are configured in such a way that allows extremely fast provisioning of network resources. This allows for dynamic control for the fluctuating bandwidth requirements.
- The light trail offers a method to group a set of nodes at the physical layer to create optical multicasting - a key feature for the success of many applications.
- The maturity of components leads to the implementation of light trails in a cost effective manner resulting in economically viable solutions for mass deployment.

5.2 Light Trail Design

To identify a set of light trails to carry the given traffic is one of the key issues in setting up light trails in a WDM network. The performance of light trail in terms of wavelength utilization also depends on the location of the light trails. The goal of the design problem therefore is to develop an effective method to groom traffic in light trail architecture and come up with a set of light trails. The light trail design problem is stated as follows:

Given graph $G(V, E)$, where $|V| = N$, and traffic matrix $D_{N \times N}$, how to define a minimum number of light trails to carry the given traffic.

The design problem is expected to be a hard problem. The approach presented here, which identifies a set of light trails to be set up in a network, consists of two steps. The first step is called *traffic matrix preprocessing*. As stated earlier, due to the power losses on the lines, a long light trail may not be advisable. The length of a light trail is limited and is specified in terms of hop-length, denoted by Tl_{max} . Therefore in the first step, a single long hop traffic is recursively divided into multiple hops.

The second step is to formulate the design problem and solve it as an ILP optimization problem, for the given network topology and refined traffic matrix obtained from step one.

The objective here is to find a minimum number of light trails that are required for the system to carry the traffic.

5.2.1 Step I: Traffic Matrix Preprocessing

In the preprocessing of the traffic matrix, a single long hop traffic is divided into multiple hops to satisfy the hop-length constraint. Recall the distance matrix $H_{N \times N} = \{h_{st}\}$, where h_{st} denotes the physical distance from node s to node t .

The length of a light trail is a main constraint due to the loss both at nodes and over the links. Let Tl_{max} be the maximum length of a light trail. For traffic between s-d pair (i, j) , where $h_{st} > Tl_{max}$, it is not possible to accommodate this traffic on a direct light trail. Thus this traffic will need to go through multiple hops. Here one light trail is counted as one “hop”. This necessitates the first step in our approach, namely *traffic matrix preprocessing*.

Let $D_{N \times N} = \{d_{st}\}$ denote the given (estimated) traffic matrix. Traffic matrix pre-processing will return a modified traffic matrix that satisfies: $D_{N \times N} = \{d_{st} : h_{st} \leq Tl_{max}, \forall d_{st} > 0\}$. Figure 5.6 provides the pseudo code for traffic matrix preprocessing algorithm.

In this step, the traffic on s-d pair (s, t) with $h_{st} > Tl_{max}$, will be reallocated on multiple hops. The goal is to find a node n such that path from node s to node n forms the first hop which is less than Tl_{max} in distance. A next intermediate node n is found recursively for the source node. Among all possible intermediate nodes, n is chosen to be as close to the destination node as possible, as shown in step 1 in Figure 5.6. This is done in order to reduce the number of hops that the original traffic has to take.

After the preprocessing of the traffic matrix, each non-zero element in the modified traffic matrix would have corresponding distance less than Tl_{max} , which is the maximum length allowed for a light trail.

5.2.2 Step II: ILP Formulation

Given the network topology $G_p(V, E)$, and the traffic matrix obtained from *step I*, we first list all possible paths with the hop-length limit constraint for each s-d node pair, this can be

<p>INPUT: Graph $G = (V, E)$ and a traffic matrix $D_{N \times N}$.</p> <p>OUTPUT: Rearranged traffic matrix $D_{N \times N}$ and the distance matrix $H_{N \times N}$.</p> <p>ALGORITHM:</p> <p><i>Step 0:</i> Apply Dijkstra's shortest path algorithm, calculate distance matrix $H_{N \times N}$.</p> <p><i>While</i> (find $(s, t) : d_{st} > 0, h_{st} > Tl_{max}$)</p> <p>{</p> <ol style="list-style-type: none"> 1. Pick an intermediate node n: $n = \arg \min_{v \in V} \{d_{vt} d_{sv} \leq Tl_{max}\};$ 2. Update traffic matrix $D_{N \times N}$: <ol style="list-style-type: none"> (a) $d_{sn} \leftarrow d_{sn} + d_{st}$; (b) $d_{nt} \leftarrow d_{nt} + d_{st}$; (c) $d_{st} \leftarrow 0$. <p>}</p>
--

Figure 5.6 Light trail design step 1: Traffic matrix preprocessing.

accomplished by applying *breadth first search* for each node. These eligible paths form a set of all possible light trails. Among all these possible choices, we then choose an optimal set of paths to form the light trail network, such that the total number of light trails are minimized. This problem is formulated as an ILP optimization problem. We also assume that each request can not be divided into different parts and transferred separately.

5.2.3 Notations

5.2.3.1 Parameters

For the given directed graph $G_p(V, E)$, $N = |V|$, let LT be the set of all the possible light trails within hop-length limit Tl_{max} , and $\tau = 1, 2, \dots, |LT|$ be the number assigned to each light trail in the LT .

We consider only fractional wavelength capacity in this study, therefore, $d_{st} \leq C$. We

assume the network is a single fiber network. In the absence of wavelength converters, the wavelength continuity constraints still need to hold for light trail networks. Here, we do not impose constraints on the number of wavelengths available per link. Yet, as we will see later on, the number of wavelengths required for establishing the light trails is not high.

5.2.3.2 Variables

- μ_{st}^τ : (binary variable) route indicator, takes value of 1 if request (s, t) takes light trail τ ; zero otherwise. This also implies that node s and t are on trail τ and s is t 's upstream node. Notice that node s and t do not have to be neighbors in a light trail.
- δ^τ : (binary variable) light trail usage indicator, takes value of 1 if trail τ is used by any request; zero otherwise.

5.2.3.3 ILP Formulation

1. Objective:

$$\min \sum_{\tau} C_{\tau} \times \delta^{\tau}. \quad (5.1)$$

When $C_\tau = 1$, the objective is to minimize the number of light trails that are required in the network. When C_τ is defined as the *hop-length* of light trail τ , the problem becomes to minimize the total wavelength-links in the network, which represents the total reserved capacity in the networks. This can be used to optimize the wavelength capacity utilization, while it might consume more light trails.

2. *Assignment constraint*: Each request is assigned to one and only one light trail.

$$\sum_{\tau} \mu_{st}^{\tau} = 1 \quad \forall (s, t) : d_{st} \in D, d_{st} > 0 \quad (5.2)$$

3. *Light trail capacity constraint*: The aggregated request capacity on a light trail should not exceed the full wavelength capacity.

$$\sum_{(s,t)} \mu_{st}^\tau d_{st} \leq C \quad (5.3)$$

4. *Light trail usage constraint:* If any of the s-d pair is assigned on light trail τ , δ^τ is set to 1; otherwise, if none of the s-d pairs picked light trail τ , $\delta^\tau = 0$. Recall that δ^τ is a binary variable.

$$\delta^\tau \geq \mu_{st}^\tau \quad \forall (s, t) : d_{st} \in D \quad (5.4)$$

5.2.4 Solution Consideration

The light trail design is a challenging problem for the following reasons.

First, in order to use a wavelength fully, one would like to *groom* near full-wavelength capacity traffic onto the wavelength. This is similar to a normal traffic grooming problem, which is often formulated as a *bin packing problem* and it is known to be an NP-complete problem. However, we cannot simply set up a light trail for any set of traffic requests that add up to C . For example, given that $d_{12} + d_{13} + d_{16} = C$, it might not be possible to establish the desired light trail due to the physical hop-length constraint. Hence, the light trail hop-length limit also adds to the complexity of the problem.

Second, the ILP formulation of the light trail design problem is similar to the *bin packing* problem, which is an NP-hard problem. However, if we treat light trails as the “bins”, and elements in the given traffic matrix as the “items” in bin packing problem, this problem differs from a normal bin packing problem due to a potential physical route constraint that an item cannot be put in any of the given bins, but only a sub-set of the bins. More specifically, an s-d pair can be assigned to the routes which satisfy: 1) node s and t belong to the route; 2) node s is the upstream node of node t along the route. Hence, the approximate algorithms for solving normal bin packing problems cannot be directly applied here for solving this light trail design problem.

5.3 Light Trail Design: Heuristic Approaches

We propose the following heuristic algorithms for light trail design. As it is well known, first-fit and best-fit are two common and effective heuristic algorithms for solving bin packing problems. Here we choose best-fit algorithm for solving the light trail design problem.

5.3.1 The Best-Fit Approach

Recall that after the traffic matrix preprocessing, each request in the newly obtained traffic matrix satisfies the light trail hop-length limit, that is, the shortest hop-length for each $s - d$ pair is no greater than Tl_{max} .

The goal of the second step is to identify a set of light trails for carrying the given traffic. To do this, we first pick up the $s - d$ pair which has the longest distance in the distance matrix H_{st} . Since a light trail between this s-d pair will be eventually required.

Once we pick up an s-d pair with the longest physical hop-length, the *head* and *tail* of a light trail are decided. The goal now is to find the *best* eligible light trail between these two end nodes. This is analogous to fully pack a “bin” in the bin packing problem. There are two subproblems need to be solved. First, the selection of a path (within the hop-length limit) between these two nodes is required. Second, the assignment of requests to this light trail needs to be identified.

In order to find the best light trail between the known *head* and *tail* nodes, we perform an exhausting search among all the possible paths between these two nodes. *Best-fit* here tries to pick up the path between the given two end nodes that is the *best* among all the paths between these *head* and *tail* nodes, instead of all candidate paths. This is still a *local* search, therefore, the final results might not be global optimal.

For each eligible path between the known *head* and *tail* nodes, we first sort all possible s-d pairs along this path according to their required capacity. There are two different ways of packing them onto a path rather than do it randomly. One is to allocate the smallest requests first, which is called *increasing packing*, the other way is to allocate the biggest requests first, hence it is named *decreasing packing*.

- Increasing packing tries to allocate finer requests first, so that the number of requests that can be packed onto this path is maximized. There might still be some capacity left on this light trail, but that is not sufficient for the next smallest request. This approach would groom as many requests as possible onto the light trail, thereby, leaving the rest of the network with fewer number of requests that are left to be allocated. The expectation is that this contributes to the saving on total number of light trails that are needed in the network. However, for each light trail, the packing efficiency might not be the most efficient, in other words, the spare capacity might not be minimized.
- Decreasing packing tries to allocate bigger requests first, and leaves the light trail with minimum spare capacity. However, since the big requests are allocated first, the total number of requests that can be carried by the light trail might be less than that of the allocation on *Increasing packing*. Therefore, it could leave more requests unallocated in the network and more light trails might need to be set up later on in order to carry all the requests. The spare capacity on each light trail is minimized in this approach at the time of allocating the capacity.

It is not clear which approach works better and always gives the minimum number of light trails required in the network. It depends on the traffic patterns. A preferred approach is to try both and choose the one that provides a better solution for the given data.

5.3.2 Algorithm Design

With the known graph, we first find out all possible paths for each s-d pair, save the path information in the following structure called $KSPath[N][N][NRoute_{max}]$ which contains the path information for each route in the network.

For later convenience usage, we sort the paths according to their physical hop-length, such that $KSPath[head][tail][1]$ contains the path information (*hop-length, intermediate nodes along this path*) of the first shortest path from **head** to **tail**.

Figure 5.7 gives the pseudo code of the local best-fit algorithm. In this pseudo code, *seq* is used to denote which route among all valid routes from **head** and **tail** is chosen to be the trail.

Also noticing that we are only dealing with sub-wavelength level requests here, by default, a shortest path will be chosen as the light trail to carry a given request if no better path can be found. That is, initially $seq = 1$.

More criteria can be added when there is a tie of selecting a route. We choose the one which can accommodate more requests, this is not included in the pseudo code in Figure 5.7. As mentioned earlier, sorting $AllRequest[]$ in different ways gives us different algorithms namely, *local best-fit decreasing packing* and *local best-fit increasing packing*.

5.3.3 Discussions

The proposed heuristic algorithm has two steps, as shown in Figure 5.6 and 5.7. Both the first and second step would need the information of paths between each $s - d$ pairs. Therefore, we first find out all possible paths for each s-d pairs. The worst case complexity of the exhausting search for each s-d pair is $O(N^3)$. The total running time for finding all possible routes is $O(RN^3)$, where R is the number of s-d pairs (requests). In fact, instead of searching for all paths, we can search among K -shortest path with K being big enough. This could reduce the complexity to $O(N(E + N \log N + KN))$ for all node pairs [56]. This may be a promising choice for big networks.

In best-fit packing of step 2, for each s-d pair, we search among all K paths for the best-fit one. For path τ with n_τ nodes, there are maximum $t = (n_\tau - 1) + (n_\tau - 2) + \dots + 1 = O(n_\tau^2)$ s-d pairs, where n_τ is bounded by Tl_{max} , hence $t = O(Tl_{max}^2)$. The sorting takes $O(t \log t)$ loops, and packing takes another t loops. Totally $O(t \log t)$ loops for each path. There are K paths, and the same procedure will be performed on the selected best-fit path. Therefore, totally $O(K(t \log t)) = O(K(Tl_{max}^2 \log Tl_{max}))$ loops are needed for each s-d pair. At least one s-d pair will be eliminated from matrix R in Figure 5.7, the program stops when R is empty.

5.4 Performance Study

To evaluate the performance of the above ILP formulations and the heuristic algorithms that we proposed earlier, experiments are performed on a physical topology given in Figure 5.8.

INPUT: Graph $G = (V, E)$, the rearranged traffic matrix $D_{N \times N}$ and distance matrix $H_{N \times N}$.

OUTPUT: A collection of light trail.

ALGORITHM:

Initializations: $d = 0$, $R = \{(m, n) : d_{m,n} > 0\}$.

Do {

1. $(m, n) = \arg \max\{h_{m,n} : (m, n) \in R\}$.
 $head = m$, $tail = n$.
2. $Trail_{cap} = d_{m,n}$, $newstream = Trail_{cap}$,
 $best = 0$, $seq = 1$.
3. **for**($\tau = 1$; $\tau \leq NRoute_{max}$; $\tau ++$)
if($KSP[head][tail][\tau].length \leq Tl_{max}$)
 - (a) Copy all s-d pairs along path $KSP[head][tail][\tau]$ that need to be allocated to array $AllRequest[\]$.
The length of $AllRequest[\]$ is known and denoted by NSD ;
 - (b) Sort $AllRequest[\]$ according to the capacities;
 - (c) **for**($tmp = 1$; $tmp \leq NSD$; $tmp ++$)
if ($newstream + AllRequest[tmp].cap \leq C$)
 $newstream = newstream + AllRequest[tmp].cap$;
 - (d) **if** ($newstream > best$)
 - {
 - $best = newstream$;
 - $seq = \tau$;
 - }
4. Copy all s-d pairs along path $KSP[head][tail][seq]$ that need to be allocated to array $AllRequest[\]$.
The length of $AllRequest[\]$ is known and denoted by NSD ;
5. **for**($tmp = 1$; $tmp \leq NSD$; $tmp ++$)
if ($newstream + AllRequest[tmp].cap \leq C$)
 - {
 - $Trail_{cap} = Trail_{cap} + AllRequest[tmp].cap$;
 - $d_{AllRequest[tmp].src, AllRequest[tmp].dst} = 0$;
 - }

} *While* ($R \neq \Phi$)

Figure 5.7 Light trail design step 2: Best-Fit approach.

To simplify the problem, we assume each physical link is bidirectional with the same length.

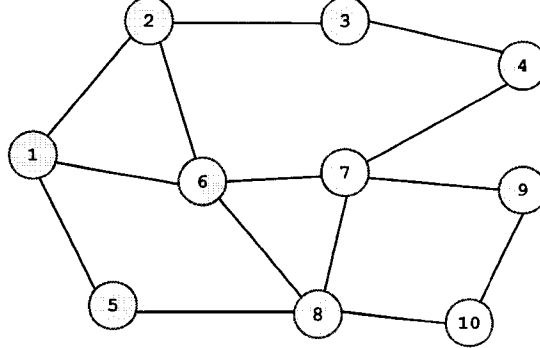


Figure 5.8 A 10-node example network.

Table 5.1 gives a randomly generated traffic matrix for this example. The integer numbers indicate the requested capacity in unit of OC-1 (51.84 Mbps), the entire wavelength capacity is OC-48. Here we only consider the fractional wavelength capacity for traffic grooming in light trail networks. Intuitively, if every $s-d$ pair requires capacity greater than half of the full wavelength capacity, no two requests can be groomed on a light trail. Thus, it is that most $s - d$ pairs request a small fractional capacity of the full wavelength channel. Hence, we randomly generate requested capacities between 0 and 11 as shown in Table 5.1.

Table 5.1 Traffic matrix for a 10-node network.

	1	2	3	4	5	6	7	8	9	10
1	0	5	8	11	3	8	5	7	8	10
2	3	0	8	4	0	5	1	2	3	1
3	9	3	0	7	3	10	11	8	0	6
4	6	0	8	0	2	5	5	2	1	1
5	0	6	10	4	0	2	11	10	5	2
6	11	3	4	4	3	0	2	6	8	3
7	0	2	10	2	11	5	0	1	6	0
8	0	5	6	2	3	1	11	0	5	0
9	4	5	11	8	8	2	3	1	0	5
10	0	9	9	3	7	10	1	2	1	0

5.4.1 Light Trail Hop-Length Limit: $Tl_{max} = 4$

We use CPLEX Linear Optimizer 7.0 [57] to solve the ILP formulation proposed in 5.2.2. We assume that each candidate path can be used once, that is, $u = 1$. Assume the hop-length limit $Tl_{max} = 4$, from the topology we can observe that all s-d pairs have paths within this hop-length limit, hence, the *traffic matrix preprocessing* will not make any change in the given traffic matrix.

Table 5.2 presents the results from solving the ILP formulation with hop-length limit $Tl_{max} = 4$. It can be observed that $W = 4$ is sufficient on each link, although we do not impose constraints on number of wavelengths.

Table 5.2 ILP: Resulting light trails $Tl_{max} = 4$.

No.	Light Trails	Hop-length	Accommodated $s - d$ Pairs	Load
1	{2, 3, 4, 7, 9}	4	(3,7) (3,4) (2,7) (2,9) (4,9)	23
2	{3, 2, 6, 8, 10}	4	(2,6) (2,8) (2,10) (3,6) (3,8) (3,10)	32
3	{4, 3, 2, 1, 5}	4	(4,1) (4,3) (4,5) (3,5) (1,5) (3,1) (2,1)	34
4	{4, 7, 6, 8, 10}	4	(6,8) (6,10) (4,6) (4,7) (4,8) (4,10)	22
5	{5, 1, 2, 3, 4}	4	(1,2) (1,3) (1,4) (5,2) (5,3) (5,4) (2,4)	48
6	{5, 1, 6, 7, 9}	4	(1,7) (1,9) (6,9)	21
7	{5, 1, 6, 8, 10}	4	(1,8) (1,10) (1,6) (5,6)	27
8	{5, 8, 7, 9, 10}	4	(9,10) (8,9) (5,9) (5,8) (5,7) (7,9) (5,10)	44
9	{9, 7, 4, 3, 2}	4	(9,2) (9,3) (9,4) (7,3) (7,2) (3,2)	39
10	{9, 7, 6, 1, 5}	4	(7,6) (6,5) (9,1) (9,6) (6,1)	25
11	{10, 8, 6, 2, 3}	4	(10,3) (10,2) (8,3) (8,2) (6,3) (6,2) (2,3)	44
12	{10, 8, 6, 7, 4}	4	(10,6) (10,4) (7,4) (6,4) (6,7) (8,4) (8,6) (8,7)	35
13	{10, 9, 7, 8, 5}	4	(10,9) (10,8) (10,7) (10,5) (9,8) (9,7) (9,5) (8,5) (7,8) (7,5)	38

Table 5.2 shows the 13 light trails are needed to carry the given traffic. The traffic assignment obtained from solving ILP formulation is also listed. For each light trail, the summation of all the traffic it carries is calculated and shown in the right most column in Table 5.2.

Table 5.3 presents the results from solving the local best-fit heuristic algorithm proposed in Section subsection:BestFitApproach. In this example, local best-fit increasing packing approach gives a solution 16 light trails.

5.4.2 Light Trail Hop-Length Limit: $Tl_{max} = 3$

When the light trail hop-length limit is set to $Tl_{max} = 3$, requests between some node pairs in the network shown in Figure 5.8 have to be divided and allocated to multiple light

Table 5.3 Local Best-Fit: Resulting light trails $Tl_{max} = 4$.

No.	Light Tails	Hop-length	Accommodated $s - d$ Pairs	Load
1	{3, 2, 6, 8, 10}	4	(3,10) (2,10) (2,8) (3,2) (6,10) (2,6) (6,8) (3,8) (3,6)	44
2	{10, 8, 6, 2, 3}	4	(10,3) (8,6) (10,8) (6,2) (6,3) (8,2) (8,3) (2,3) (10,2)	47
3	{1, 6, 2, 3, 4}	4	(1,4) (6,4) (2,4) (1,2) (3,4) (1,3) (1,6)	47
4	{1, 5, 8, 10, 9}	4	(1,9) (10,9) (5,10) (1,5) (8,9) (5,9) (1,8) (1,10)	41
5	{2, 6, 8, 7, 9}	4	(2,9) (2,7) (6,7) (7,9) (6,9) (8,7)	31
6	{3, 4, 7, 8, 5}	4	(3,5) (7,8) (4,5) (4,8) (8,5) (4,7) (7,5) (3,7)	38
7	{4, 3, 2, 6, 1}	4	(4,1) (2,1) (4,6) (4,3) (3,1) (6,1)	42
8	{4, 7, 9, 10}	3	(4,10) (4,9) (9,10)	7
9	{5, 8, 7, 4, 3}	4	(5,3) (8,4) (7,4) (5,4) (5,8) (7,3)	38
10	{9, 7, 6, 2, 1}	4	(9,1) (9,6) (7,2) (9,7) (7,6) (9,2)	21
11	{9, 7, 4, 3}	3	(9,3) (9,4)	19
12	{9, 10, 8, 5}	3	(9,5) (9,8) (10,5)	16
13	{10, 8, 6, 7, 4}	4	(10,4) (10,6) (10,7)	14
14	{1, 5, 8, 6, 7}	4	(1,7) (5,6) (5,7)	18
15	{5, 1, 2}	2	(5,2)	6
16	{6, 1, 5}	2	(6,5)	3

trails. More specifically, the shortest paths between Node 3 and Node 10 have hop-length of 4. Therefore, the request between these two nodes cannot be accommodated on single light trails. The *traffic matrix preprocessing* heuristic re-arranges the original traffic $d_{3,10}$ onto $d_{3,8}$ and $d_{8,10}$. Similarly, the request from Node 10 to Node 3 is aggregated onto node-pair (10,2) and (2,3). The resulting traffic matrix is shown in Table 5.4.

Table 5.4 Traffic matrix for a 10-node network: After traffic matrix pre-processing.

	1	2	3	4	5	6	7	8	9	10
1	0	5	8	11	3	8	5	7	8	10
2	3	0	17	4	0	5	1	2	3	1
3	9	3	0	7	3	10	11	14	0	0
4	6	0	8	0	2	5	5	2	1	1
5	0	6	10	4	0	2	11	10	5	2
6	11	3	4	4	3	0	2	6	8	3
7	0	2	10	2	11	5	0	1	6	0
8	0	5	6	2	3	1	11	0	5	6
9	4	5	11	8	8	2	3	1	0	5
10	0	18	0	3	7	10	1	2	1	0

Solving the ILP formulation with this modified traffic matrix gives an optimal solution consisting of 23 light trails as shown in Table 5.5. Experiments by using both local best-fit

increasing and decreasing packing algorithms are performed, and the better solution with a result of 24 light trails is chosen. The detailed results are shown in Table 5.6.

Table 5.5 ILP: Resulting light trails $Tl_{max} = 3$.

No.	Light Trails	Hops	Accommodated s-d Pairs	Load
1	{1, 6, 7, 4}	3	(1,4) (6,4)	15
2	{1, 6, 7, 9}	3	(1,6) (1,7) (1,9) (6,7) (7,9)	29
3	{1, 5, 8, 10}	3	(1,8) (1,10)	17
4	{2, 3, 4, 7}	3	(2,4) (3,4) (3,7)	22
5	{2, 6, 7, 9}	3	(2,6) (2,7) (2,9) (6,9)	17
6	{2, 6, 8, 10}	3	(2,8) (2,10) (6,8) (6,10) (8,10)	18
7	{3, 2, 1, 5}	3	(3,2) (3,1) (3,5) (2,1) (1,5)	21
8	{3, 2, 6, 8}	3	(3,6) (3,8)	24
9	{4, 7, 6, 1}	3	(4,6) (4,1)	11
10	{4, 7, 8, 5}	3	(4,7) (4,8) (4,5) (7,8) (7,5) (8,5)	24
11	{4, 7, 9, 10}	3	(4,9) (4,10)	2
12	{5, 1, 2, 3}	3	(5,2) (5,3) (1,2) (1,3) (2,3)	46
13	{5, 8, 7, 4}	3	(5,8) (5,7) (5,4) (8,7) (8,4)	38
14	{5, 8, 6}	2	(5,6)	2
15	{5, 8, 10, 9}	3	(5,10) (5,9) (8,9)	12
16	{6, 8, 5, 1}	3	(6,5)	3
17	{8, 6, 2, 3}	3	(8,3) (6,3)	10
18	{9, 7, 6, 1}	3	(9,1) (7,6) (6,1)	20
19	{9, 7, 6, 2}	3	(9,6) (9,2) (7,2)	9
20	{9, 7, 4, 3}	3	(9,7) (9,4) (9,3) (7,4) (7,3) (4,3)	42
21	{9, 10, 8, 5}	3	(9,10) (9,8) (9,5) (10,5)	21
22	{10, 8, 6, 2}	3	(10,8) (10,6) (10,2) (8,6) (8,2) (6,2)	39
23	{10, 9, 7, 4}	3	(10,9) (10,7) (10,4)	5

5.4.3 Light Trail Hop-Length Limit: $Tl_{max} = 5$

When Tl_{max} increases to 5, the running time to solve ILP formulation increases dramatically. This is because, as earlier mentioned, the number of candidate paths increases very fast as Tl_{max} increases. This increase introduces a significant number of variables and constraints in the ILP formulation. The optimal solution contains 10 light trails, the detailed results are shown in Table 5.7. The heuristic algorithms give solutions in seconds. The better solution obtained from using both best-fit increasing packing order and best-fit decreasing order packing consists of 13 light trails as shown in Table 5.8.

Table 5.6 Local Best-Fit: Resulting light trails $Tl_{max} = 3$.

No.	Light Trails	Hops	Accommodated s-d Pairs	Load
1	{1, 6, 7, 4}	3	(1,4) (1,6) (1,7) (6,4) (7,4) (6,7)	32
2	{1, 6, 7, 9}	3	(1,9) (6,9) (7,9)	22
3	{1, 5, 8, 10}	3	(1,10) (5,8) (1,8) (8,10) (1,5) (5,10)	38
4	{2, 6, 7, 9}	3	(2,9) (2,6) (2,7)	9
5	{2, 6, 8, 10}	3	(2,10) (2,8) (6,8) (6,10)	12
6	{3, 2, 1, 5}	3	(3,2) (3,1) (3,5) (2,1)	18
7	{3, 4, 7, 8}	3	(3,8) (3,7) (3,4) (4,7) (4,8) (7,8)	40
8	{4, 7, 6, 1}	3	(4,6) (4,1) (6,1) (7,6)	27
9	{4, 7, 8, 5}	3	(4,5) (7,5) (8,5)	16
10	{4, 7, 9, 10}	3	(4,9) (4,10) (9,10)	7
11	{5, 1, 2, 3}	3	(5,2) (5,3) (1,2) (1,3) (2,3)	46
12	{5, 8, 7, 4}	3	(5,4) (5,7) (8,7) (8,4)	28
13	{5, 8, 10, 9}	3	(5,9) (8,9) (10,9)	11
14	{8, 6, 2, 3}	3	(8,3) (8,6) (8,2) (6,3) (6,2)	19
15	{9, 7, 6, 1}	3	(9,1) (9,7) (9,6)	9
16	{9, 7, 6, 2}	3	(9,2) (7,2)	7
17	{9, 7, 4, 3}	3	(9,3) (9,4) (7,3) (4,3)	37
18	{9, 10, 8, 5}	3	(9,5) (9,8) (10,8) (10,5)	18
19	{10, 8, 6, 2}	3	(10,2) (10,6)	28
20	{10, 8, 7, 4}	3	(10,4) (10,7)	4
21	{2, 3, 4}	2	(2,4)	4
22	{3, 2, 6}	2	(3,6)	10
23	{5, 1, 6}	2	(5,6)	2
24	{6, 1, 5}	2	(6,5)	3

Table 5.7 ILP: Resulting light trails $Tl_{max} = 5$.

No.	Light Trails	Hops	Accommodated s-d Pairs	Load
1	{1, 2, 3, 4, 7, 6}	5	(1,4) (1,6) (1,7) (3,6) (4,6)	39
2	{2, 1, 6, 7, 9, 10}	5	(2,1) (2,6) (2,7) (2,9) (2,10) (1,9) (1,10) (9,10) (6,9) (6,10)	47
3	{3, 4, 7, 8, 10, 9}	5	(3,7) (3,8) (3,10) (4,7) (4,8) (4,9) (4,10) (7,8) (7,9) (10,9)	42
4	{4, 3, 2, 1, 5, 8}	5	(4,1) (4,5) (3,2) (3,1) (3,5) (1,5) (1,8) (2,8)	35
5	{5, 1, 6, 2, 3, 4}	5	(5,6) (5,4) (1,2) (1,3) (6,2) (6,3) (2,3) (2,4) (3,4)	45
6	{5, 8, 10, 9, 7, 6}	5	(5,10) (5,9) (8,9) (8,7) (8,6) (10,6) (9,6) (7,6)	41
7	{6, 1, 5, 8, 7, 4}	5	(6,1) (6,5) (6,8) (6,7) (6,4) (5,8) (5,7)	47
8	{9, 7, 8, 5, 1, 2}	5	(9,7) (9,5) (9,1) (9,2) (7,5) (7,2) (8,2) (5,2)	44
9	{9, 10, 8, 7, 4, 3}	5	(9,8) (9,4) (9,3) (10,8) (10,7) (10,4) (8,4) (7,4) (7,3) (4,3)	48
10	{10, 8, 5, 1, 2, 3}	5	(10,5) (10,2) (10,3) (8,5) (8,3) (5,3)	44

Table 5.8 Local Best-Fit: Resulting light trails $Tl_{max} = 5$.

No.	Light Trails	Hops	Accommodated $s-d$ Pairs	Load
1	{3, 2, 6, 7, 8, 10}	5	(3,10) (3,6) (3,8) (6,8) (2,6) (3,2) (6,10) (2,8) (6,7) (2,7) (2,10) (7,8)	48
2	{10, 8, 7, 6, 2, 3}	5	(10,3) (2,3) (8,3) (8,2) (7,6) (6,3) (6,2) (10,8) (7,2) (10,7) (8,6)	46
3	{1, 5, 8, 6, 7, 4}	5	(1,4) (1,6) (1,8) (1,7) (5,4) (6,4) (1,5) (5,6) (8,4) (7,4)	48
4	{1, 2, 3, 4, 7, 9}	5	(1,9) (1,3) (3,4) (7,9) (1,2) (4,7) (2,4) (2,9) (4,9)	47
5	{1, 5, 8, 7, 9, 10}	5	(1,10) (8,7) (5,8) (5,9) (8,9) (9,10) (5,10)	48
6	{3, 4, 7, 6, 8, 5}	5	(3,5) (3,7) (7,5) (4,6) (6,5) (8,5) (4,5) (4,8)	40
7	{4, 3, 2, 6, 1}	4	(4,1) (6,1) (3,1) (4,3) (2,1)	37
8	{4, 7, 8, 10}	3	(4,10)	1
9	{5, 8, 7, 6, 2, 3}	5	(5,3) (5,7) (7,3) (5,2)	37
10	{9, 10, 8, 6, 2, 1}	5	(9,1) (10,6) (10,2) (9,2) (9,6) (9,8)	31
11	{9, 10, 8, 7, 4, 3}	5	(9,3) (9,4) (9,7) (10,4)	25
12	{9, 10, 8, 5}	3	(9,5) (10,5)	15
13	{6, 8, 10, 9}	3	(6,9) (10,9)	9

5.4.4 Discussions

An observation from the optimal solutions obtained by solving ILP formations is that only the longest candidate paths are chosen as light trails. This is due to the fact that only the number of light trails is being minimized. The program stops searching as the number of light trails does not decrease, even though it is possible to substitute some light trails with shorter paths.

The problem becomes unmanageable to ILP approach as the problem size increases. In these scenario, relaxation techniques could be a preferred choice. When the traffic is uniform or the variation among different requests are small enough that they can be approximately treated as uniform traffic, $D_{N \times N} = \{d_{s,t} = \bar{d} | \forall (s,t)\}$. LP relaxation is a very effective means for obtaining fast solutions. This can be achieved by modifying ILP formulation 5.2.2 as follows, and the rest of the formulation remains the same.

$$\sum_{(s,t)} \mu_{s,t}^{\tau} \leq \lfloor C/\bar{d} \rfloor \quad (5.5)$$

$$0 \leq \delta^{\tau} \leq 1 \quad (5.6)$$

$$0 \leq \mu_{s,t}^{\tau} \leq 1 \quad (5.7)$$

In this formulation, the coefficient matrix of the variables is totally unimodular, hence, the LP relaxation still yields integer solutions. This can be applied to solve light trail design problem where the traffic requests have similar capacities.

5.5 Summary

The concept of light trails has been proposed as a novel architecture designed for carrying finer granularity IP burst traffic. The fast access of lightpath communication and the flexible dynamic sub-wavelength provisioning make light trail architecture a strong candidate for transporting IP traffic over optical networks. As a newly proposed concept, light trail architecture also brings up various issues in designing optical networks for transporting IP centric traffic.

How to identify a set of light trails in the design phase is one of the key issues in light trail implementations. In this chapter we proposed an exact ILP formulation for obtaining optimal light trail design with minimum cost (in terms of number of light trails as well as the number of wavelengths). A simplified formulation with possible LP-relaxations is given as well. We also designed two algorithms, namely *local best-fit increasing packing* and *local best-fit decreasing packing*. Heuristic algorithms do not guarantee the optimality of the solution. However, their capability of obtaining fast and near optimal solutions is still preferred, especially when the problem is unmanageable to ILP approaches.

CHAPTER 6. Survivable Grooming Network Design

6.1 Introduction

WDM significantly increases the capacity of a fiber by allowing simultaneous transmission of multiple wavelengths (channels), each operating at rates up to 10Gb/s. There are several critical issues involved in using WDM optical networks effectively. We address two important issues of current interest in this chapter.

1. Due to the high bandwidth involved, any link failure that leaves fiber unusable will have catastrophic results. Thus protection and restoration schemes for the interrupted services must form an integral part of the network design and operation strategies. Although network survivability can be achieved at the higher layers above the optical layer, e.g., self-healing in SONET rings, using alternate ATM virtual path, fast rerouting in MPLS, and changing routes using dynamic routing protocols in the IP layer, it is advantageous to use optical WDM survivability mechanisms since they offer a common and fast survivability platform for services to the higher layers. Moreover, due to the availability of multiple paths on the same fiber, the higher layers may not be aware of and may plan to use an alternate path through the same fiber, obviously that will not work.
2. The bandwidth on a wavelength is close to the peak electronic transmission speed and has steadily increased from OC-48 (2.5 Gbps) to OC-192 (10Gbps), and is expected to increase up to OC-768 (40 Gbps). The available bandwidth on a wavelength is becoming too large for certain traffic. Several types of further traffic multiplexing on a wavelength are thus proposed [21, 25, 13]. One approach to provisioning fractional wavelength capacity is to multiplex traffic on a wavelength. The resulting networks are referred to as

WDM grooming networks. The aim of this research is to enable grooming capability in the design of survivable WDM mesh networks.

This chapter deals with lightpath protection schemes for subwavelength level traffic grooming networks, which are defined as shared-wavelength grooming networks with wavelength continuity constrained grooming nodes. This chapter is organized as follows: the remainder of Section 6.1 reviews prior work on survivable WDM network design. The ILP formulations for enabling grooming in survivable WDM network are presented in Section 6.2. Results of ILP formulations are given in Section 6.3. Our approaches of survivable grooming network design is extended to partially protected WDM grooming networks in Section 6.4. Section 6.5 presents the conclusions.

6.1.1 Related Work

Joint working (primary) and spare (backup) capacity planning in mesh-survivable WDM networks design has gained a lot of attention in optical community [58],[40], [41], [59].

The study in [58] proposed an optimal design scheme to achieve fast restoration in survivable WDM transport networks by using predetermined restoration paths. The problem was formulated as an Integer Linear programming (ILP) problem to optimally determine the working paths and their corresponding restoration paths, together with the number of fibers in each span, and the optical crossconnects in each node. The study in [40] examined different approaches to protect mesh-based WDM optical networks from single-link failures. The problems of determining the capacity requirements for a static traffic demand based path/link protection/restoration schemes were formulated into ILP optimization problems. Joint optimization of primary and restoration routes to minimize the network capacity was studied in [41]. The study also tried to determine the best restoration route for each wavelength demand, the capacities, and primary routes of all demands, given network topology. They considered a static traffic demand and optimized the network cost assuming various cost models and survivability paradigms. The study in [59] formulated various operational phases in survivable WDM networks as a single ILP optimization problem, and proposed a fast algorithm for fast

online reconfiguration based on LP-relaxation technique to solve the ILP problem.

The above algorithms are designed for a network scenario where the full wavelength is the minimum unit of the bandwidth on a link. The algorithms cannot be directly applied for grooming WDM networks design. For example, it is assumed in [59] that if a wavelength is used by any primary path, it cannot be used by any backup paths. This constraint holds in WDM networks without grooming and it helps to simplify the ILP formulation for the survivable network design. However, in grooming WDM networks this primary path wavelength restriction might not be necessary where the subwavelength level primary and backup paths could be groomed on the same wavelength on a link.

On the other hand, most early work on traffic grooming had focused on SONET ring, which deals with known and static traffic. Only few recent studies focusing on non-ring topologies. This is appropriate because today's backbone transport infrastructures are organized in rings. However, as networks evolve to become more IP-centric, grooming for IP traffic will become an important area for future work. In the IP environment, the network topology could be general mesh and the traffic is typically neither static nor known in advance. Grooming in mesh-based networks with dynamic traffic will become an important extension to current ring-based grooming algorithms.

By the time we completed our study on the full protection in survivable grooming network design again single link failure [60], there had been only a few papers on this topic in literature. The study in [61] addressed the problem of dynamically establishing dependable low-rate traffic stream connections in WDM mesh networks with traffic grooming capabilities. To establish a dependable connection, they pre-computed link-disjoint primary and backup paths between the source and destination node and use backup multiplexing to reduce the overhead of backup traffic streams. Two schemes for grooming traffic streams onto wavelengths were proposed, namely *Mixed Primary-Backup Grooming Policy* (MGP) and *Segregated Primary-Backup Grooming Policy* (SGP). Their simulation results showed that SGP performs better in mesh networks and MGP performs better in ring networks. Similar study in the context of IP/MPLS protection/restoration with dynamic traffic has been done in [62], where k-shortest

paths were pre-computed for each request and wavelength assignment followed the first-fit (FF) policy. The authors also applied backup multiplexing technique to reduce the redundant reserved spare capacity. Benefits gained by dynamically provisioning low-rate traffic streams at the IP/MPLS layer in IP over WDM optical networks are shown through simulations.

More research interests have been focused on the issue of survivability in grooming networks lately. In [63], the authors proposed three approaches, namely protection-at-lightpath (PAL) level, mixed protection-at-connection (MPAC) level, and separate protection-at-connection (SPAC) level, for grooming a connection request with shared protection. In shared protection, backup paths can share resources provided their corresponding working paths are unlikely to fail simultaneously. Different ways of backup sharing as well as the tradeoff between wavelengths and grooming ports were studied in this paper. They concluded that when the lower bandwidth connections outnumber higher bandwidth connections, it is beneficial to groom working paths and backup paths separately, especially when the number of grooming ports is sufficient; when the number of grooming ports is moderate or small, protecting each specific lightpath achieves the best performance. The same problem with dedicated protection was studied in [64]. Two approaches, protection-at-lightpath (PAL) level and protection-at-connection (PAC) level, for grooming a connection request were studied. Their study showed that under the same assumption in [63] when the lower bandwidth connections outnumber higher bandwidth connections, PAC outperforms PAL given large number of grooming ports are available; otherwise, when the number of grooming ports is moderate or small, PAL performs better.

The above studies are based on simulations. We investigate the problem of how to *groom* subwavelength level requests efficiently in mesh restorable WDM networks, and formulate the corresponding path selection and wavelength assignment problem as ILP optimization problems. We also extend our solutions to the partially protected grooming networks, based on the same design idea, we develop a heuristic algorithm for routing dynamic traffic in grooming networks.

6.2 Formulation of the Optimization Problem

6.2.1 Network Model

A network with W wavelengths and K disjoint alternate paths for each s-d pairs can be viewed as $W \times K$ networks, each of them representing a single wavelength network. Here we choose $K = 2$. The first W networks contain the first alternate path for each s-d pair on each wavelength, number the networks from 1 to W according to the wavelengths associated with them. The second W networks contain the second alternate path for each s-d pair on each wavelength, similarly, number them from $W + 1$ to $2W$, where the $(W + i)$ th network represents the same wavelength as the i th network, where $i = 1, 2, \dots, W$. Figure 6.1 illustrates this layered model of a 6-node network with 3 wavelengths, 2 connections with each has 2 link disjoint alternate paths. We can also observe from Figure 6.1 that, for example, a path among network 1 to W is selected as a primary path for a request, its backup paths can only be selected from the network $W + 1$ to $2W$ in this layered network model, so as to guarantee that the primary and backup paths are link disjoint.

6.2.2 Restoration Models

We consider 100% restoration guarantee for any single link failure for protected connections. This implies that the primary (working) paths and the restoration (backup) paths are assigned the same capacity and are link disjoint, assuming that it is possible in the network topology.

6.2.2.1 Backup Multiplexing

An efficient way of assigning backup capacities is to employ *backup multiplexing* technique to improve the network resource utilization. This technique allows many restoration paths, belonging to different source-destination node pairs, to share a wavelength w on a link l if and only if their corresponding primary paths are link disjoint. This is based on the fact that a single link failure will not break down two link disjoint paths.

In grooming WDM networks, the capacity reserved for restoration paths is more complicated. Let $B = \{b_1, b_2, \dots, b_k\}$ denotes the set of backup paths that traverse the wavelength w

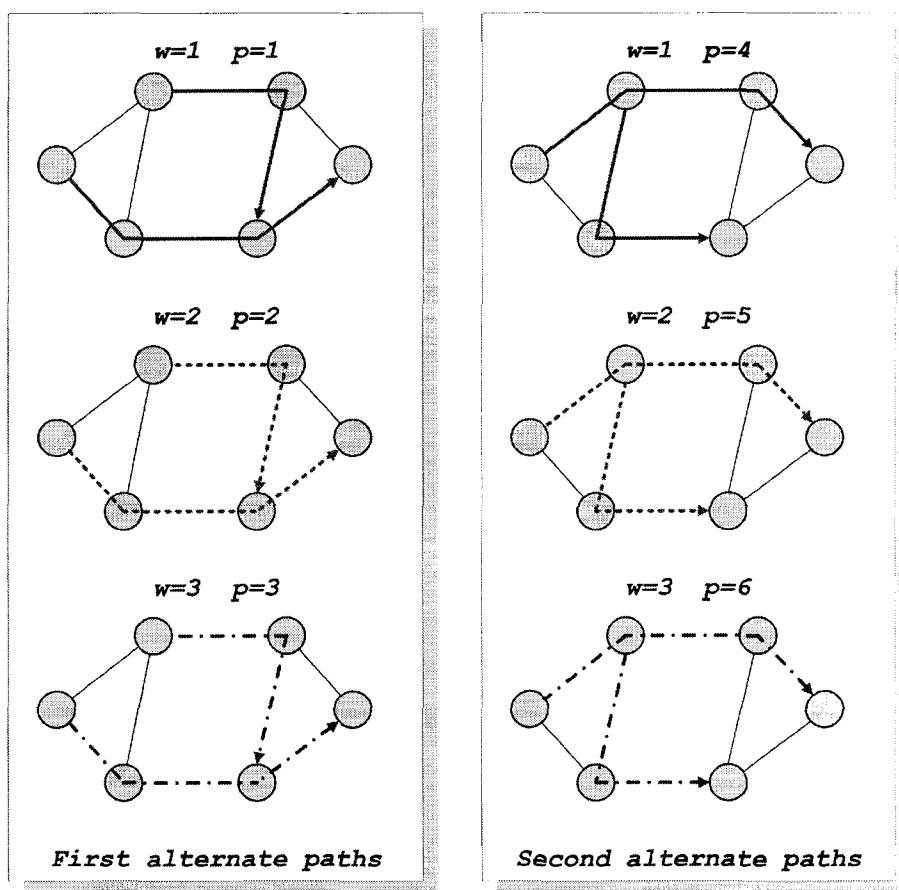


Figure 6.1 An example of layered network model with $W = 3$, $K = 2$.

on link l . Let their respective capacities be $D = \{d_1, d_2, \dots, d_k\}$, and their respective primary paths be $P = \{p_1, p_2, \dots, p_k\}$. If none of the p_i 's have common links, the needed capacity on w is $\max(d_1, d_2, \dots, d_k)$. If some of the p_i 's have common links, their backup paths can still be groomed on wavelength w . However, the capacity to be reserved must be up to the summation of their capacities. The primary paths can be grouped according to their common links. Let $P^l = \{p_1^l, p_2^l, \dots, p_a^l\}$ denote the group of primary paths that have link l as their common link. The capacity required by this group for back up of link l is then given by $D^l = (d_1^l + d_2^l + \dots + d_a^l)$. It is possible that one primary path belongs to more than one group. The reserved capacity on wavelength w on link l is therefore the maximum value of the capacities required by all the groups, that is $D = \max(D^l)$.

6.2.2.2 Dedicated Backup Reservation

One simple and effective way of assigning backup capacities is to reserve dedicated capacity for each backup path. While choosing primary paths, instead of simply choosing the shortest path, we try to *minimize* the total *link-primary-sharing* (MLPS). The link-primary-sharing is defined as following,

$$s_l = \max(0, P_l - 1) \quad (6.1)$$

where s_l denotes the link-primary-sharing of link l and P_l denotes the total number of primary paths that utilize link l . s_l can be viewed as the penalty assigned to link l when it is used by more than one primary path.

Backup multiplexing and dedicated backup reservation schemes with MLPS have been formulated in ILP optimization problems in Section 6.2.5 and 6.2.6, respectively.

6.2.3 Assumptions

To formulate the grooming survivable network design problem in a WDM mesh network with static traffic pattern as an ILP problem, we make the following assumptions.

1. The network is a single-fiber general mesh network.

2. A connection request cannot be divided into several lower speed connection requests and routed separated from the source to the destination. The data traffic on a connection request should always follow the same route.
3. The transceivers in a network node are fixed, hence wavelength continuity constraint applies.
4. Each grooming node has unlimited multiplexing and demultiplexing capability. This means that the network node can multiplex/demultiplex as many low-speed traffic streams to a lightpath as needed, as long as the aggregated traffic does not exceed the lightpath capacity.

6.2.4 Notations

The following cost parameter is employed.

- C_l : Cost of using link l .

The following information is given regarding link usage and whether two given paths are link and node disjoint.

- $I_{(i,p),(j,r)}$: Takes a value of one if paths (i, p) and (j, r) have at least one link in common; zero otherwise. If two routes share a link, then all lightpaths using those routes have the corresponding I value set to one; else zero. (data).

The following notations are for path-related information.

- $\delta^{i,p}$: Path indicator. It takes a value of one if (i, p) is chosen as a primary path; zero otherwise (binary variable).
- $\nu^{i,r}$: Path indicator. It takes a value of one if (m, r) is chosen as a restoration path; zero otherwise (binary variable).
- $\epsilon_l^{i,p}$: Link indicator. It takes a value of one if link l is used in path (i, p) ; zero otherwise (data).

- $\psi_w^{i,p}$: Wavelength indicator. It takes a value of one if wavelength w is used by the path (i, p) ; zero otherwise (data).

The following variables are used to present wavelength assignment in this grooming network.

- $p_{l,w}^i$: Takes a value of one if wavelength w on link l is used by primary path of demand i ; zero otherwise (binary variable).
- $r_{l,w}^i$: Takes a value of one if wavelength w on link l is used by backup path of demand i ; zero otherwise (binary variable).
- W_l : Total number of wavelengths required on link l (nonnegative integer).
- $M_{l,w}$: Total capacity assigned to primary paths on wavelength w on link l (nonnegative integer).
- $R_{l,w}$: Total capacity reserved for backup paths on wavelength w on link l (nonnegative integer).

6.2.5 ILP Formulation I: Backup Multiplexing

1. Objective:

The objective is to minimize the total wavelength links. Given a network topology and a set of point-to-point demands and their link disjoint primary and backup routes, assign the primary and backup routes in an optimal way that the total wavelength links is minimized. Here we choose $C_l = 1$, hence, the objective is to minimize the total number of *wavelength-links*.

$$\min \sum_{l \in E} C_l \times W_l \quad (6.2)$$

2. *Constraints on physical route variables*: A lightpath can carry traffic for a s-d pair only if it is in the physical route of this request.

$$p_{l,w}^i = \sum_{p=1}^{KW} \delta^{i,p} \epsilon_l^{i,p} \psi_w^{i,p} \quad (6.3)$$

$$r_{ij,w}^m = \sum_{r=1}^{KW} \nu^{i,r} \epsilon_l^{i,r} \psi_w^{i,r} \quad (6.4)$$

3. *Constraints on path indicators:* One and only one path will be assigned as a primary(backup) path for each request.

$$\sum_{p=1}^{KW} \delta^{i,p} = 1 \quad (6.5)$$

$$\sum_{r=1}^{KW} \nu^{i,r} = 1 \quad (6.6)$$

4. *Constraints on topology diversity of primary and backup paths:* Primary and restoration paths of a given demand should be node and link disjoint.

$$\sum_{p=1}^W \delta^{i,p} = \sum_{r=W+1}^{KW} \nu^{i,r} \quad (6.7)$$

$$\sum_{p=W+1}^{KW} \delta^{i,p} = \sum_{r=1}^W \nu^{i,r} \quad (6.8)$$

5. *Constraints on wavelength capacity:* Primary capacities are aggregated. For each wavelength, the sum of primary capacities and backup capacities should not exceed the total wavelength capacity.

$$M_{l,w} = \sum_i d_i \times p_{l,w}^i \quad (6.9)$$

$$M_{l,w} + R_{l,w} \leq C \quad (6.10)$$

6. *Constraints on fiber capacity:* The number of wavelengths used on a fiber should not exceed the total number of wavelengths carried by the fiber. Equations (6.12), (6.13),

and (6.14) together set $u_{l,w} = 1$, if $x_{l,w} \geq 1$, and zero otherwise. $x_{l,w}$ counts the number of primary and backup paths that use wavelength w on link l , and W_l counts the number of wavelengths used on link l . Recall that we assume single-fiber networks here.

$$x_{l,w} = \sum_i (r_{l,w}^i + p_{l,w}^i) \quad (6.11)$$

$$u_{l,w} \leq x_{l,w} \quad (6.12)$$

$$KN(N-1)u_{l,w} \geq x_{l,w} \quad (6.13)$$

$$u_{l,w} \in \{0, 1\} \quad (6.14)$$

$$W_l \geq \sum_w u_{l,w} \quad (6.15)$$

$$W_l \leq W \quad (6.16)$$

7. *Constraints on backup multiplexing:* The capacity reserved for backup paths on a link need to take the correlations between the corresponding primary paths into account. If the primary paths do not have common links, their backup paths can share the same wavelength on their common links, the reserved capacity will be the maximum requested capacity among them. Otherwise, the capacity for their backups on the same wavelength will also be aggregated. Recall $R_{l,w}$ denotes the capacity assigned to backup paths on wavelength w on link l , $R_{l,w}$ is given as:

$$\begin{aligned}
R_{l,w} \geq & d_i \times \nu^{i,p} \epsilon_l^{i,p} \psi_w^{i,p} \\
& + \sum_{j \geq i} d_n \times \nu^{j,p,i,p} \epsilon_l^{j,p} \psi_w^{j,p} \times I_{(i,\bar{p}),(j,\bar{p})} \\
& + \sum_{j \geq i} d_j \times \nu^{j,\bar{p},i,p} \epsilon_l^{j,\bar{p}} \psi_w^{j,\bar{p}} \times I_{(i,p),(j,p)} \\
& + \sum_{j \geq i} d_j \times \nu^{j,p,i,\bar{p}} \epsilon_l^{j,p} \psi_w^{j,p} \times I_{(i,\bar{p}),(j,\bar{p})} \\
& + \sum_{j \geq i} d_j \times \nu^{j,\bar{p},i,\bar{p}} \epsilon_l^{j,\bar{p}} \psi_w^{j,\bar{p}} \times I_{(i,p),(j,\bar{p})}
\end{aligned} \tag{6.17}$$

where $\nu^{j,p,i,p}$ is a binary variable which takes value of one when $\nu^{j,p} = 1$ and $\nu^{i,p} = 1$. It is given by Equation (6.18), (6.19) and (6.20).

$$\nu^{j,p,i,p} \geq \nu^{j,p} + \nu^{i,p} - 1 \tag{6.18}$$

$$\nu^{j,p,i,p} \leq \nu^{j,p} \tag{6.19}$$

$$\nu^{j,p,i,p} \leq \nu^{i,p} \tag{6.20}$$

6.2.6 ILP Formulation II: Dedicated Backup with MLPS

1. Objective:

The objective is to minimize the total wavelength-links as well as total link-primary-sharing. Recall that s_l denotes the link-primary-sharing on link l . Let C_{share}^l be the weight of s_l . The objective function is hence give as:

$$\min(\sum_{l \in E} C_l \times W_l + C_{share}^l \times s_l). \tag{6.21}$$

Constraints 6.3-6.15 are still applicable, only the backup capacities are calculated in a different way.

2. *Constraints on backup capacity:* Backup capacities are aggregated when dedicated backup reservation is applied.

$$R_{l,w} = \sum_i d_i \times r_{l,w}^i. \quad (6.22)$$

3. *Constraints on link-primary-sharing:* Recall the definition of s_l in Section 6.2.2.2, s_l is nonnegative and given as following.

$$s_l \geq \sum_i \sum_w p_{l,w}^i - 1 \quad (6.23)$$

$$s_l \leq \sum_i \sum_w p_{l,w}^i \quad (6.24)$$

6.3 Numerical Results

6.3.1 Experimental Design

This section presents numerical results of the ILP formulations given in Section 6.2.5 and 6.2.6 on physical topologies given in Figure 6.2(a) and (b).

The performance of grooming depends on the efficiency of *grooming* fractional wavelength traffic onto full or almost-full wavelength, hence, it also depends on the traffic pattern. When most of the traffic are of full-wavelength capacity or almost full-wavelength capacity, grooming will not bring much improvement on wavelength utilization. In this example traffic is randomly generated with each request having a capacity of OC-12, which is 1/4 of the full wavelength capacity. Two link disjoint alternate paths for each connection are pre-computed based on fixed shortest-paths routing algorithm.

6.3.2 Experiment I

We use CPLEX Linear Optimizer 7.0 [57] to solve the ILP formulation I and II. Tables 6.1 and 6.2 show the path selection and wavelength assignment results of the same set of requests on topology given by Figure 6.2(a) with ILP formulation I and II, respectively.

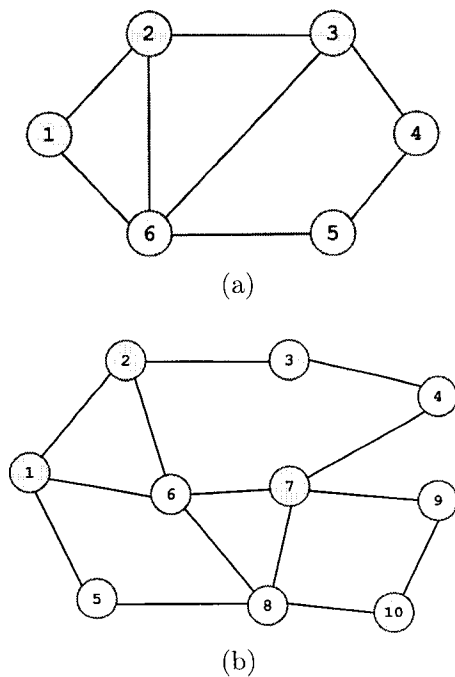


Figure 6.2 Physical topologies used in experiments.

Table 6.1 Solution from ILP formulation I: Requires 21 wavelength-links.

Seq. No.	s-d pair	Formulation I			
		Primary		Backup	
1	1-3	1-2-3	w_3	1-6-3	w_2
2	1-4	1-2-3-4	w_3	1-6-5-4	w_2
3	1-5	1-2-3-4-5	w_3	1-6-5	w_2
4	2-4	2-3-4	w_2	2-6-5-4	w_4
5	2-5	2-6-5	w_4	2-3-4-5	w_3
6	2-6	2-6	w_4	2-1-6	w_2
7	3-5	3-4-5	w_3	3-6-5	w_4
8	3-6	3-2-6	w_4	3-6	w_4
9	4-2	4-3-2	w_4	4-5-6-2	w_2
10	4-5	4-3-6-5	w_4	4-5	w_2
11	5-2	5-6-2	w_2	5-4-3-2	w_4
12	5-3	5-4-3	w_4	5-6-3	w_2
13	6-1	6-2-1	w_2	6-1	w_1
14	6-3	6-3	w_2	6-2-3	w_2
15	6-4	6-3-4	w_2	6-5-4	w_2

Table 6.2 Solution from ILP formulation II: Requires 21 wavelength-links.

Seq. No.	s-d pair	Formulation II			
		Primary		Backup	
1	1-3	1-2-3	w_3	1-6-3	w_3
2	1-4	1-6-5-4	w_3	1-2-3-4	w_3
3	1-5	1-6-5	w_3	1-2-3-4-5	w_3
4	2-4	2-3-4	w_2	2-6-5-4	w_1
5	2-5	2-6-5	w_1	2-3-4-5	w_2
6	2-6	2-6	w_1	2-1-6	w_3
7	3-5	3-4-5	w_2	3-6-5	w_1
8	3-6	3-6	w_1	3-2-6	w_1
9	4-2	4-3-2	w_1	4-5-6-2	w_3
10	4-5	4-5	w_2	4-3-6-5	w_1
11	5-2	5-6-2	w_3	5-4-3-2	w_1
12	5-3	5-6-3	w_3	5-4-3	w_1
13	6-1	6-1	w_1	6-2-1	w_3
14	6-3	6-3	w_3	6-2-3	w_3
15	6-4	6-5-4	w_3	6-3-4	w_3

Tables 6.1 and 6.2 shows that 21 wavelength-links are needed to carry all the 15 requests. The solution for the same request set in the network without traffic grooming capability can be obtained from formulation I as a special case where each request has full wavelength capacity. The results are shown in Table 6.3. It turned out that minimum 52 wavelength-links are required in the network without traffic grooming capability.

From pre-computed path sets, we can calculate the maximum wavelength-links that are needed to establish all the primary and backup paths. Notice that without traffic grooming and backup multiplexing, 64 wavelength-links are needed, while backup multiplexing helps to reduce it to 52. The gain by using backup multiplexing is then 18.75%, and 8 wavelength-links are saved.

With subwavelength traffic grooming, 21 wavelength-links are sufficient, which means another 31 wavelength-links are saved. If we take the wavelength capacity granularity into account, the total required capacity is $64/4 = 16$ OC-12 capacity units. Without grooming, each lightpath uses full OC-48 capacity, although the requested capacity is OC-12, so totally 52 OC-48 capacity units have been occupied. With traffic grooming, although 21 wavelength-links

Table 6.3 Solution without traffic grooming: Requires 52 wavelength-links.

Seq. No.	s-d pair	No Traffic Grooming			
		Primary		Backup	
1	1-3	1-2-3	w_6	1-6-3	w_6
2	1-4	1-2-3-4	w_3	1-6-5-4	w_1
3	1-5	1-6-5	w_3	1-2-3-4-5	w_2
4	2-4	2-3-4	w_4	2-6-5-4	w_7
5	2-5	2-6-5	w_2	2-3-4-5	w_7
6	2-6	2-6	w_8	2-1-6	w_2
7	3-5	3-6-5	w_8	3-4-5	w_5
8	3-6	3-6	w_6	3-2-6	w_7
9	4-2	4-3-2	w_6	4-5-6-2	w_2
10	4-5	4-5	w_4	4-3-6-5	w_7
11	5-2	5-6-2	w_4	5-4-3-2	w_7
12	5-3	5-6-3	w_5	5-4-3	w_1
13	6-1	6-1	w_3	6-2-1	w_2
14	6-3	6-3	w_4	6-2-3	w_2
15	6-4	6-5-4	w_5	6-3-4	w_6

have been used, it is still possible to pack other lightpaths on to some wavelengths even without taking backup multiplexing into account, because some wavelengths still have free bandwidth, and the total used capacity is exactly 16 OC-12 capacity units. This example clearly shows the improvement of capacity utilization by enabling subwavelength level grooming in the restorable WDM network design.

Although in the above example, backup multiplexing and dedicated backup with MLPS perform the same in terms of wavelength-links. This will not always happen. However in this scenario MLPS is preferred because fewer working paths will be touched by single-link failures. For example, from Table 6.1, the failure of link (2, 3) would affect 4 working paths in formulation I and 2 in formulation II as shown in Table 6.2. Additionally, with the objective to minimize the total wavelength-links, backup multiplexing stops when the objective value does not decrease any more. It is still possible to reallocate some primary paths so that there could be more chances to multiplex backup paths onto some wavelength, and result in more spare capacity on the utilized wavelengths. But the value of the objective function will stay the same.

Different path selections can be observed from the Tables 6.1 and 6.2. In order to simply minimize the total wavelength-links, grooming tends to exhaust one wavelength before using another wavelength. While link-primary-share is taken as a link penalty, in formulation II, it would be preferred to have more balanced load for primary paths.

6.3.3 Experiment II

We also performed experiments on the topology in Figure 6.2(b), which is a 10-node network with 14 bi-directional links. The randomly generated traffic matrix is shown in Table 6.4.

Table 6.4 Traffic matrix for the 10-node-14-link network.

	1	2	3	4	5	6	7	8	9	10
1	0	0	0	12	1	0	0	0	0	0
2	1	0	0	0	0	0	0	0	0	12
3	0	3	0	0	0	0	0	0	0	0
4	0	0	0	0	3	1	0	3	12	12
5	0	0	0	0	0	0	0	0	1	0
6	0	0	3	0	0	0	0	0	0	0
7	0	0	0	0	0	0	0	0	3+1	0
8	1	0	12+12	0	0	0	1	0	0	0
9	0	3	0	0	12	3+3	0	0	0	0
10	3	0	0	0	0	0	0	0	0	0

The solution from formulation I shows that by employing backup multiplexing technique 28 wavelength-links are needed, while formulation II gives a solution requires 33 wavelength-links. The detailed results on path selection and wavelength assignment are shown in Table 6.5 and Table 6.6 respectively.

In general, formulation II requires more wavelength-links in comparison to formulation I. However, this becomes affordable in networks with subwavelength grooming capability, where the wavelength utilization is significantly improved by traffic grooming. Moreover, from the respect of ILP formulation, formulation II has less complexity than formulation I in terms of number of constraints and variables, which makes formulation II less computationally expensive and hence more practical.

Table 6.5 Solution from ILP formulation I: Requires 28 wavelength-links.

Seq. No.	s-d pair	Formulation I			
		Primary		Backup	
1	9-2	9-10-8-5-1-2	w_1	9-7-6-2	w_1
2	3-2	3-2	w_1	3-4-7-6-2	w_1
3	7-9	7-9	w_1	7-8-10-9	w_1
4	8-7	8-6-7	w_1	8-7	w_1
5	9-6	9-7-6	w_1	9-10-8-6	w_1
6	2-1	2-1	w_1	2-6-1	w_1
7	1-4	1-6-7-4	w_1	1-2-3-4	w_1
8	4-9	4-7-9	w_1	4-3-2-6-8-10-9	w_1
9	10-1	10-8-5-1	w_1	10-9-7-6-1	w_1
10	4-8	4-7-8	w_1	4-3-2-6-8	w_1
11	4-5	4-3-2-1-5	w_1	4-7-8-5	w_1
12	8-1	8-5-1	w_1	8-6-1	w_1
13	9-5	9-10-8-6-1-5	w_1	9-7-8-5	w_1
14	5-9	5-1-6-8-10-9	w_1	5-8-7-9	w_1
15	8-3	8-6-2-3	w_1	8-7-4-3	w_1
16	7-9	7-9	w_1	7-8-10-9	w_1
17	2-10	2-6-8-10	w_1	2-3-4-7-9-10	w_1
18	9-6	9-10-8-6	w_1	9-7-6	w_1
19	4-6	4-3-2-6	w_1	4-7-6	w_1
20	6-3	6-2-3	w_1	6-7-4-3	w_1
21	8-3	8-7-4-3	w_1	8-6-2-3	w_1
22	1-5	1-6-8-5	w_1	1-5	w_1
23	4-10	4-3-2-6-7-9-10	w_1	4-7-8-10	w_1

Table 6.6 Solution from ILP formulation II: Requires 33 wavelength-links.

Seq. No.	s-d pair	Formulation II			
		Primary		Backup	
1	9-2	9-10-8-5-1-2	w_1	9-7-6-2	w_1
2	3-2	3-2	w_1	3-4-7-6-2	w_1
3	7-9	7-9	w_1	7-8-10-9	w_1
4	8-7	8-7	w_1	8-6-7	w_1
5	9-6	9-7-6	w_1	9-10-8-6	w_1
6	2-1	2-1	w_1	2-6-1	w_1
7	1-4	1-6-7-4	w_1	1-2-3-4	w_1
8	4-9	4-7-9	w_1	4-3-2-6-8-10-9	w_1
9	10-1	10-9-7-6-1	w_1	10-8-5-1	w_1
10	4-8	4-7-8	w_1	4-3-2-6-8	w_1
11	4-5	4-7-8-5	w_1	4-3-2-1-5	w_1
12	8-1	8-5-1	w_1	8-6-1	w_1
13	9-5	9-7-8-5	w_1	9-10-8-6-1-5	w_1
14	5-9	5-8-7-9	w_1	5-1-6-8-10-9	w_1
15	8-3	8-7-4-3	w_2	8-6-2-3	w_1
16	7-9	7-9	w_1	7-8-10-9	w_1
17	2-10	2-6-8-10	w_1	2-3-4-7-9-10	w_1
18	9-6	9-7-6	w_1	9-10-8-6	w_1
19	4-6	4-7-6	w_1	4-3-2-6	w_1
20	6-3	6-2-3	w_2	6-7-4-3	w_1
21	8-3	8-6-2-3	w_1	8-7-4-3	w_1
22	1-5	1-5	w_1	1-6-8-5	w_1
23	4-10	4-7-8-10	w_1	4-3-2-6-7-9-10	w_1

6.4 Partial Protection

Our approaches of survivable grooming network design can be extended to the partial protection in WDM grooming networks. As aforementioned in Chapter 2.2, the grooming capability of the network makes partial protection a possible solution when the network resource is not sufficient to provide full protection for every request.

For a request m , its requested capacity for primary or working path is given as d_m , the minimum capacity for its backup is given as b_m . The difference between partial protection and full protection is that here $0 < b_m < d_m$, while in the full protection, $b_m = d_m$. Just for the sake of completeness, when $b_m = 0$, it is called no protection for request m . The problem is partial protection is to find a primary path for request m , assigning capacity of d_m to it, and find a backup path with capacity c_m such that $b_m \leq c_m \leq d_m$. The higher the value of c_m , the better protection request m has.

6.4.1 Optimal Design for Partial Protection

The exact ILP formulations earlier in this chapter can be modified to solve the partial protection problems in grooming networks as well. However, a direct modification makes the formulations nonlinear, because in partial protection problems, the backup capacity becomes unknown.

If we reconsider the motivation of the partial protection in grooming networks, the problem might be solved differently. The main reason partial protection is adopted is that we do not have enough wavelength resource to provide full protection for each request. In other words, we may not want to exploit one extra wavelength just to provide more than the minimum capacity requirement of the backups. In this situation, the partial protection problem can be divided into two subproblems.

1. Resource minimization: Given the network resource and minimum backup requirement, try allocate each request m with primary capacity of d_m and backup capacity of b_m .
2. Protection maximization: Given all the requests are accommodated with the minimum

protection requirement being satisfied, the second step is to optimally distribute the residual network capacity to provide better protection to some, if not all, of the requests.

We propose a two-phase ILP formulation with dedicated backup reservation for the partial protection design in WDM grooming networks as follows.

6.4.2 ILP Formulation I: Resource Minimization

1. Objective:

The objective is to minimize the total wavelength-links as well as the total link-primary-sharing.

$$\min\left(\sum_{(i,j) \in E} w_{ij}^c \times \lambda_{ij} + w_{ij}^s \times s_{ij}\right). \quad (6.25)$$

The constraints in Equations 6.3 - 6.8, and 6.11 - 6.16, and 6.22 - 6.24 still apply here.

The modified constraints are following.

2. *Constraints on wavelength capacity variables:* Primary capacities are aggregated. Backup capacities are aggregated when dedicated backup reservation is applied.

$$\alpha_{ij,w} = \sum_m d_m \times p_{ij,w}^m \quad (6.26)$$

$$\beta_{ij,w} = \sum_m b_m \times r_{ij,w}^m. \quad (6.27)$$

For each wavelength, the sum of primary capacities and backup capacities should not exceed the total wavelength capacity.

$$\alpha_{ij,w} + \beta_{ij,w} \leq C \quad (6.28)$$

6.4.3 ILP Formulation II: Protection Maximization

After solving the ILP formulation in Section 6.4.2, it is guaranteed that each request m has its minimum protection requirement being satisfied, which is b_m . In the grooming WDM network, it is quite possible that there are still fractional wavelength resource available in the network. This second step is to optimally allocate the residual capacity so that some if not all the requests can achieve better protection than their minimum requirements.

After we solved the ILP formulation presented in Section 6.4.2, the primary and backup paths for each request m are known, with d_m reserved for primary path and b_m for the backup path. That is the variables in aforementioned ILP formulations are the data for this formulation. The are as follows.

- $\Delta^{m,p}$: Path indicator that takes a value of one if (m, p) is chosen as a primary path; zero otherwise (binary data).
- $\Gamma^{m,r}$: Path indicator that takes a value of one if (m, r) is chosen as a restoration path; zero otherwise (binary data).
- $P_{ij,w}^m$: binary data, 1 if wavelength w on link (i, j) is used by primary path of demand m ; 0 otherwise.
- $R_{ij,w}^m$: binary data, 1 if wavelength w on link (i, j) is used by backup path of demand m ; 0 otherwise.
- Λ_{ij} : nonnegative integer, total number of wavelengths required on link (i, j) .

The new variable here is,

- c_m : capacity assigned to the backup path of request m .

1. Objective:

The objective here is to maximize the protection. We use $c_m - b_m$ to indicate the quality of the protection, where $b_m \leq c_m \leq d_m$. w_m^p is the weight assigned to the request m .

$$\max(\sum_m w_m^p \times (c_m - b_m)). \quad (6.29)$$

2. *Constraints on wavelength capacity variables:* Primary and backup capacities are aggregated.

$$\sum_m (d_m \times P_{ij,w}^m + c_m \times R_{ij,w}^m) \leq C \quad (6.30)$$

$$b_m \leq c_m \leq d_m \quad (6.31)$$

6.4.4 Experimental Results

We use CPLEX Linear Optimizer 7.0 [57] to solve the two ILP formulations developed above, namely *resource minimization* and *protection maximization*. The experiments are performed on the same 10-node network topology shown in Figure 6.2 (b). For the sake of convenience, the topology is redrawn in Figure 6.3. It is assumed that each link is bi-unidirectional.

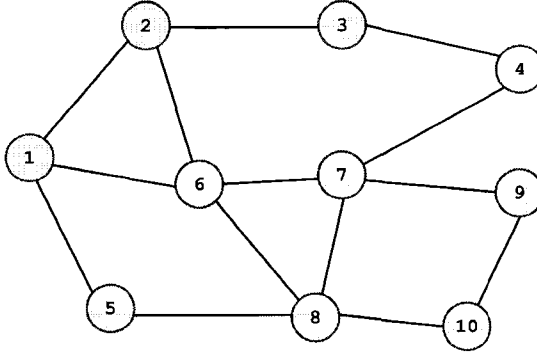


Figure 6.3 Physical topologies used in experiments.

6.4.4.1 Experiment I

The first experiment uses the same randomly generated 23 requests as shown in Table 6.4. We also assume each link has single fiber that carries 2 wavelengths. As presented in Section 6.3.3, 33 wavelength-links are needed with full protection for each request. We present the solutions with capacity assigned on primary and backup paths here in Table 6.7. As it shows, wavelength 2 is only used by two requests on their primary paths. Obviously wavelength 2 is not fully utilized on those corresponding links in this example.

Table 6.7 Solution with full protection: Requires 33 wavelength-links.

Seq. No.	s-d pair	Primary Path			Backup Path		
		path	w	cap	path	w	cap
1	9-2	9-10-8-5-1-2	w_1	3	9-7-6-2	w_1	3
2	3-2	3-2	w_1	3	3-4-7-6-2	w_1	3
3	7-9	7-9	w_1	3	7-8-10-9	w_1	3
4	8-7	8-7	w_1	1	8-6-7	w_1	1
5	9-6	9-7-6	w_1	3	9-10-8-6	w_1	3
6	2-1	2-1	w_1	1	2-6-1	w_1	1
7	1-4	1-6-7-4	w_1	12	1-2-3-4	w_1	12
8	4-9	4-7-9	w_1	12	4-3-2-6-8-10-9	w_1	12
9	10-1	10-9-7-6-1	w_1	3	10-8-5-1	w_1	3
10	4-8	4-7-8	w_1	3	4-3-2-6-8	w_1	3
11	4-5	4-7-8-5	w_1	3	4-3-2-1-5	w_1	3
12	8-1	8-5-1	w_1	1	8-6-1	w_1	1
13	9-5	9-7-8-5	w_1	12	9-10-8-6-1-5	w_1	12
14	5-9	5-8-7-9	w_1	1	5-1-6-8-10-9	w_1	1
15	8-3	8-7-4-3	w_2	12	8-6-2-3	w_1	12
16	7-9	7-9	w_1	1	7-8-10-9	w_1	1
17	2-10	2-6-8-10	w_1	12	2-3-4-7-9-10	w_1	12
18	9-6	9-7-6	w_1	3	9-10-8-6	w_1	3
19	4-6	4-7-6	w_1	1	4-3-2-6	w_1	1
20	6-3	6-2-3	w_2	3	6-7-4-3	w_1	3
21	8-3	8-6-2-3	w_1	12	8-7-4-3	w_1	12
22	1-5	1-5	w_1	1	1-6-8-5	w_1	1
23	4-10	4-7-8-10	w_1	12	4-3-2-6-7-9-10	w_1	12

For the experiments on partial protection, we define the *minimum backup capacity* and *protection ration* as follows.

$$b_m = \lceil c_m \times P_{ratio} \rceil \quad (6.32)$$

where P_{ratio} is referred to as the *protection ratio*.

In this experiment, $P_{ratio} = 0.6$. The path selection and wavelength assignment results are presented in Table 6.8. Totally 28 wavelength-links are required in this scenario when partial protection with $P_{ratio} = 0.6$ is provided. It also shows that only one wavelength is used in the network. It can also be seen that some of the requests are provided with more capacity than their minimum requirement fully protected and some are fully protected.

Table 6.8 Solution with partial protection ($P_{ratio} = 0.6$): Requires 28 wavelength-links.

Seq. No.	s-d pair	Primary Path			Backup Path		
		Path	w	cap	Path	w	cap
1	9-2	9-7-6-2	w_1	3	9-10-8-5-1-2	w_1	3
2	3-2	3-2	w_1	3	3-4-7-6-2	w_1	3
3	7-9	7-9	w_1	3	7-8-10-9	w_1	3
4	8-7	8-7	w_1	1	8-6-7	w_1	1
5	9-6	9-10-8-6	w_1	3	9-7-6	w_1	3
6	2-1	2-1	w_1	1	2-6-1	w_1	1
7	1-4	1-2-3-4	w_1	12	1-6-7-4	w_1	12
8	4-9	4-7-9	w_1	12	4-3-2-6-8-10-9	w_1	8
9	10-1	10-9-7-6-1	w_1	3	10-8-5-1	w_1	3
10	4-8	4-7-8	w_1	3	4-3-2-6-8	w_1	2
11	4-5	4-7-8-5	w_1	3	4-3-2-1-5	w_1	2
12	8-1	8-5-1	w_1	1	8-6-1	w_1	1
13	9-5	9-7-8-5	w_1	12	9-10-8-6-1-5	w_1	12
14	5-9	5-8-7-9	w_1	1	5-1-6-8-10-9	w_1	1
15	8-3	8-6-2-3	w_1	12	8-7-4-3	w_1	8
16	7-9	7-9	w_1	1	7-8-10-9	w_1	1
17	2-10	2-6-8-10	w_1	12	2-3-4-7-9-10	w_1	9
18	9-6	9-7-6	w_1	3	9-10-8-6	w_1	3
19	4-6	4-7-6	w_1	1	4-3-2-6	w_1	1
20	6-3	6-2-3	w_1	3	6-7-4-3	w_1	3
21	8-3	8-7-4-3	w_1	12	8-6-2-3	w_1	12
22	1-5	1-5	w_1	1	1-6-8-5	w_1	1
23	4-10	4-7-8-10	w_1	12	4-3-2-6-7-9-10	w_1	12

6.4.4.2 Experiment II

In the second experiment, 50 requests are randomly generated as it is shown in Table 6.9, in which each request has a capacity of 12. Given total number of wavelength $W = 3$, there is no solution for full protection ($P_{ratio} = 1$).

When the protection ratio reduces to $P_{ratio} = 0.5$, the *resource minimization* step gives a solution of 59 wavelength-links, where all backup paths are given their minimum capacity, which is 6 in this scenario. Based on this routing and wavelength assignment results obtained from *resource minimization*, we perform *protection maximization*. The results show that some of the requests gain more backup capacity and reach to its full protection level, the improved requests are shown in Table 6.10.

Table 6.9 Traffic matrix for the 10-node-14-link network: 50 requests.

	1	2	3	4	5	6	7	8	9	10
1	0	0	0	12	12	0	12	0	0	12
2	0	0	0	12	0	0	0	0	0	12+12
3	12+12	12	0	0	12	12+12	0	12	12+12	0
4	0	12	0	0	0	0	12	12	12	12
5	12+12	0	0	0	0	12	12+12	0	0	0
6	0	0	12	12	0	0	0	12+12	12+12	0
7	0	0	0	12	0	0	0	0	12+12+12	12
8	12	12	12	0	0	0	12	0	0	0
9	0	0	12+12	0	0	0	0	0	0	0
10	12	0	12+12	12	0	12	12	0	12	0

Table 6.10 Requests with improved protection: Given $P_{ratio} = 0.5$.

Seq. No.	s-d pair	Primary Path			Backup Path		
		Path	w	cap	Path	w	cap
5	10-9	9-7-6-2	w_3	12	10-8-7-9	w_2	12
18	7-10	7-9-10	w_1	12	7-8-10	w_1	12
24	8-1	8-6-1	w_2	12	8-5-1	w_1	12
27	6-8	6-8	w_1	12	6-7-8	w_3	12
30	1-7	1-6-7	w_1	12	1-5-8-7	w_3	12
31	6-3	6-2-3	w_1	12	6-7-4-3	w_3	12
47	3-5	3-2-1-5	w_3	12	3-4-7-8-5	w_1	12

6.4.5 Shortest-Available-Least-Congested Routing

This section deals with partial protection design in WDM grooming networks with dynamic traffic patterns. The basic ideas of solving two subproblems are applied in dynamic routing. The idea of *resource minimization* is conveyed to the *shortest-available* routing strategy on primary path allocation, and the idea of *protection maximization* is realized by looking for the *least-congested routing* for the backup path.

More specifically, for each node pair, K alternate paths are pre-computed, as the candidate routes for the primary path. As a request comes, the shortest available path, \hat{p} , is selected first as the temporary primary path. By removing all the links involved in path \hat{p} , a reduced network topology is generated. In this reduced graph, find L alternative paths as the corresponding backup path candidates for the temporary primary path \hat{p} . Among these L backup path candidates, select the one which has the maximum free capacity to be the backup path given \hat{p} being the temporary primary path. Such a backup route is also referred to as the *least congested route* among all the L backup path candidates.

Let \hat{b} denote the least congested route given \hat{p} as the temporary primary path. If \hat{b} satisfies the protection requirement, the call is accepted with \hat{p} being the primary path and \hat{b} being the backup path. Depending on the free capacity on path \hat{b} , the request is at least protected with its minimum requirement or being full protected in the best case.

Otherwise, if \hat{b} , the one which has the maximum free capacity among all L backup candidates, can not meet the minimum protection requirement of the current request, then none of the L backup candidates can satisfy the protection requirement. \hat{p} is removed from the list of the eligible primary path candidates, and the next shortest available path is then selected as the new temporary primary path, its backup candidates will be generated and checked accordingly. This algorithm terminates either the request is accepted, or all K alternate paths as the primary path candidates have been checked. If either primary or backup path can not be found, the request is said to be blocked.

This routing scheme is therefore called *shortest-available-least-congested* routing for partial protected WDM grooming networks. The main idea of this design is to first assign the minimum

resource, in terms of wavelength-links, to the primary path. Given the primary path is decided, the second step is to select a backup path. Among all the L backup path candidates, select the one which has the maximum free capacity to be the backup path. Essentially, this is the same as the design idea in ILP, in which we solve two subproblems, namely *resource minimization* and *protection maximization* in order to obtain an optimal partial protection in grooming WDM networks.

6.4.6 Simulation Results

We perform our simulations on the same topology shown in Figure 6.3. Each link has a single fiber which carries 3 wavelengths. It is assumed that random requests arrive at each node according to a Poisson process with rate λ . Each request is equally likely to be destined to any of the remaining nodes. The holding time of the requests are exponentially distributed with mean $1/\mu$. Hence, the Erlang load offered by a node is $\rho = \lambda/\mu$. The requested capacity is uniformly distributed between a given lower-bound and an upper-bound, the full wavelength capacity is chosen to be OC-48. The minimum backup capacity is specified by the *protection ratio* as defined earlier in Section 6.4.4.1.

A request is said to be accepted if and only if both of its primary path and backup path are successfully allocated. If a primary path can not be found, the request is said to be blocked due to *primary blocking*. Otherwise, given its primary path being successfully allocated, if no backup paths are found to satisfy the protection requirement, the request is said to be blocked due to *backup blocking*. These terms are used to analyze the simulation results.

6.4.6.1 Experiment I

In this experiment, the request capacity is uniformly distributed between OC-1 and OC-36, with the given full wavelength capacity being OC-48. Figure 6.4 presents the networking blocking performance as the node load changes. For each node load, we perform simulations in 10 rounds, with each round having 100000 random requests. An average value is taken as the blocking probability for the given node load value. The number of primary blocking and

backup blocking are presented in Figures 6.5 and 6.6, respectively.

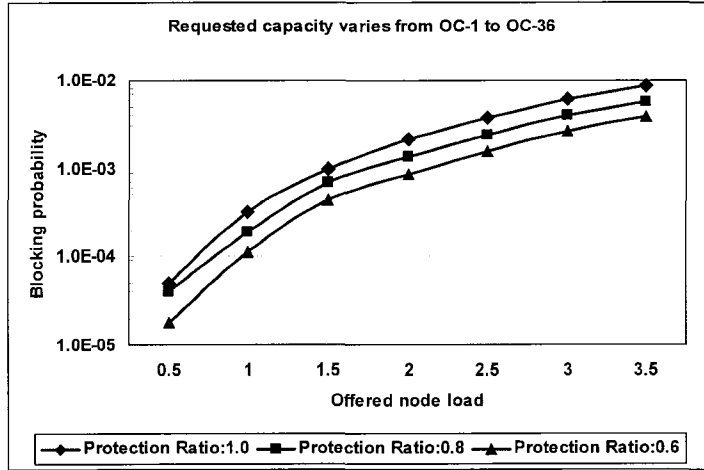


Figure 6.4 Blocking performance for traffic capacity varies from OC-1 to OC-36.

6.4.6.2 Experiment II

In this experiment, the request capacity is uniformly distributed between OC-24 and OC-36. In comparison to the traffic pattern in Experiment I in Section 6.4.6.1, the average load here is higher, also the variance of the requested capacity is smaller. And hence, the traffic pattern in this experiment is called the *heavy traffic*, while the traffic pattern in Section 6.4.6.1 is referred to as the *light traffic*.

Figure 6.7 presents the blocking performance as the node load changes. For each node load, we also perform simulations in 10 rounds, each consisting 100000 random requests. The number of primary blocking and backup blocking are presented in Figures 6.8 and 6.9 respectively.

As it can be observed from Figures 6.4 and 6.7, as the protection ratio goes down, the network blocking performance improves. In the network with high load as shown in Figure 6.7, a greater improvement on blocking performance can be seen as the protection ratio goes from 0.8 to 0.6, while in the network with light load as a comparison, the improvement is more even. The reason being is that the wavelength resource is more constrained when the traffic

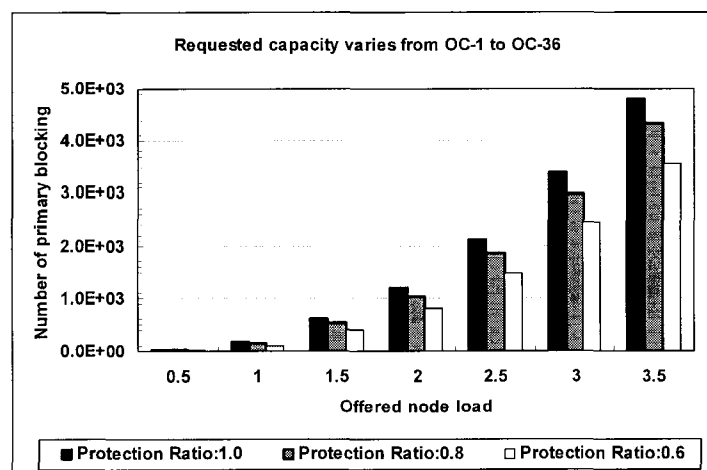


Figure 6.5 Number of call blocked due to primary blocking.

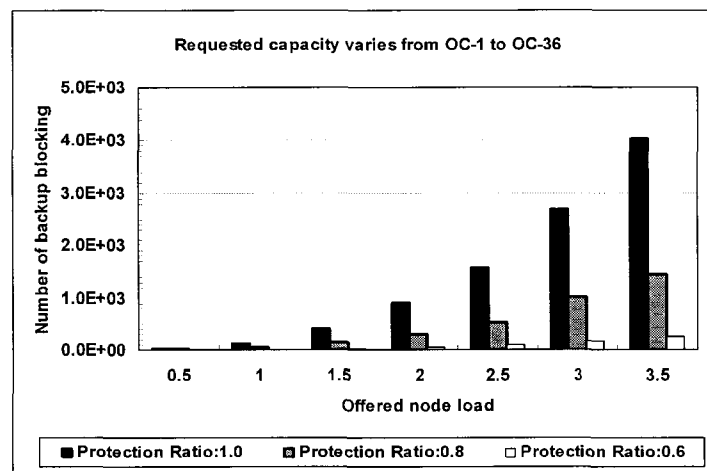


Figure 6.6 Number of call blocked due to backup blocking.

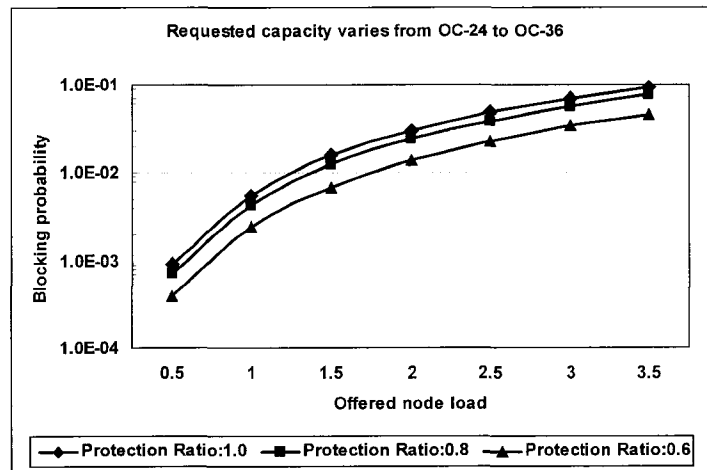


Figure 6.7 Blocking performance for traffic capacity varies from OC-24 to OC-36.

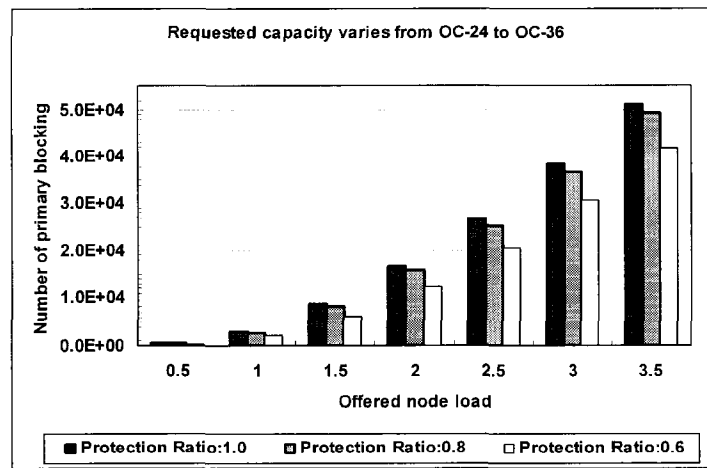


Figure 6.8 Number of call blocked due to primary blocking.

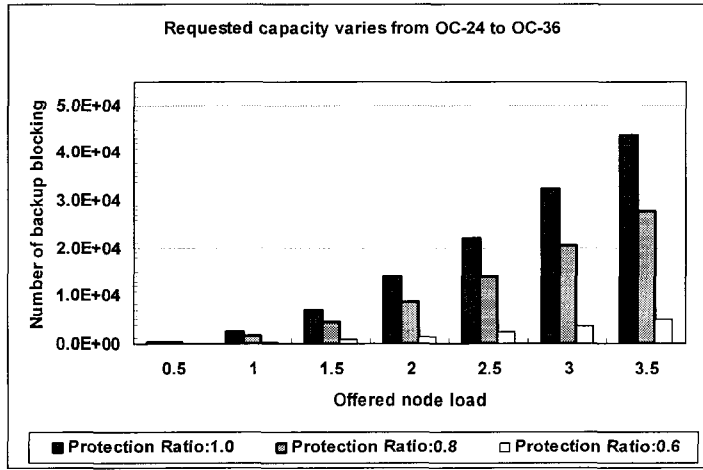


Figure 6.9 Number of call blocked due to backup blocking.

load is high.

Figures 6.5 and 6.8 show the number of primary blocking also goes down as the value of protection ration decreases. This is due to the fact that as less resource is reserved for backup paths, the chance of establishing the primary paths increases. A very sharp reduce on the number of backup blocking can be seen in both Figure 6.6 and Figure 6.9. This is mainly due to the reduce on protection value that leads to lower backup capacity requirement. For the same reason as it is in the blocking performance improvement, as the protection ration goes down, greater improvement is seen on both number of primary blocking as well as the number of backup blocking in the network with heavy load.

6.5 Summary

This chapter addresses two important issues in WDM network design, survivability and traffic grooming. The aim is to enable subwavelength level traffic grooming in survivable WDM network design. In order to provide 100% protection under single link failure, two link-disjoint alternate paths for each connection are pre-computed. The path selection and wavelength assignment schemes are formulated as ILP optimization problems. Two exact formulations

are given for employing backup multiplexing and dedicated backup (with MLPS) respectively. Illustrative examples are given to show the improvement of wavelength utilization of the two schemes and the difference path selections.

Backup multiplexing has been extensively studied in mesh-restoration WDM networks, it helps to reduce the amount of spare capacity by allowing multiple backup paths to share the same wavelength on their common links given their corresponding primary paths are link disjoint. Backup multiplexing becomes much more complicated in WDM grooming networks as we analyze in Section 6.2.2.1. It can still be applied in WDM grooming networks, however, it becomes much more expensive in computation than it is in the network without traffic grooming. Since the network grooming capability leads to a significant improvement on wavelength utilization, the dedicated backup reservation becomes affordable to provide 100 % restoration for any single link failure. Furthermore, by minimizing the total Link-Primary-Sharing (MLPS), the number of affected working paths due to single link failure is reduced, so that the recovering signalling is simplified. It would be ideal to employ both backup multiplexing and MLPS scheme. However that will be too costly in computation and therefore infeasible for practical usage.

The approaches we proposed here can be easily adapted to solve partial protection problems in grooming network design. The partial protection design is decomposed into two subproblems, namely *resource minimization* and *protection maximization*. Each subproblem is formulated as an ILP optimization problem. We apply this design idea in dynamic traffic scenario, and propose a routing scheme called *shortest-available-least-congested* algorithm to deal with the problem of routing partial protected requests in grooming networks. The essence of our design is to make the best out of the network resource that meets the minimum protection requirement before exploiting more wavelengths. The results for both static and dynamic traffic scenarios are obtained and presented. The results show that partial protection is a useful compromise when the network resource is restrained and not sufficient to provide full protection for every request.

CHAPTER 7. Summary and Future Work

As technology develops, the networking infrastructure evolves towards the slim two-layer model of IP over WDM. The need of ATM, SONET/SDH diminishes and their functions are divided by IP and WDM layers. Challenges remain as changes happen. We have addressed several prominent issues of the design in optical layer in the context of IP over WDM.

Routing and wavelength assignment is a key problem that needs to be solved. The data traffic keep increasing while the wavelength resource is still limited. The wavelength continuity constraint in WDM layer leads to higher blocking probability in a network without wavelength conversion capability, in comparison to a network which wavelength converters are equipped. How to route and assign wavelength on a request efficient to avoid employing the expensive network equipment like wavelength converters, or adding transmitters and receivers remains to be a significant problem.

We consider the power budget scenario in optical networks when the total number of usable wavelengths in a fiber is limited to a certain maximum number due to power considerations. The total number of available wavelengths in the fiber can be more than the maximum usable number, this is referred to as the *wavelength usage constraint*. This research gives a viable solution of establishing lightpaths without involving wavelength converters but still achieves similar blocking performance. We develop an analytical model for evaluating the blocking performance of WDM optical networks with wavelength usage constraint. This model is verified to be accurate by comparing the results obtained from the simulations. We also evaluate the performance of first-fit wavelength assignment strategy and compare its performance with that of random wavelength assignment strategy. Our results show that with an increase of few extra wavelengths in the fiber, the blocking performance is similar to that when full-

wavelength conversion is employed. Moreover, the number of extra wavelengths required to achieve a certain blocking performance is lesser when first-fit wavelength assignment strategy is employed. We conclude that employing extra wavelengths in practical WDM optical networks is an attractive alternative compared to full-wavelength conversion even in the presence of power budget constraints. Strictly speaking, the wavelength usage constraint is an estimation of the power limit on each fiber link. It would be accurate to use the actual power that every wavelength introduces to the fiber link in order to measure the exact power level of this fiber link. This can be another challenging research problem.

As the capacity of a single wavelength keeps increasing, there exists a big gap between the huge wavelength capacity and the fractional wavelength level users requirements, it is of great importance to develop efficient wavelength sharing techniques. This motivated our investigation on IP traffic grooming in both conventional WDM optical networks as well as in a recently proposed architecture called *light tail*. IP traffic grooming here is referred to as the traffic aggregation performed at IP routers. It helps to alleviate the complexity of performing subwavelength level grooming in WDM layer.

The concept of virtual topology is used to solve the IP traffic grooming problem with objective to minimize the network cost in terms of number of transmitters and receivers. We formulate the transmitter/receiver minimization problem as an ILP optimization problem, and also design a simple heuristic approach, called the *traffic aggregation algorithm*. The IP traffic aggregation algorithm effectively reduces the number of transmitters/receivers as well as the overhead IP traffic in big networks where it is impractical to apply ILP approaches.

For a given estimated traffic matrix, a virtual topology can be obtained by applying either of the above approaches. We then propose three different routing strategies for dynamic routing in the resulting virtual topology, namely *fixed path routing (FPR)*, *least congested routing (LCR)*, and *preferred path first (PPF)*. The blocking performance of these routing schemes is compared through simulations with different traffic patterns and virtual topologies. Our simulation results show that given a virtual topology with high designed link load, PPF is a preferred choice among the three routing schemes. When the designed link load is low, LCR outperforms

PPF and FPR.

The light trail has been proposed as a novel architecture designed for carrying finer granularity IP burst traffic. The fast access of light trail communication and the flexible dynamic sub-wavelength provisioning make light trail architecture a strong candidate for transporting IP traffic over optical networks. As a newly proposed concept, light trail architecture also brings up various issues in designing optical networks for transporting IP centric traffic.

We study the problem of how to identify a set of light trails at the design phase, which is one of the key issues in light trail implementations. Both mathematical formulation and heuristic algorithms are developed for obtaining a solution with minimum number of light trails to carry the given traffic. This problem is also referred to as the *light trail design problem*. We have not proved but we believe that light trail design problem is NP-complete. This proof remains to be one of the future projects. Dynamic routing in light trail optical networks is another topic worth investigating. Finally, to come up with a better cost function is still an interesting problem for both conventional WDM networks as well as in the light trail architecture.

Another major issue in optical fiber network is the management of fault. Even a single link failure is expensive in optical networks due to the huge amount of traffic carried by a single fiber. We study the resource planning in WDM grooming networks where a single link failure is part of the design and operation process. We propose two exact formulations for employing backup multiplexing and dedicated backup respectively in survivable grooming networks. Backup multiplexing has been extensively studied in mesh-restoration WDM networks, it leads to the save on the reserved capacity by allowing backup paths to share the wavelength capacity if their corresponding primary paths are link disjoint and will not fail due to the same single link failure. However, backup multiplexing becomes much more computational expensive than it is in networks without grooming functionality.

Our study shows that dedicated backup reservation becomes affordable and appears to be more desired in survivable grooming networks, where the wavelength utilization has significantly improved by the grooming capability of the network. Furthermore, by adding a constraint to minimize the total link-primary-sharing, the number of affected working paths

due to single link failure is reduced. This effectually prevents failure from spreading and simplifies the recovering signalling as the same time.

When network resource is restrained and insufficient to provide 100% protection to every request, one solution is to provide partial protections. The ratio between the reserved backup capacity to the primary capacity is called the *protection ratio*. Our methods for survivable WDM grooming network design can be easily adapted to solve the routing and wavelength assignment problem in partial protected grooming networks. We solve this problem by dividing it into two subproblems: 1) resource minimization, and 2) protection maximization. Based on this design idea, we formulate each subproblem as an ILP optimization problem for the static traffic scenario, and develop a routing scheme called *shortest-available-least-congested* algorithm to solve routing and wavelength assignment problem in dynamic traffic scenario. Our approaches first allocate the minimum required network resource to meet the partial protection requirement, then maximize the residual network resource to provide better protection for some of the requests if it is impossible for all the requests. Our results show that partial protection is an effective compromise when the network resource is limited.

Survivable design in grooming network is still a relatively new territory. The protection and restoration design in grooming networks is more complicated than that of the conventional WDM networks, which does not have grooming capability. However, the wavelength resource in grooming networks is not as restricted as it is in conventional WDM networks. Other than minimizing the spare capacity reserved in the network, which is a common objective of general WDM network, different aspects of the protection and restoration design can be considered. For example, future research projects can focus on the quality of protection or the failure propagation in grooming networks.

BIBLIOGRAPHY

- [1] R. Jain and S. Dharanikota, "Internet protocol over DWDM - recent developments, trends and issues," in *Global Optical Communications - Business Briefing*, London, UK, July 2001, World Market Research Centre Ltd (www.wmrc.com).
- [2] P. Bonenfant, A. Rodrigues-Moral, and J.S. Manchester, "IP over WDM: The missing link," Tech. Rep., white paper, Lucent Technologies, 1999.
- [3] J. Anderson, J.S. Manchester, A. Rodrigues-Moral, and M. Veeraraghavan, "Protocols and architectures for IP optical networking," *Bell Labs Technical Journal*, pp. 105–124, January–March 1999.
- [4] A. Banerjee, J. Drake, and *et al.*, "Generalized multiprotocol label switching: An overview of routing and management enhancements," *IEEE communication magazine*, pp. 144–150, January 2001.
- [5] J. Y. Wei, "Advances in the management and control of optical internet," *IEEE Journal on Selected Areas in Communications*, vol. 20, no. 4, pp. 768–785, May 2002.
- [6] P. Gambini and *et al.*, "Transparent optical packet switching: network architecture and demonstrators in the KEOPS project," *IEEE Journal on Selected Areas in Communications*, vol. 16, no. 7, pp. 1245–1259, Sept 1998.
- [7] Y. Yamada and *et al.*, "Optical output buffered ATM switch prototype based on FRON-TIERNET architecture," *IEEE Journal on Selected Areas in Communications*, vol. 16, no. 7, pp. 1298–1307, Sept 1998.

- [8] M. Mahony, D. Simeonidou, D. Hunter, and A. Tzanakaki, “The application of optical packet switching in future communication networks,” *IEEE Communication Magazine*, pp. 128–135, March 2001.
- [9] G. K. Chang and *et al.*, “A proof-of-concept, ultra-low latency ols testbed demonstration for next generation internet networks,” in *OFC’2000*, Baltimore, MD, March 2000, paper WD5, pp. 56–58.
- [10] B. Rajagopalan and *et al.*, “IP over optical networks, a framework.,” IETF Internet Draft, March 2001, Available: <http://www.ietf.org/internet-drafts/draft-many-ip-optical-framework-03.txt> (date accessed: July 16, 2001).
- [11] J. Fang, R. Srinivasan, and A. K. Soman, “Performance analysis of WDM optical networks with wavelength usage constraint,” *Journal of Photonic Network Communications*, vol. 5, no. 2, pp. 137–146, March 2003.
- [12] O. Gerstel, R. Ramaswami, and G. H. Sasaki, “Cost-effective traffic grooming in WDM rings,” *IEEE Transactions on Networking*, vol. 8, no. 5, pp. 618–630, October 2000.
- [13] E. Modiano and P. J. Lin, “Traffic grooming in WDM networks,” *IEEE Communications Magazine*, vol. 39, no. 7, pp. 124–129, July 2001.
- [14] R. Srinivasan and A. K. Soman, “A generalized framework for analyzing time-space switched optical networks,” in *Proceedings of IEEE INFOCOM’01*, 2001, pp. 179–188.
- [15] C. Guillemot and *et al.*, “Transparent optical packet switching: The european ACTS KEOPS project approach,” *Journal of Lightwave Technology*, vol. 16, no. 12, pp. 2117–2134, December 1998.
- [16] H. J. S. Dorren, M. T. Hill, and *et al.*, “Optical packet switching and buffering by using all-optical signal processing methods,” *Journal of Lightwave Technology*, vol. 21, no. 1, pp. 2–12, 2003.

- [17] D. J. Blumenthal, "Photonic packet switching and optical label swapping," *Optical Networks Magazine*, vol. 2, no. 6, pp. 54–65, 2001.
- [18] S. Amstutz, "Burst switching - an introduction," *IEEE Communications*, November 1983.
- [19] L. Xu, H. Perros, and G. Rouskas, "Techniques for optical packet switching and optical burst switching," *IEEE Communications Magazine*, pp. 136–142, Jan 2001.
- [20] M. Yoo, M. Jeong, and C. Qiao, "A high speed protocol for bursty traffic in optical networks," *SPIE's All-Optical Communication Systems*, vol. 3230, pp. 79–90, 1997.
- [21] C. Qiao and M. Yoo, "Optical burst switching (OBS) - a new paradigm for an optical internet," *Journal of High Speed Networks*, vol. 8, no. 1, pp. 69–84, 1999.
- [22] I. Widjaja, "Performance analysis of burst admission control protocols," *IEEE Proceedings on Communications*, vol. 142, pp. 7–14, Feb 1995.
- [23] E. Vararigos and V. Sharma, "The ready-to-go virtual-circuit protocol: a loss-free protocol for multigigabit networks using fifo buffers," *IEEE/ACM Transactions on Networking*, vol. 5, pp. 705–718, Oct 1999.
- [24] J. Y. Wei and R. I. McFarland, "Just-in-time signaling for WDM optical burst switching networks," *Journal of lightwave technology (JLT)*, vol. 18, no. 2, December 2000.
- [25] J. S. Turner, "Terabit burst switching," *Journal of High Speed Networks*, vol. 8, no. 1, pp. 3–16, March 1999.
- [26] I. Chlamtac and A. Gumaste, "Light-trails: A solution to IP centric communication in the optical domain," in *Second International Workshop on Quality of Service in Multiservice IP Networks (QoS-IP 2003)*. 2003, pp. 634–644, Springer-Verlag, Heidelberg.
- [27] A. Ganz I. Chlamtac and G. Karmi, "Lightpath communications: An approach to high bandwidth optical WANs," *IEEE Transactions on Communications*, vol. 40, pp. 1171–1182, July 1992.

- [28] R.A. Barry and P.A. Humblet, "Models of blocking probability in all-optical networks with and without wavelength changers," *IEEE Journal on Selected Areas in Communications*, vol. 14, no. 5, pp. 858–867, June 1996.
- [29] A. Birman, "Computing approximate blocking probabilities for a class of all-optical networks," in *Proceedings of IEEE INFOCOM'95*, April 1995, pp. 651–658.
- [30] M. Kovacevic and S. Acampora, "On wavelength translation in all-optical networks," in *Proceedings of IEEE INFOCOM'95*, April 1995, pp. 413–422.
- [31] M. Kovacevic and S. Acampora, "Benefits of wavelength translation in all-optical clear-channel networks," *IEEE Journal on Selected Areas in Communications*, vol. 14, no. 5, pp. 868–880, June 1996.
- [32] K. -C. Lee and V. O. K. Li, "A wavelength-convertible optical network," *Journal of Lightwave Technology*, vol. 11, no. 5, pp. 962–970, May-June 1993.
- [33] S. Subramaniam, M. Azizoglu, and A. K. Soman, "All-optical networks with sparse-wavelength conversion," *IEEE/ACM Transactions on Networking*, vol. 4, no. 4, pp. 544–557, August 1996.
- [34] R. Ramaswami and G. Sasaki, "Multiwavelength optical networks with limited wavelength conversion," *IEEE/ACM Transactions on Networking*, vol. 6, no. 6, pp. 744–754, December 1998.
- [35] T. Tripathi and K.N. Sivarajan, "Computing approximate blocking probabilities in wavelength-routed all-optical networks with limited-range wavelength conversion," in *Proceedings of IEEE INFOCOM'99*, March 1999, vol. 1, pp. 329–336.
- [36] L. Li and A.K. Soman, "A new analytical model for multi-fiber WDM networks," in *Proceedings of IEEE Global Telecommunications Conference (GLOBECOM)*, 1999, vol. 1B, pp. 1007–1011.

- [37] N. Wauters and P. Demeester, "Wavelength conversion in optical multi-wavelength multi-fiber transport networks," *International Journal of Optoelectronics*, vol. 11, no. 1, pp. 53–70, Janurary/February 1997.
- [38] J. Yates, J. Lacey, and D. Everitt, "Blocking in multiwavelength TDM networks," in *4th International Conference on Telecommunication Systems, Modeling, and Analysis*, March 1996, pp. 535–541.
- [39] R. Srinivasan and A. K. Somani, "Request-specific routing in WDM grooming networks," *IEEE International Conference on Communications (ICC)*, vol. 5, pp. 2876–2880, 2001.
- [40] S. Ramamurthy and B. Mukherjee, "Survivable WDM mesh networks, part i-protection," in *Proceedings of IEEE INFOCOM*, March 1999, vol. 2, pp. 744–751.
- [41] B.T. Doshi, S. Dravida, P. Harshavardhana, O. Hauser, and Y. Wang, "Optical network design and restoration," *Bell Labs Technical Journal*, pp. 58–83, January-March 1999.
- [42] G. Mohan and A. K. Somani, "Routing dependable connections with specified failure restoration guarantees in WDM networks," in *Proceedings of IEEE INFOCOM*, March 2000, pp. 1761–1770.
- [43] D. Bertsekas and R. Gallager, *Data Networks*, Prentice Hall, Englewood Cliffs, N.J., U.S.A., 1992.
- [44] A. L. Chiu and E. H. Modiano, "Traffic grooming algorithms for reducing electronic multiplexing costs in WDM ring networks," *Journal of Lightwave Technology*, vol. 18, no. 1, pp. 2–12, January 2000.
- [45] H. Ghafouri-Shiraz, G. Zhu, and Y. Fei, "Effective wavelength assignment algorithms for optimizing design costs in SONET/WDM rings," *Journal of Lightwave Technology*, vol. 19, no. 10, pp. 1427–1439, October 2001.
- [46] R. Dutta and G. N. Rouskas, "On optical traffic grooming in WDM rings," *IEEE Journal on Selected Areas in Communications*, vol. 20, no. 1, pp. 110–121, January 2002.

- [47] M. Kodialam and T. V. Lakshman, “Integrated dynamic IP and wavelength routing in IP over WDM networks,” in *Proceedings of IEEE INFOCOM*, 2001.
- [48] H. Zhu, H. Zang, K. Zhu, and B. Mukherjee, “A novel generic graph model for traffic grooming in heterogeneous WDM mesh networks,” *IEEE Transactions on Networking*, vol. 11, no. 2, pp. 285–299, April 2003.
- [49] J. John and T. Mueller, “From ring to mesh: why, when and how?” Tech. Rep., Bell Labs, Lucent Technologies, 2002.
- [50] O. Gerstel, P. J. Lin, and G. H. Sasaki, “Wavelength assignment in WDM rings to minimize system cost instead of number of wavelengths,” in *Proceedings of IEEE INFOCOM*, 29 March - 2 April 1998, vol. 1, pp. 94–101.
- [51] O. Gerstel, P. J. Lin, and G. H. Sasaki, “Combined WDM and SONET network design,” in *Proceedings of IEEE INFOCOM*, 1999.
- [52] V. R. Konda and T. Y. Chow, “Algorithm for traffic grooming in optical networks to minimize the number of transceivers,” in *IEEE Workshop on High Performance Switching and Routing*, 2001, pp. 218–221.
- [53] R. K. Ahuja, T. L. Magnanti, and J. B. Orlin, *Network flows: theory, algorithms, and applications*, Prentice Hall, Upper Saddle River, N.J., U.S.A., 1993.
- [54] A. Feldmann, A. Greenberg, C. Lund, N. Reingold, J. Rexford, and F. True, “Deriving traffic demands for operational IP networks: methodology and experience,” in *SIGCOMM*, 2000, pp. 257–270.
- [55] A. Medina, N. Taft, K. Salamatian, S. Bhattacharyya, and C. Diot, “Traffic matrix estimation: Existing techniques and new directions,” Pittsburgh, Pennsylvania, August 19-23 2002, SIGCOMM’02.
- [56] D. Eppstein, “Finding the k shortest paths,” in *IEEE Symposium on Foundations of Computer Science*, 1994, pp. 154–165.

- [57] ILOG CPLEX 7.0 Reference Manual <http://www.cplex.com>" (date accessed: November 20, 2004).
- [58] Y. Miyao and H. Saito, "Optimal design and evaluation of survivable WDM transport networks," *IEEE Journal on Selected Areas in Communications*, vol. 16, no. 7, pp. 1190–1198, September 1998.
- [59] M. Sridharan, M. V. Salapaka, and A. K. Somani, "A practical approach to operating survivable WDM networks," *IEEE Journal on Selected Areas in Communications*, vol. 20, no. 1, pp. 34–46, January 2002.
- [60] J. Fang and A. K. Somani, "Enabling subwavelength level traffic grooming in survivable WDM optical network design," in *IEEE Global Telecommunications Conference (GLOBECOM)*, vol. 5, pp. 2761–2766.
- [61] S. Thiagarajan and A. K. Somani, "Traffic grooming for survivable WDM mesh networks," in *OptiComm2001: Optical Networking and Communications*, 2001, vol. 4599, pp. 54–65.
- [62] C. Assi, Y. Ye, A. Shami, S. Dixit, I. Habib, and M.A. Ali, "On the merit of IP/MPLS protection/restoration in IP over WDM networks," in *IEEE Global Telecommunications Conference (GLOBECOM)*, 2001, vol. 1, pp. 65 –69.
- [63] C. Ou, K. Zhu, and *et al.*, "Traffic grooming for survivable WDM networks - shared protection," *IEEE Journal on Selected Areas in Communications*, pp. 1367–1383, November 2003.
- [64] C. Ou, K. Zhu, and *et al.*, "Traffic grooming for survivable WDM networks - dedicated protection," *Journal of Optical Networking*, pp. 50–74, January 2004.